Feasibility study of an innovative surveillance system for space debris observations in LEO based on optical telescopes

Relatore: Prof. Michèle Lavagna

Corelatore: Lorenzo Cibin

Tesi di laurea magistrale di

Francesco Villa 70884

Anno accademico 2009/2010

Contents

Acknowledgement

A

scrivi

Sommario

Lo scopo di questa tesi è lo studio di fattibilità di un sistema di osservazioni ottiche per i debris, in particolare per quelli in fascia LEO, la zona più vicina alla Terra. Il problema dei debris nello spazio che circonda la Terra è di attuale importanza, alla luce di alcune recenti collisioni ed esplosioni di satelliti avvenute in orbita e considerando il fatto che la popolazione di debris è destinata ad aumentare sempre di più nel corso dei prossimi anni. Bisogna tenere presente che per la maggior parte di questi oggetti sono sconosciute sia le caratteristiche fisiche che i parametri orbitali. L'osservazione, il monitoraggio e la determinazione orbitale dei debris sono quindi temi fondamentali che trovano il forte interessamento di tutte le principali agenzie spaziali del mondo: in particolare la NASA che cataloga debris da alcuni decenni, e l'ESA, che si sta affacciando da pochi anni all'osservazione di questi oggetti. L'osservazione dei debris viene tipicamente effettuata da stazioni radar (per i debris alle quote più basse, in LEO) o da stazioni ottiche (per i debris a quote più alte, in GEO e MEO). In questa tesi verrà analizzato un approccio alternativo alle osservazioni di debris in fascia LEO (in particolare nella parte più alta della fascia LEO), che utilizza osservazioni ottiche come valida alternative in termini di costi alle osservazioni radar nella stessa zona.

Il primo capitolo introduce il problema dei debris nelle regioni attorno alla Terra.

Il secondo capitolo è una panoramica sui debris e sul loro studio. Il capitolo descrive le varie tipologie di oggetti presenti nello spazio attorno alla Terra, come essi sono distribuiti (con particolare attenzione ai debris in LEO) e come vengono monitorati dalle agenzie spaziali, considerando sia i sistemi per osservarli che i metodi di determinazione orbitale.

Il terzo capitolo mostra lo studio di fattibilità di un sistema innovativo per le osservazioni ottiche dei debris in fascia LEO. Questo studio fa parte di un progetto svolto per l'ESA dalla *Carlo Gavazzi Space* e verranno analizzate (con le relative ipotesi) le osservazioni simulate create da un'apposita interfaccia software tra i tool STK e Matlab.

Il quarto capitolo mostra i risultati ottenuti dalle osservazioni simulate, dopo aver analizzato alcuni aspetti importanti che riguardano l'osservazione ottica di debris, quali il network di stazioni, l'analisi della situazione meteorologica e le proprietà ottiche dei debris.

Il quinto capitolo descrive lo studio di fattibilità per l'osservazioni di debris tramite un satellite disposto in orbita bassa attorno alla Terra. Definendo alcune opportune strategie di osservazione, questo sistema si pone come supporto alle osservazione da Terra di debris in LEO.

Il sesto capitolo presenta le conclusioni dello studio e i possibili sviluppi futuri.

Abstract

The purpose of this thesis is the feasibility study of a system for optical debris observation, particularly debris in LEO band, the closest area to the Earth. The debris problem around the Earth is now important, considering some recent satellites collisions and explosions occurred in orbit and considering that the debris population will grow increasingly over the next years. Both physical characteristics and orbital parameters of most of these objects are completely unknown and this represents an important limit in debris observations. The debris observation and orbit determination are fundamental issues analysed from the major space agencies in the world: in particular NASA has classified debris for decades and ESA is beginning debris observations. Debris observations are tipically performed by radar stations (for lower altitude debris in LEO) or by optical stations (for higher altitude debris in GEO or MEO). In this thesis an alternative approach for debris observation in LEO (in particular in the upper part of LEO region) is investigated; this approach uses optical observations as valid alternatives for costs to radar observations in the same region.

The first chapter introduces the debris problem in regions around Earth.

The second chapter is an overview of actual debris studies. This chapter describes debris types, debris distribution around the Earth (in particular the debris in the LEO band) and how debris are observed by space agencies, considering also their orbit determination.

The third chapter shows the system feasibility study for an innovative debris optical observations in LEO. This study is part of a project carried out for ESA by *Carlo Gavazzi Space* and debris simulated observations created by a special software interface (between STK and Matlab tools) will be analysed with their assumptions.

The fourth chapter shows results for simulated observations, after an analysis of some importance aspects related to debris optical observations, such as the stations network, weather conditions and debris optical properties.

The fifth chapter describes the feasibility study for debris observations with a in-orbit satellite. After defining some observation strategies, this concept is a support for LEO debris ground observations.

The sixth chapter presents study conclusions and possible future developments.

Chapter 1

Introduction

There is perhaps one single environment near us that had remained virgin and unexploited from the human race: the space. But in the middle of last century, the first artificial satellite, Sputnik 1, was launched by the USSR on October 4, 1957, and also space began to be polluted by human presence. A few years later, in the 1961 the first known break up in orbit, the explosion of the Transit 4A rocket body took place. From this explosion, the repetition of these two events (launches of new satellites and break-up of spacecraft in orbit) contributed to build up a huge population of objects that are now polluting, perhaps in an irreversible way, the space around us. All these objects are called space debris: they include operational spacecraft, non-operational (inactive or retired) spacecraft and rocket bodies, as well as debris from a variety of sources. Debris can be released intentionally from a spacecraft or rocket body, but many times are generated from accidental rocket bodies explosion, accidental or intentional satellites collisions. Space debris are often objects with unknown physical and orbital characteristics, so it's very difficult to observe them.

The large number of debris around Earth is a risk for the operative satellites safety, but also for the impact of these objects on the Earth. So it's very important to monitoring space debris with different methods and to know their orbits in order to prevent collisions. To protect critical space assets (including satellites, the ISS, the Space Shuttle, and future exploration vehicles), a reliable orbital debris environment definition is needed. A better understanding of the environment is also a key for appropriate protection and for this reason the most important space agencies in the world are very interested in the debris observation in order to prevent the safety of their operative satellites. For debris observations radar and optical stations are active, but also in situ measurements (e.g. optical observations from satellites) are efficient. Low altitude debris are usually observed by radar ground stations while high altitude debris are observed by optical ground stations. Debris observations are analysed from some mathematical methods in order to obtain the debris orbits.

The region with the most debris concentration is the LEO region where the most important spacecraft collisions or explosions happened. As baseline for LEO debris observations, radar stations are often used because radar is more efficient than telescope for lower altitude observations. This thesis wants to study the feasibility of a new approach for LEO debris surveillance, based

on optical observation only. Presently the LEO radar covers the full 200-2000 km altitude LEO region, but with the new approach the upper part of the LEO region (between 1000-2000 km altitude) might also be surveyed by ground based telescopes, which would significantly reduce the performance requirements for the radar system and could reduce costs of the system. This study is part of a project developed by the *Carlo Gavazzi Space* for the ESA SSA study about innovative system surveillance for optical observations in LEO region. ESA wants to have an independent debris surveillance system for LEO and GEO debris; it considers as baseline, radar observations for LEO region and optical observation for GEO region, but radar observations have great costs, so it's important to study alternative optical approaches in LEO.

Below 1000 km altitude is very difficult to observe debris with ground optical stations, so this thesis also propose a debris system surveillance based on satellites with optical telescopes. Considering that radars are efficient with reasonable costs till 700 km, it's possible to observe with an optical satellite constellation debris region from 700 to 1000 km altitude.

For the debris surveillance system study, simulated debris observations will be generated in order to analyse the system efficiency for debris detectability and not for debris orbit determination. Simulated observations are achieved with ad-hoc software interface between STK and Matlab tools created for this study. Study assumptions has been decided by the *Carlo Gavazzi Space*, but the debris simulated observations software interface between STK and Matlab tools and the debris detection analysis program have been developed in this thesis with these assumptions. It will be shown that simulated results of this thesis are similar to real observations from best optical ground stations in the world (US telescope used for LEO debris). In this study only objects from 3 cm to 25-26 cm are analysed: small objects observations is more difficult because they have less observations than large objects.

Considering that debris physical characteristics are important for debris observation, but completely unknown, this thesis also analyses the state of art knowledge about the most important debris optical parameter (i.e. the albedo) and some realistic asteroid models are proposed to calculate debris magnitude (absolute and apparent) because the actual knowledge concerning debris magnitude computation is very poor. Asteroid models used for debris magnitude calculation represent a limit for this study, but it's possible to suppose that these asteroid models are appropriate also for debris.

Chapter 2

The orbital debris environment

This chapter is an overview of the state-of-the-art knowledge about space debris. After a discussion about sources of debris and their distribution around Earth (in particular the LEO region, subject of this thesis), it's presented how space debris are monitored. Observations of space debris are achieved mainly with ground radar or optical stations; these observation methods are described considering positive and negative aspects and it's important to know that space around Earth is divided into two main regions: radars observe LEO region while telescope observe mainly GEO or MEO regions. The most important US and European radar and optical stations in the world are described and they are compared, considering that US was the first nation that built radar and optical stations for the debris surveillance and at now US has a better knowledge about space debris than other nations in the world. It's important to show that there are also debris in situ measurements to define the debris environment.

In this chapter is also presented how debris observations are elaborated to obtain information about debris (orbit determination, physical characteristics) and the importance of surveillance systems are described: the US SSN and the development of the new ESA SSA system are analysed. SSA system is the context of this thesis that considers a ESA SSA proposal to develop the study. The debris orbit determination is an important aspect of this thesis, in particular the innovative orbit determination method proposed by the Department of Mathematics of the University of Pisa is analysed. Debris observations and their elaborations are used to define space debris models that define the space debris environment.

The debris hazard is also discussed and the chapter ends with some considerations about the actual situation of debris observations and it's presented the new alternative observation approach of this thesis.

2.1 Sources of debris and distributions

In this section it's now presented the debris distribution around Earth considering all regions (LEO, MEO and GEO). The knowledge of the debris population distribution is very important to understand the most populated debris regions around Earth and to prevent collision between operative satellites and other debris. In this section also the main debris sources are described

and the future debris environment is presented. Two important and recent events (the Iridium 33 and the Cosmos-2251 collision and the explosion of the Chinese satellite Fengyun-1C) are also presented in order to show how these events improved the debris population and how space objects can represent an important risk for the operative spacecraft safety.

2.1.1 Sources of debris

Presently more than 12000 artificial objects with diameter larger than 10 cm are orbiting the Earth and they are monitored and catalogued by a large worldwide network of sensors. More than 500000-600000 debris have diameter larger than 1 cm, while those larger than 1 mm could be more than $3e^8$ (but no one really knows the exact population). These objects populate different regions of the circum-terrestrial space ranging from about 150 km of altitude above the Earth surface up to the geostationary radius, at an altitude of about 36000, and beyond. Many different kind of objects compose the Earth orbiting population. A part from the satellites (active and non-operational), rocket upper stages and a large number of debris, produced by different source mechanisms ranging from high energy fragmentation of large spacecraft to slow diffusion of liquid metal, are present. The density of objects in Earth orbit is such that in certain regions of space impact against a space debris is a now serious risk.

Artificial debris includes spent satellites, cast off Yo-Yo de-spinners (used to de-spin spacecraft after launch), tools dropped during spacewalks, discarded rocket upper stages and the fragmentary remains of craft that have exploded or otherwise broken up.

Only about 7% of the objects in the SSN catalog (the US catalog for space debris, for more information see sec. 2.3.1) are operative satellites. Approximately 20% is composed by non-operative spacecraft; around 14% by the upper stages of the rockets used to place the satellite in orbit. Since the Sputnik I, about 6600 payloads have been launched, with approximately 4600 launches. Note that, among the launched objects, some 3400 satellites and 3500 upper stages have re-entered in the atmosphere. The other spacecraft are still orbiting and represent most of the large (> 1 m) objects in orbit. About 13% consist of mission related debris, that is relatively small objects released mainly during the initial phases of a mission (e.g., sensors caps, yo-yo masses used to slow down the spacecraft spin, etc). Finally about half of the catalogued objects are debris generated mostly by about 200 fragmentations that happened in orbit. About 99% of the mass in orbit is due to the large objects included in the catalog. The figure 2.1 summarizes on-orbit objects by type, while the figure 2.2 shows on-orbit objects catalogued during years.
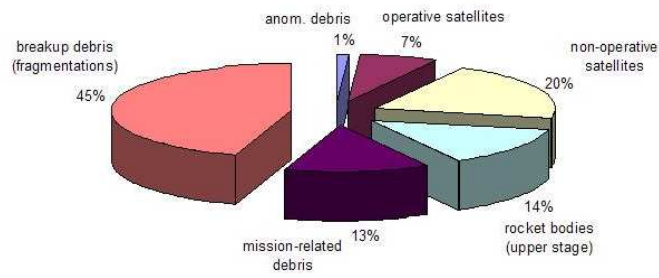
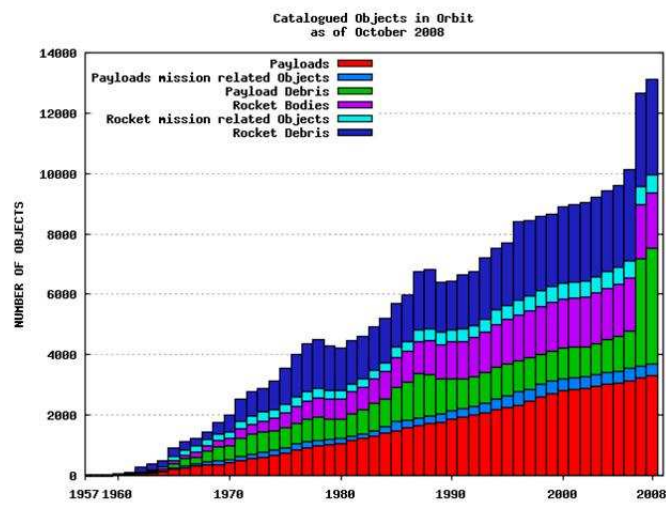Figure 2.1: On-Orbit objects by type until 2009 (from [7])

Figure 2.2: On-orbit objects catalogued during years until October 2008 (from [68])

The figure 2.3 represents all the debris generated by fragmentations that happened in orbit. The primary source of this debris was the intentional destruction of the Chinese Fengyun-1C spacecraft (see sec. 2.1.1).
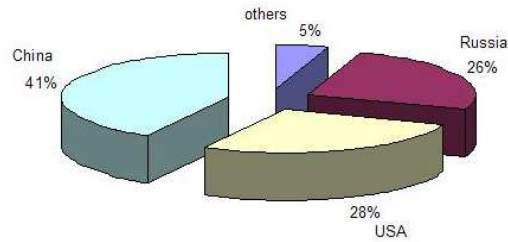
Figure 2.3: Satellite breakup debris in orbit as of 1 January 2008 (from [42])

The major sources of orbital debris are now described.

Mission-Related debris

Mission-related debris are objects intentionally discarded during satellite delivery or satellite operations. Most missions have very few pieces of this type of debris, and many times the objects have lower ballistic coefficients (mass, multiplied by the inverses of the drag coefficient and the area). LEO objects of this type will reenter the Earth's atmosphere more rapidly. Since the turn of the century, the absolute number of mission related debris in Earth orbit has declined due to increasing adoption of mitigation measures and design modifications. Mission related debris includes the release of payload attachment devices, sensor covers, explosive bolt fragments, and straps and wires. Such objects are often seen immediately after launch or release and are cataloged quickly. The release of debris from space stations has been a common occurrence for more than 30 years. The generation of debris onboard a space station is a natural consequence, but its accumulation can present a direct or indirect hazard to the crew as well as result in reduced productivity. Hence, the jettison of debris into space, in special cases, can be the most viable option. The Mir space station, which supported crews over a span of 14 years, created more than 300 cataloged debris, but its rate of release was significantly lower than its predecessor's rate. By contrast, the amount of cataloged debris released from ISS has been considerably less: only three dozen in more than 7 years of operations. Debris can be generated either deliberately or accidentally. During spacewalks (EVA), debris, both small and large, are often thrown off the station for convenience, although sometimes tools unintentionally slip away. The sizes of debris released from space stations vary dramatically from small, untrackable debris to the 10 m diameter KRT-10 antenna. Typically, debris experience rapid orbital decay and reenter the atmosphere within about one month. However, some objects have taken more than 100 days to fall back to Earth.

Fragmentation debris

Since the first recognized fragmentation in the 1961, over 200 objects (payloads, rocket bodies, and mission-related debris) have experienced on-orbit breakups. On-orbit fragmentations can result from accidental or intentional explosions, accidental or intentional collisions, or aerodynamic

forces as an object nears atmospheric reentry. Accidental collisions (e.g. satellites collisions) are not many, but are expected to increase as more objects are placed into orbit. Aerodynamic breakups, while relatively common, produce very few long-lived debris and are a non-factor in the long-term orbital debris problem. However, the intentional breakup of the Fengyun-1C spacecraft in January 2007 via hypervelocity collision with a ballistic object created the most severe artificial debris cloud in Earth orbit since the beginning of space exploration. Before the Fengyun-1C event, accidental explosions have dominated the long-lived debris generating events. Because of the energy associated with an explosion, these events can have hundreds of trackable objects, and probably tens-of-thousands of smaller pieces. It is these events that the international space agencies are focusing on reducing or eliminating. The accidental explosion event causing the most objects still in orbit today was the explosion of the Soviet Cosmos 1275 payload. A (probable) battery explosion 50 days into the lifetime of the satellite led to 259 objects. A close second place is the United States Nimbus 4 rocket body, which first fragmented in 1970, but has experienced up to six sub-events as late as 1995. These events released over 370 trackable objects, with over 240 pieces of debris still in Earth orbit. In terms of official debris, the explosion of a Pegasus HAPS (Hydrazine Auxiliary Propulsion System) orbital stage in June 1996 is the worst explosion on record creating more than 700 cataloged debris pieces. Immediately after the fragmentation many debris will be close to other debris or the parent object. The low altitude of the breakup has also presented special concerns for other spacecraft in low Earth orbit, in particular the Space Shuttle and the Hubble telescope. Examples of the most important and recent accidental collisions in LEO are in sec. 2.4: these collisions usually involve satellites or upper stages with relative small fragments and only one collision between two satellites it's known (the Iridium 33-Cosmos 2251 collision,see sec. 2.1.1).

Anomalous/Deterioration debris

As spacecraft spend many years in the space environment, many deteriorate to the point of pieces or parts separating from the original spacecraft and causing what is referred to as *anomalous debris*. An anomalous event is the unplanned separation, usually at low velocity, of one or more detectable objects from a satellite that remains relatively intact. The disintegration of spacecraft exterior paint is thought to create many sub-millimeter pieces of debris. The cause of this paint flaking is believed to be atomic oxygen erosion of the organic binder in the paint. Stage and spacecraft separation processes that occur in orbit also frequently release small debris.

Slag and NaK debris

Many small orbital debris particles are created by solid rocket motor (SRM) firings, which produce aluminum oxide (Al_2O_3) particles called *slag*. These particles are formed during SRM tail-off, or termination of burn, by the rapid expansion, dissemination, and solidification of the molten Al_2O_3 slag accumulated during the burn. Since the transfer orbits are elliptical orbits, most of the particles reenter quickly because of the effects of atmospheric drag and other forces at the orbit perigee. However, the propensity of SRM to generate particles of 100 μm and larger has caused concern regarding their contribution to the debris environment. Particle sizes as large as 1 cm

have been witnessed in ground tests, and comparable sizes have been estimated via ground-based and in-situ observations of sub-orbital tail-off events. Due to the large number of particles ejected by each motor, these Al_2O_3 particles can represent a significant surface erosion and contamination threat to spacecraft. Studies are ongoing to better understand the Al_2O_3 environment because, due to their smaller sizes, they are difficult to track from ground-based sensors. As a matter of fact the solid rocket motor (SRM) exhausts are probably the main contributors to the debris population between 10 μm and 100 μm. Between 100 μm and 1 cm the SRM exhausts are again one of the main components of the population.

Another class of debris is the sodium-potassium (NaK) droplets that are released the Russian ocean surveillance satellites (RORSAT) launched between 1971 and 1988 by the Soviet Union. The nuclear reactors on board routinely released many drops of coolant into the orbital environment. The spherical NaK droplets released over a period of decades number in the thousands. Because the RORSAT objects are in circular orbits over 800 km, the lifetime of the NaK droplets will be measured in thousands of years. Attempts to quantify the NaK population have been ongoing, with observations now coming from the Haystack Radar telescopes (see sec. 2.3.2). About 70000 drops with diameter between 0.5 mm and about 5.5 cm have been estimated to orbit the observed region.

The figure 2.4 summarizes debris sources for the country of origin. This table is updated at the destruction of the Chinese Fengyun-1C spacecraft, so it's possible to notice the large fragmentation debris population produced by China (PRC). CIS represents the debris produced by Russia.

on-orbit	US	CIS	France	PRC	India	Japan	ESRO/ESA	Other	totals
payloads	1063	1324	44	61	33	103	36	387	3051
rocket bodies	542	837	97	37	8	35	6	27	1589
debris dispensed	0	0	0	0	0	0	0	0	0
mission related debris	781	507	92	62	1	36	12	5	1496
fragmentation debris	1666	1524	126	2315	97	2	18	35	5783
anomalous debris	142	82	3	0	0	0	0	0	227
totals	4194	4274	362	2475	139	176	72	454	12146

decayed or beyond Earth orbit	US	CIS	France	PRC	India	Japan	ESRO/ESA	Other	totals
payloads	800	1860	8	50	9	22	18	49	2816
rocket bodies	631	2367	55	68	8	53	5	7	3194
debris dispensed	0	1250	0	0	0	0	0	0	1250
mission related debris	783	4300	123	113	8	81	8	54	5470
fragmentation debris	2835	3272	474	179	249	22	4	4	7039
anomalous debris	74	5	2	0	0	2	0	0	83
totals	5123	13054	662	410	274	180	35	114	19852

								Grand Total ->	31998

Figure 2.4: Debris source vs. type accounting: types of objects both in-orbit and decayed, by country of origin (epoch date of 2 August 2007, from [41])

Breakups causes

It's now important to understand breakup debris causes, because they are the greatest debris portion in the space (see figure 2.1). The cause of debris-generating and fragmentation events is still unknown. Causes that are known include deliberate explosion (or collision), propulsion events, battery explosion events, unintentional collisions, and aerodynamic events.

- Deliberate. Deliberate actions, often associated with activities related to national security, were formerly the most frequently occurring class, but only four such events have happened since 1997, the latest being the Fengyun-1C deliberate collision.

- Propulsion. Propulsion-related events are the most frequent type of satellite fragmentation. Over half of all breakups with known causes are a result of a propulsion explosion (88 propulsion events as of February 2007). Causes of propulsion events include catastrophic malfunctions during orbital injection or maneuvers, subsequent explosions based on residual propellants, and failures of active attitude control systems. Breakups of rocket bodies due to propulsion failures are usually more prolific and produce longer-lived debris than the intentional destruction of payloads, often due to higher altitudes of the malfunctioning rocket bodies rather than the mechanics of the explosive event.

- Battery. Explosions of pressurized batteries present a non-trivial contribution to the debris environment. While only eight events have been confirmed as related to battery explosions, debris remaining from these eight events are the second largest contributor to the debris still on-orbit.

- Collisions. There have only been three accidental collisions of objects in space. All three involved a large intact body colliding with a much smaller piece of debris (see sec 2.4).

- Aerodynamic events. These events occur when an object is undergoing its final atmospheric demise, but puts off a small number of debris that are briefly trackable, before they demise as well.

The figure 2.5 shows causes of satellite breakups. The large percentage for deliberate actions is due the Fengyun-1C deliberate explosion.
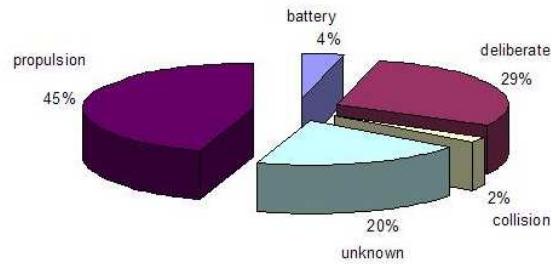
Figure 2.5: Causes of satellite breakups. Percentage by number of events (epoch date of 2 August 2007) from [41]

Future debris environment

Management of the future debris environment is critical to space operations for all nations of the world. Consequently, in the 1990s, international policies and procedures began to take form, such that all space-faring nations were making a concerted effort to maximize the ability to use space, while minimizing operations and procedures that might be destructive to the environment in the long term. As more countries gain the technology and economic means to launch spacecraft, more focus is being exerted on standardizing the procedures in each individual country, while adhering to the international agreements. Space activity is placing debris in orbit faster than the natural effects of drag can remove it. As a result, since 1980, the tracked population of orbital debris is increasing by about 160 objects per year, even though launch rates have remained relatively constant for the last couple of decades. This increase in objects per year only includes those having sizes of 10 cm or larger; the increase in the number of smaller pieces is most likely much larger. Since 1980, the population of intact spacecraft, rocket bodies, and mission-related debris is increasing by about 120 objects per year, demonstrating that despite launch rates that are relatively stable, the increase in number of objects is still dominated by intact objects. The major source of both large and small debris in LEO has been fragmentation of satellites and rocket bodies. This process has produced more large, trackable debris than has space operations, and very many more small untrackable debris. The launching of a payload into space from a booster or rocket upper stage generates orbital debris composed of spent rocket stages, clamps, shrouds, covers, and so forth, but does not produce many untrackable debris (sizes smaller than 10 cm) in LEO. As launch activity has stabilized, and a greater focus has been placed on engineering spacecraft and rocket body hardware to avoid fragmentation events, the fragmentation debris count has been relatively stable since about 1987. The debris count can be noticeably affected by the solar cycle, which lasts approximately 11 years. During periods of high solar activity, an object will see more drag from the atmosphere. Because in most cases, debris has lower ballistic coefficients (higher area-to-mass, A/M) than intact objects, debris tends to reenter the atmosphere more quickly.

Recent important events for the debris population growth in LEO

In the last years two very important e destructive events happen around the Earth in LEO improving the debris environment: the collision between two satellites in the 2009 (the Iridium 33 and the Cosmos 2251) and the explosion of the Chinese satellite FengYun-1C in the 2007.

The Iridium 33 and Cosmos 2251 collision was the first ever collision between two satellites, an operative one (Iridium, an American communication satellite) and a non-operational one (Cosmos, a Russian military satellite) [67]. They collided at 776 km altitude at a relative speed of 11.5 km/s; both were destroyed and a large amount of debris was generated in a zone around the 800 km altitude. This was the first major collision between two large spacecraft and produced two large clouds of debris. These large clouds of debris will cause an interaction, for many years to come, with the other Iridium satellites and with the other spacecraft in the region, posing a constant threat to the space environment.

The Fengyun-1C spacecraft was used as a target for the test of an anti-satellite (ASAT) system by the People's Republic of China on January 11, 2007. Impacted by a direct-ascent interceptor at a speed of approximately 9 km/s at an altitude near 850 km, the spacecraft disintegrated, spreading debris throughout LEO and beyond. This single recent event is responsible for more than 25% of all catalogued objects. By the end of the year, the US Space Surveillance Network (SSN) had officially cataloged 2317 debris, of which only 22 (less than 1%) had reentered the atmosphere. More than 2200 debris on the order of 10 cm or greater and 2400 fragments greater than 5 cm in diameter have been officially catalogued by the US Space Surveillance Network as of January 2009. The majority of these debris appear to reside in long-lived orbits. Data analysis by NASA's Orbital Debris Program personnel suggests that the total number of Fengyun-1C orbital debris one centimeter and larger was at least 150000. The SSN continues to identify new, large debris in low Earth orbit (LEO), while special observations by the Haystack radar provide insight into the much larger numbers of smaller, potentially hazardous orbital debris. The Fengyun-1C explosion unfortunately happened exactly in a critical region for the debris distribution in LEO and the related debris contribute significantly to the density peak in the region (see figures 2.6 and 2.7).
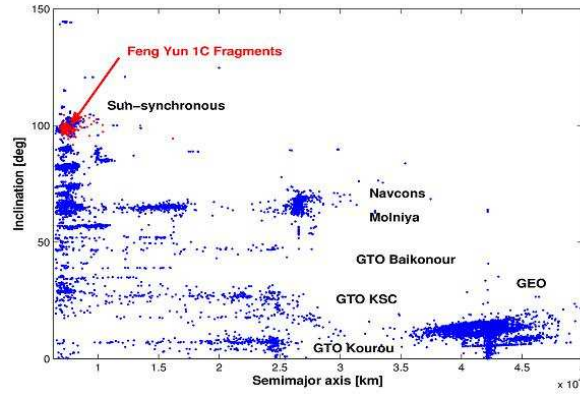
Figure 2.6: Distribution in the semimajor axis-inclination plane of objects included in the TLE Catalog. The fragments of the Fengyun-1C event are highlighted in red (from [7])
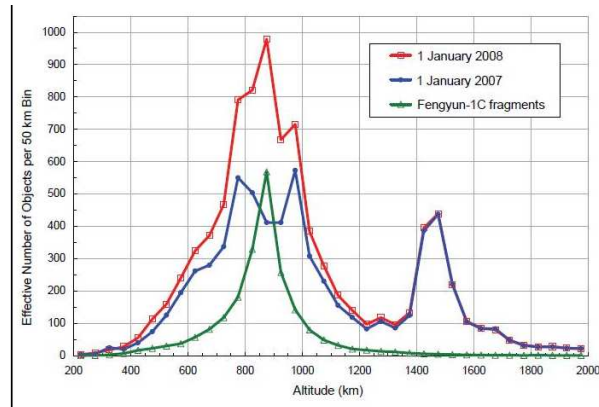
Figure 2.7: Distributions of the catalog populations in the low Earth orbit region in January 2007 (blue), January 2008 (red), and the officially cataloged Fengyun-1C fragments (from [42])

2.1.2   Distribution of debris around the Earth

All the un-classified spacecraft currently in orbit are catalogued by the United States Space Command in the Two-Line Element (TLE) catalogue [74] [75]. Two Line Elements is a format for distributing orbital elements data considering all objects orbiting around Earth (both operative satellites and debris) cataloged by NORAD (North American Aerospace Defense Command, a joint organization of Canada and US that provides aerospace warning and air sovereignty). In this catalogue about 12800 objects are listed along with their current orbital parameters (as of 1 January 2009). The limiting size of the objects included in the catalogue (due to limitations in sensors power and in observation and data processing procedures) is about 5 to 10 cm below a few thousands km of altitude (in LEO) and about 0.5 to 1 m in higher orbits (GEO). The orbits of the TLE catalogue objects are maintained thanks to the observations performed by the US Space

Surveillance Network (SSN). With 75.7%, the vast majority of catalogue objects reside in the LEO region. Another 8.7% of the catalogue objects are in or near the GEO ring. The remainder of the catalogue mainly belongs to the MEO region. It's important to remind that the region around Earth are defined in table 2.1.

Table 2.1: Space region around Earth (from [10])

Space region	Altitude (km)
LEO	from 120 to 2000
MEO	MEO-Low from 2000 to 15000
	MEO-High from 15000 to 33786
GEO	from 34000 to 38000

The population of objects smaller than several centimetres is statistically known thanks mainly to sporadic radar campaigns. Whereas the fragmentation debris were thought to be the only small particles present in space until about 10 years ago, the radar and in-situ measurements brought to light a series of new unexpected population of debris.

The figure 2.8 shows the density of objects for the 3 different size regimes as a function of altitude and highlight the three main zones of accumulation in space: the region of the Low Earth Orbits (LEO), the Medium Earth Orbits (MEO) and the Geostationary Orbits (GEO). It's possible to notice the great debris population in LEO.
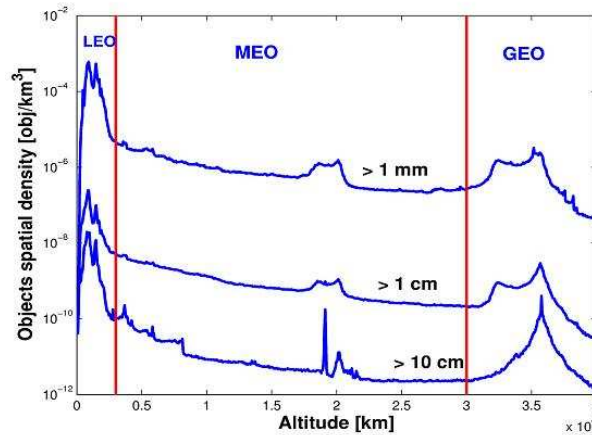
Figure 2.8: Density of objects as a function of altitude for three different size thresholds: objects with diameter larger than 1 mm, 1 cm and 10 cm (from [45])

Figures 2.9 and 2.10 show debris distribution as function of inclination for all space region around Earth for debris larger 10 cm and 1 cm. It's possible to notice all debris families: Sun-

synchronous orbits and GTO orbits (from the most important launch bases) in LEO, Molniya orbits and some navigation constellations orbits in MEO and the population in GEO.
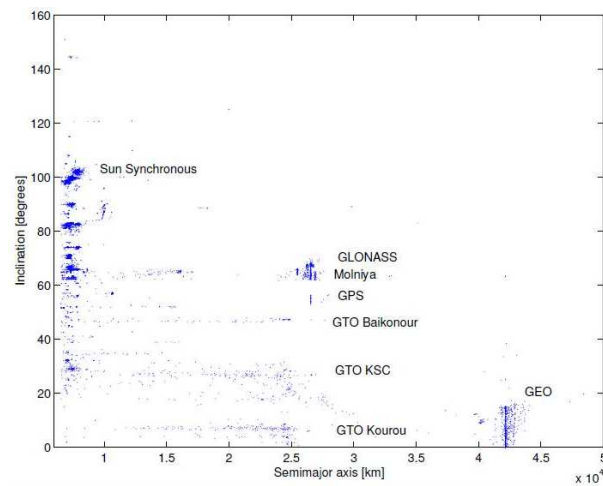
Figure 2.9: Distribution in the semimajor axis-inclination plane of the objects included in the TLE Catalog larger than 10 cm (from [45])
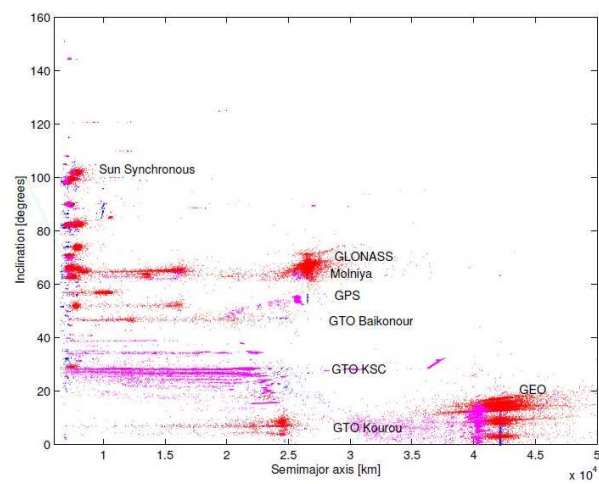
Figure 2.10: Distribution in the semimajor axis-inclination plane of the objects larger than 1 cm (from [45])

It's now presented the debris distribution in regions around Earth.

MEO region

The figure 2.11 shows a detail of the spatial density of objects in the MEO region, highlighting the main assets present in this zone: the navigation constellations.

Figure 2.11: Density of objects with diameter larger than 10 cm in MEO, as a function of altitude. The vertical lines mark the location f the GPS, GLONASS and GALILEO orbits (from [7])

The navigation constellations are the satellite systems providing autonomous positioning with global coverage of the globe. The US GPS satellites ($a = 26560\,km$ and $i = 55°$) and their Russian analogues GLONASS ($a = 25510\,km$ and $i = 64.8°$) are the two currently deployed navigation constellations. The Eur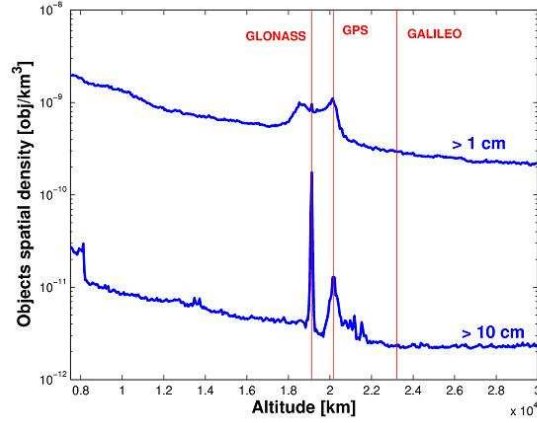opean GALILEO and the Chinese COMPASS systems are going to be launched in the next few years on similar circular MEO orbits.

The group of the Russian communication satellites in Molniya orbits ($a \simeq 26000 km$, $e \simeq 0.7$, $i \simeq 63°$) can be found in figure 2.9. The Russian territories are mostly at high latitudes, where the geostationary ring lies very low above (or even below) the horizon. Therefore, geosynchronous satellites are not well suited for communications in those regions and, since the Soviet era, the communication satellites were put on these high eccentricity orbits, having an inclination around $63°$, the so-called critical inclination. Along with the Russian telecommunication spacecraft in Molniya orbits, they are the most sensible objects orbiting the MEO region. Actually most of the objects in MEO are clustered about the Molniya orbits and have therefore a minimal interaction with the navigation constellations. But, even if we exclude the objects close to Molniya orbits, about 16000 objects with diameter larger than 1 cm have orbits potentially crossing the navigation constellations. In particular, the GPS orbit appears within reach of several thousand objects, due to the nonzero eccentricity of most of the debris in the MEO zone.

From figures 2.9 and 2.10 three horizontal stripes of dots can be also seen spanning from LEO to about 26000 km. The clusters at $a = 25000\,km$ refer to the objects in Geostationary Transfer Orbits (GTO). These are mostly upper stages launched from Kourou (ESA Ariane rockets, $i \simeq 7°$), from the Kennedy Space Centre ($i \simeq 27°$) and from Baikonour ($i \simeq 48°$). The inclination of a GTO is determined by the latitude of the launch site and the launch azimuth. The upper stages of the rockets used to bring the satellites to GEO are usually left stranded in GTO. If the

perigee of the GTO is low enough for the air drag to be effective, the rocket can reenter into the atmosphere in a few years, but some higher apogee (with a perigee altitude > 600 km) upper stages can spend decades in orbit, contributing to the space debris pollution in LEO and MEO. With growing distance from the center of the Earth, different perturbations become important. While the main effects are still due to the term, J2, the gravitational perturbations due to the differential attraction of Sun and the Moon, become comparable. The lunisolar attraction induce long-term and sometimes secular variation in the eccentricity, inclination, argument of the node and of perigee. As a matter of fact, lunisolar perturbation, coupled with air drag, may play a role in speeding the orbital decay of certain classes of highly eccentric orbits, by lowering the perigee height. On the other hand air drag is of course negligible for circular MEO, due to the absence of any residual atmosphere. Another non-gravitational perturbation starts to play a role: the solar radiation pressure. The solar radiation pressure is due to the absorption and reflection of photons by the surface of the body and depends again on the area to mass ratio of the spacecraft. For objects with area to mass ratios in the range 0.01 to 0.1, typical of orbiting spacecraft, its effect is mainly a long periodic.

About 2% of the US SSN catalogue population is related to MEO. Observations for this region are often achieved with telescopes. The lower density of objects makes the collision probability in MEO about two orders of magnitude lower than in LEO. Recent studies, based on the current limited knowledge of the MEO environment, evaluate the collision risk in MEO at the level of about 1 collision between objects larger than 10 cm in the next 200 years (close to the diameter of the objects capable of producing a catastrophic fragmentation of a satellite in MEO), in a worst case scenario.

GEO region

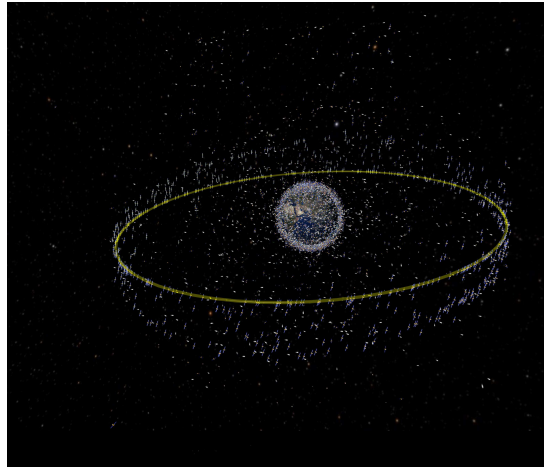The figure 2.12 shows the debris distribution in the GEO region.

Figure 2.12: Debris distribution in the GEO region (the yellow circle represents the GEO ring) (from [65])

In figure 2.9 it's possible to note the geosynchronous satellites. A geosynchronous orbit is an orbit around the Earth with the orbital period matching the Earth's sidereal rotation period. Most of the telecommunication and weather satellites are placed in this peculiar orbit, since an object there will appear motionless from the ground station easing antenna pointing and control. Notwithstanding its paramount importance, the population of spacecraft and debris in the GEO region is still quite uncertain, mainly due to the physical distance which prevents its mapping by radars. Dedicated optical observation campaigns are performed to characterize the environment in this orbital region. About 1040 objects have been detected near GEO. Only 340 are active satellites, while the rest are debris, mostly uncatalogued objects. The source of this objects remains still uncertain since only two explosions have been recorded in GEO and these two events cannot account for all the observed debris. Probably ten more unrecorded fragmentation events must have happened in GEO. Of course the number of non-trackable objects, smaller than the telescope detection threshold, should be much larger than 1000. A large uncertainty remains in the geostationary region and international efforts are under way to improve our knowledge in this area.

The peculiarities of the GEO region are mainly the absence of any natural decay mechanism, such as air drag. For this reason the useful space in the GEO region is actually operationally limited since an orbital slot not freed by a 'dead' satellite (or a debris) is not any more usable by other spacecraft. Moreover any debris created in the region will stay there almost for ever. Note that, during their operative lifetime, the satellites are periodically maneuvered to keep them inside the slot, counteracting the perturbations that would tend to change their orbital parameters.

Taking also into account the typical large dimensions of the solar panels and antennas of the geostationary satellites, in the GEO region the solar radiation pressure becomes relatively more important. Large area to mass ratios are also quite common between GEO spacecraft, leading to even higher accelerations. The main effect of the solar radiation pressure is to induce long periodic (i.e. approximately yearly) variations in eccentricity. More complex effects, leading to

long term perturbations on the semimajor axis, inclination and node, can be caused by the effect of the radiation pressure on the spacecraft antenna. In recent years a peculiar population of objects having an high eccentricity (as high as 0.55) was detected by the ESA telescope in Tenerife [47] [48]. It was shown that these are objects with very high area to mass ratio whose dynamics is therefore strongly perturbed by the solar radiation pressure that significantly affects their eccentricity with small effects on the total energy of the orbit and, therefore, on the semi-major axis or mean motion. Most probably these objects are remnants of thermal blankets or multi-layer insulation (MLI) either detached from aging spacecraft or ejected by explosive fragmentations of old spacecraft. So far, however, only two fragmentations have been confirmed in the geostationary region and the identification of further explosions is complicated by the long time that has elapsed since the events. Orbital characteristics indicate that they could also be pieces of thermal blankets of satellites. Approximately 50% of the newly discovered objects, in recent GEO observations, are high area to mass ratio objects.

2.2 The space debris population in LEO

It's now presented the space debris population in LEO, a vital region around Earth with a lot of operative and non-operative satellites and so with a lot of space debris. LEO region is limited under 2000 km of altitude. The figure 2.13 represents the debris density in this region.
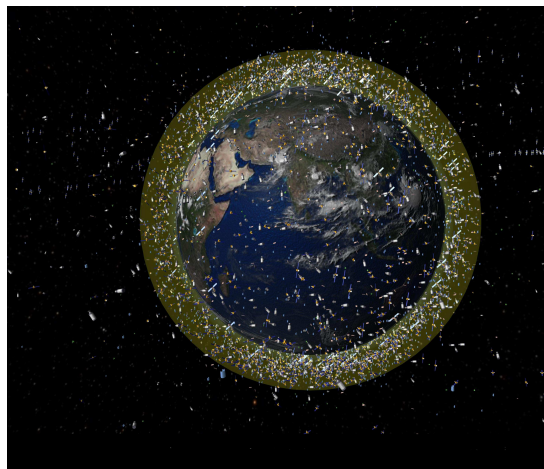
Figure 2.13: Debris distribution in the LEO region (from [65])

LEO is by far the most crowded zone in the circumterrestrial space. As can be seen also from figure 2.6, the Fengyun-1C and a lot of spacecraft explosions or collisions unfortunately happened exactly in this critical region and related debris contribute significantly to the density peak in the LEO region. The major density of explosion or collision observations in this region respect other regions (GEO or MEO) is due to the greater density of debris population and operative satellites in LEO and to the fact that debris observations in LEO (mainly with radar but also with telescope) are easier than other regions because objects are at low altitudes. For this reason first debris observations were performed in LEO in order to understand risks for a lot of satellites that

populate this important region. LEO satellites are in many different orbital planes providing global coverage, in particular in polar orbits. In LEO collisions occur at very high relative velocities, typically several km/s. In this region a collision creates debris that crosses other orbits increasing the debris population.

Some analysis about debris population in LEO have been achieved in order to understand the debris distribution in this region. Analysis have been produced using a particular *MASTER 2005* population file, integrated with the recent in-orbit collisions (Fengyun-1C, Iridium-Cosmos). The *MASTER 2005* file contains the larger objects taken from the TLE plus the smaller objects generated with ad-hoc source models (see sec. 2.6). In this particular population file all objects are considered (not only non-operational objects, but also operative satellites) with diameter d, $3\,cm < d < 31.73\,m$. All objects in the file are crossing the LEO with the perigee altitude, h_p, included between about 200 km and 2000 km. Among these objects 21481 are single objects and 10201 are sampled objects, i.e. an object in the file accounts for several 'real' objects. So the total number of objects represented in the files, once de-sampled, are 73594. In order to understand the debris LEO population, a few subsets has been produced with different size and perigee limits. The number of objects included in these sub-samples are listed below (table 2.2 considers the number of objects in the file, 31682).

Table 2.2: Characteristics of the population model from the particular *MASTER 2005* file

	d>3 cm	**d>5 cm**	**d>10 cm**
h_p>**800 km**	16061 objects	11347 objects	7471 objects
h_p>**1000 km**	8260 objects	6334 objects	3923 objects
h_p>**1300 km**	6005 objects	4616 objects	2800 objects

Figures 2.14 and 2.15 represent the debris distribution of objects larger than 3 cm in LEO from the particular *MASTER 2005* population file.
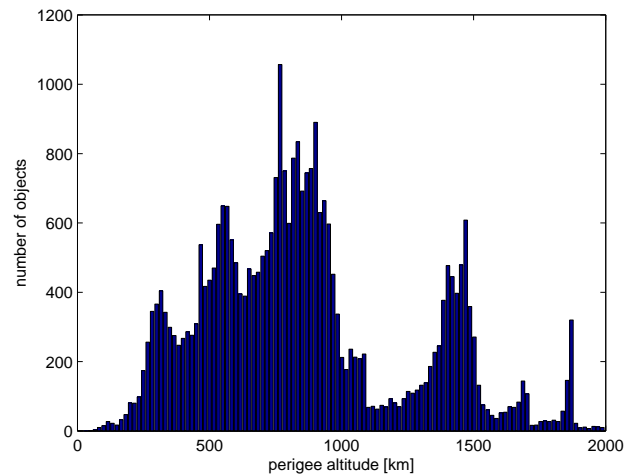
Figure 2.14: Perigee altitude distribution of the population in LEO
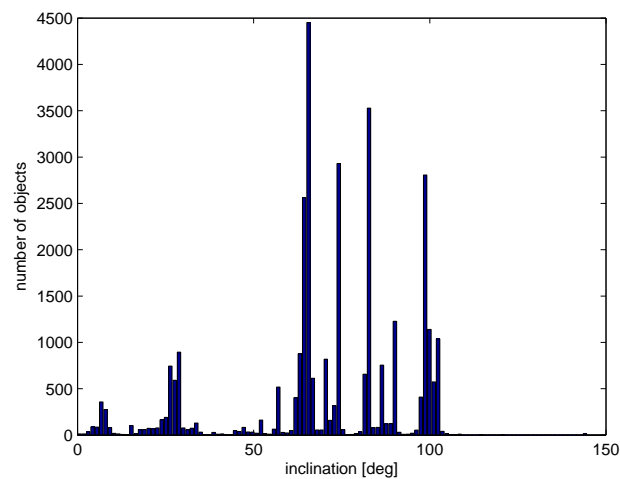
Figure 2.15: Inclination distribution of the population in LEO

In LEO there is a debris distribution over all orbits inclination and orbits altitude. Figure 2.9 and figure 2.10 clearly highlight some features in the distribution of objects with the spacecraft (and the resulting debris) being clearly grouped in 'families' according to their different purpose and to the different launching bases. It's possible to distinguish the satellites in Sun-synchronous orbits ($i \simeq 100°$), the satellites in polar orbits ($i \simeq 90°$), some families of Russian COSMOS satellites between $i \simeq 60°$ and $i \simeq 80°$, the LEO satellites launched from the Kennedy Space Center (at $i \simeq 27°$) or from others space centers.

Figure 2.14 shows some peaks of LEO catalogue objects concentration at altitudes from 800 km to 1000 km and again around 1400 km. The non-uniform density, with the highest peaks between 800 and 1000 km, is due to a large number of satellites, upper stages and fragmentation debris related to civil and military missions for Earth observation, surveillance and telecommunication.

The rapid decline of objects density below about 500 km of altitude is due to the air drag: it subtracts energy from an orbiting object causing its decay into the atmosphere. The atmospheric drag is the most important perturbation in LEO with the J2 gravitational effect. On the other hand, the atmosphere density is decreasing exponentially with the altitude, so that J2 perturbation is efficient only up to about 800 km above the Earth surface.

This density peak around 900 km is also due to the presence, in this altitude band, of a large number of sodium-potassium (NaK) liquid metal droplets (see sec. 2.1.1). The source of NaK particles from RORSAT should only exist at one inclination (65°).

Figure 2.16 shows the debris distribution in LEO in some planes considering eccentricity, semimajor axis, inclination and orbital period.

(a) `ecc-a`

(b) `incl-ecc`

(c) `incl-a`

(d) `incl-a(particular)`

(e) `period(particular)`
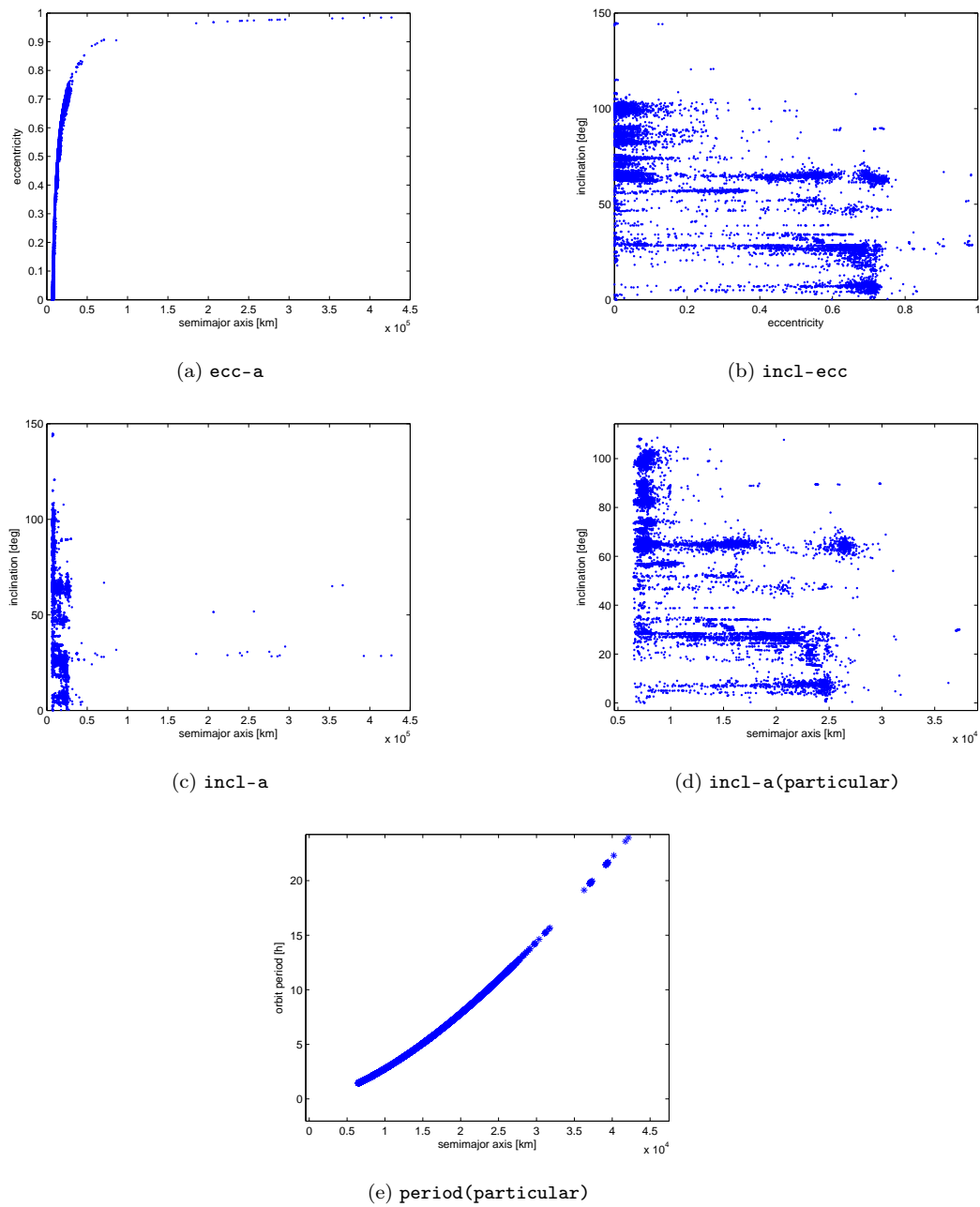
Figure 2.16: Orbital characteristics distribution in some planes of LEO debris population

Figures 2.17 and 2.18 show the debris mass and diameter distribution in LEO. It is possible to conclude that the most of debris have a little diameter (under 1-2 m) and a little mass (few grams).

(a) all

(b) particular
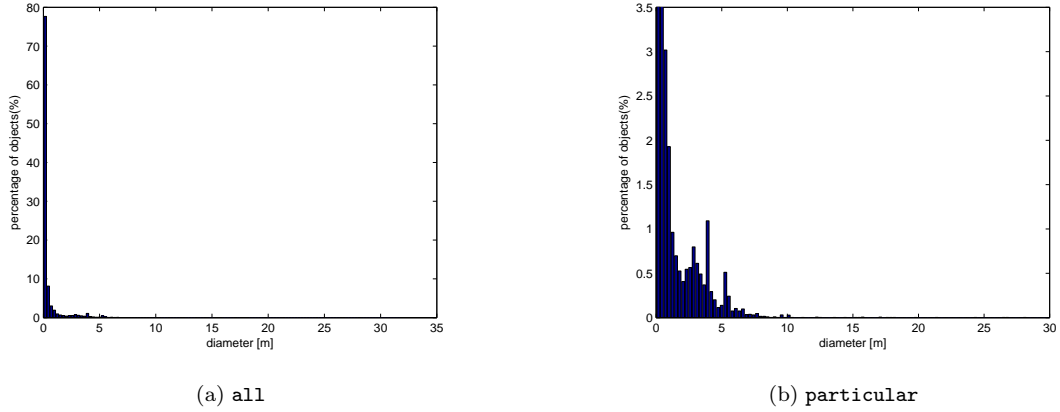
Figure 2.17: Diameter distribution for LEO objects

(a) all

(b) particular
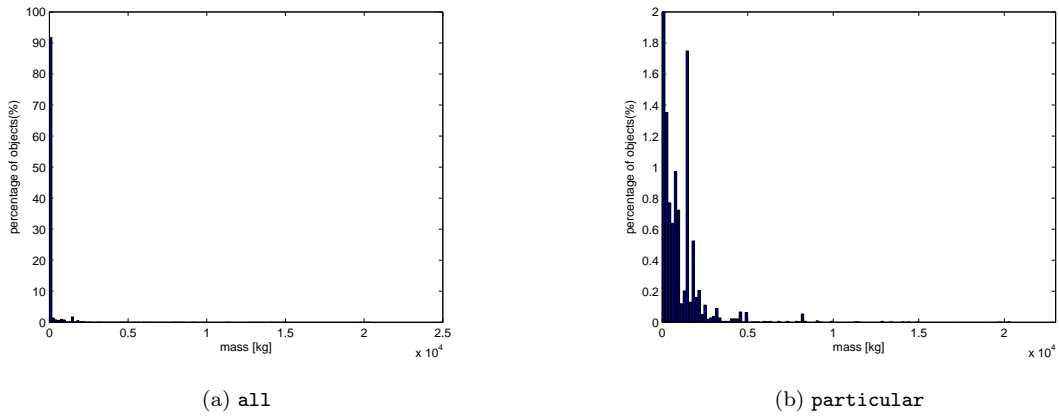
Figure 2.18: Mass distribution for LEO objects

In LEO debris population there are also transient debris with a perigee altitude under 2000 km but with an apogee altitude over 2000 km. This objects are called TLEO debris (Transient LEO) and a particular type of TLEO debris with the greatest eccentricity and the greatest apogee radius are objects in GTO (Geostationary Transfer Orbit) and in Molniya orbit. Objects in LEO are divided into 4 classes:

- resident LEO debris with apogee altitude $< 2000 km$

- transient LEO (TLEO) debris with apogee altitude $> 2200 km$

- GTO debris with semimajor axis $26600\,km > a > 24100\,km$ and eccentricity $0.74 > e > 0.59$

- Molniya debris with semimajor axis $27000\,km > a > 26000\,km$ and eccentricity $0.74 > e > 0.69$ and inclination around 63 deg

The figure 2.19 represents all debris population considering resident LEO debris and TLEO (GTO and Molniya) debris.

(a) `apogee-ecc(particular)`

(b) `ecc-perigee`

(c) `incl-ecc`

(d) `inlc-perigee`

(e) `incl-a(particular)`

(f) `mass-perigee(particular)`
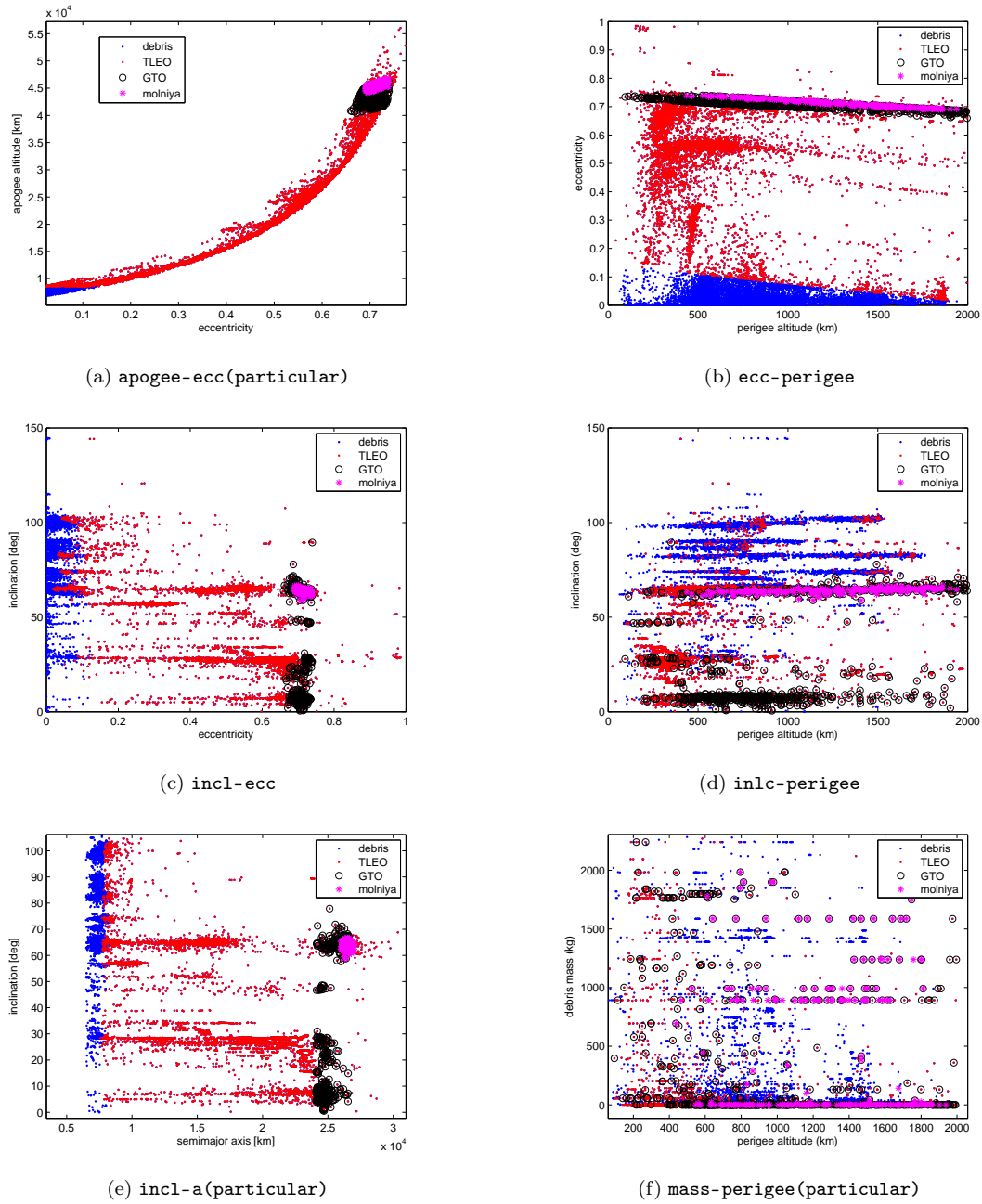
Figure 2.19: Characteristics distribution in some planes of LEO debris population (blue dots are resident LEO debris, red dots are TLEO debris, black circles are GTO debris and in magenta the Molniya debris)

It is possible to conclude that the most of TLEO debris are at low altitude (under 700 km) and GTO and debris with an high eccentricity are distributed in some precise inclination regions

because they are mostly upper stages launched from Kourou (ESA Ariane rockets, $i \simeq 7°$), from Baikonour ($i \simeq 48°$) and from the Kennedy Space Centre ($i \simeq 27°$). The GTO debris concentration around 62°-66° is probably due to the launch activities from the Russian Plesetsk Cosmodrome (62.55° of latitude), kept secret until 1983 [76]. It has been supposed that more than 1500 launches to space had been made from this site, more than for any other launch facility . Around inclination 63° it's possible to observe the great concentration of Molniya debris launched from this Russian site.

The figure 2.20 shows the population used for analysis in sec. 4.3 (debris diameter between 5 cm to 30 cm). Most Molniya debris are above 1000 km, while most GTO debris are under 1000 km. From above debris orbit definitions it's difficult to distinguish in this figure GTO debris from Molniya debris.
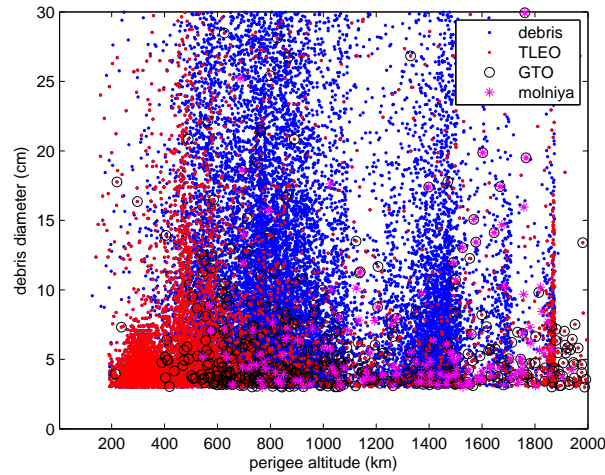
Figure 2.20: Analysed debris population distribution considering debris perigee altitude and diameter (blue dots are resident LEO debris, red dots are TLEO debris, black circles are GTO debris and in magenta the Molniya debris)

2.3 Measurements of the orbital debris environment

In this section debris measurements achieved to understand the debris environment are explained. Radar, optical and in situ measurements are described, considering negative and positive aspects. Measurements are fundamental for space debris surveillance systems, in particular the SSN and the SSA here described.

2.3.1 Introduction: The US Space Surveillance Network Catalog (SSN) and the ESA Space Situational Awareness program (SSA)

Space surveillance is the detection, correlation and orbit determination of all objects in space. At present, only the US and Russia have this operational capability with a routinely updated space

object catalogue, while ESA is working to create an autonomous similar system. Space object catalogues, as generated and maintained by space surveillance networks, are limited to larger objects, typically greater than 5-10 cm in low Earth orbits and greater than 1 m at geostationary altitudes. These sensitivity thresholds are a compromise between system cost and performance. Knowledge of the space debris environment at sub-catalogue sizes is normally acquired in a statistical manner through experimental sensors with higher sensitivities.

US *SSN* system

The United States Space Command SSN is composed of ground and space-based sensor systems whose charter is to track human-made resident space objects. These data are compiled daily into Keplerian element sets and distributed to the user community via NASA Goddard Space Flight Center's Orbital Information Group. All the un-classified spacecraft currently in orbit are cataloged by the United States Space Command in the Two Line Element (TLE) catalog (see sec. 2.1.2). The limiting size of the objects included in the catalog (due to limitations in sensors power and in observation and data processing procedures) is about 3 to 10 cm below a few thousands km of altitude and about 0.5 - 1 m in higher orbits (up to the geostationary ones).

The figure 2.21 shows the SSN network with ground sensors.

Figure 2.21: Configuration of the SSN in 2009 (from [27])
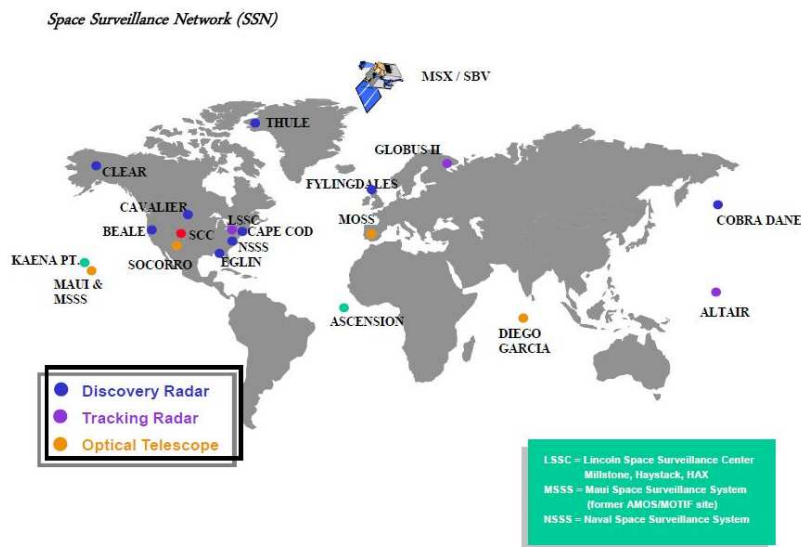
Although the origin of the SSN predates the launch of the world's first artificial satellite on 4 October 1957, the dramatic appearance of Sputnik 1 profoundly altered the course of satellite tracking in the US. For this reason the Smithsonian Astrophysical Observatory (SAO) was assigned the responsibility of designing and deploying a worldwide, satellite-tracking network. The first of

the famous Baker-Nunn cameras was completed on 2 October 1957, just two days before the Space Age was inaugurated. An equally important milestone was achieved on 5 October 1957 when the Millstone Hill radar, a product of the Massachusetts Institute of Technology's Lincoln Laboratory (MIT/LL), became operational.

Space surveillance involves detecting, tracking, cataloging, and identifying man-made objects orbiting the Earth; e.g., active and inactive spacecraft, spent rocket bodies, mission-related debris, and fragments. SSN (and in general all space surveillance systems) have to make the following actions:

- Detects new man-made objects in space;

- Produces a running catalog of man-made space objects;

- Determines which country is responsible for an orbiting or reentering space object;

- Charts the present position of space objects and plots their anticipated trajectories;

- Predicts when and where a space object will reenter the Earth's atmosphere.

A wide variety of radar, optical, and electro-optical sensors have been a part of the SSN since 1961. Now the United States Space Command SSN is composed of 25 sensors, both radars and optical sensors. Below a brief description of the most important sensor type.

- Phased-array radars can maintain tracks on multiple satellites or debris simultaneously and scan large areas of space in a fraction of a second. These radars have no moving mechanical parts to limit the speed of the radar

- Conventional radars use moveable tracking antennas or fixed detection and tracking antennas. A detection antenna transmits radar energy into space in the shape of a large fan. When a satellite or debris intersects the fan, energy is reflected back to the detection antenna, where the location of the satellite is computed. A tracking antenna steers a narrow beam of energy toward a satellite and uses the returned energy to compute the location of the satellite and to follow the satellite's motion to collect more data

- Electro-optical sensors consist of telescopes linked to video cameras and computers. The video cameras feed their space pictures into a nearby computer that drives a display scope. The image is transposed into electrical impulses and stored on magnetic media. Thus, the image can be recorded and analyzed in real-time or later

- The Midcourse Space Experiment (MSX) satellite is an Earth-orbiting satellite with a payload containing a variety of sensors, from ultra-violet to very-long-wave infrared. It has contributed significantly to the tracking of geosynchronous objects and is serving as a pathfinder for a future space-based space surveillance system

In general, electro-optical sensors are used to track objects at high altitudes (above 2000-4000 km), and radar sensors are used for lower altitude objects. By 2007, the SSN had cataloged more than 30000 space objects in orbit about the Earth. The SSN currently tracks and monitors nearly

10000 cataloged satellites, of which about 800 represent operational spacecraft. More than 19000 cataloged objects have already reentered Earth's turbulent atmosphere and they are no longer in orbit. Cataloged objects now orbiting the Earth range from debris with masses of less than 1 kg to the ISS with a mass of 186000 kg. If a new object is discovered by the SSN (e.g., insulation material that has separated from a spacecraft), the observations of that object are collected and correlated, a two-line element set is developed.

ESA *SSA* system

The Space Situational Awareness (SSA) is a initiative of ESA created in 2008 [69]. SSA is defined as a comprehensive knowledge, understanding and maintained awareness of:

- the population of space objects

- the space environment

- the existing threats and risks

The overall aim of the SSA is to support the European independent utilization of and access to space for research or services, through providing timely and quality data, information, services regarding the environment, the threats and the sustainable exploitation of the outer space surrounding our planet Earth. While some European radar and optical facilities exist for tracking and imaging space objects, Europe has no systematic, operational capability for space surveillance, and is therefore strongly dependent on external information, mainly from the US.

The objective of the SSA programme is to support Europe's independent utilisation of, and access to, space through the provision of timely and accurate information, data and services regarding the space environment, and particularly regarding hazards to infrastructure in orbit and on the ground. In general, these hazards stem from possible collisions between objects in orbit, harmful space weather and potential strikes by natural objects that cross Earth's orbit.

The SSA programme will, ultimately, enable Europe to autonomously detect, predict and assess the risk to life and property due to remnant man-made space objects, re-entries, in-orbit explosions and release events, in-orbit collisions, disruption of missions and satellite-based service capabilities, potential impacts of Near Earth Objects, and the effects of space weather phenomena on space and ground-based infrastructure. Space-based systems have become indispensable to many services critical to Europe's economies and governmental functions, including those related to security.

The SSA programme is active in three main areas:

- Space Surveillance and Tracking of objects in Earth orbit (SST): comprising active and inactive satellites, discarded launch stages and fragmentation debris that orbit the Earth

- Monitoring Space Weather (SWE): comprising particles and radiation coming from the Sun that can affect communications, navigation systems and other networks in space and on the ground

- Watching for Near-Earth Objects (NEO): comprising natural objects that can potentially impact Earth and cause damage and assessing their impact risk and potential mitigation measures

The first aspect, the survey and tracking of space debris in the SSA program, is the context of this thesis. The central aim of SST is to provide an independent ability to acquire prompt and precise information regarding objects orbiting the Earth. Using this data, a wide range of services will be provided, such as warning of potential collisions between these objects or alerting when and where debris re-enters the Earth's atmosphere. This data will be stored in a catalogue, made available to SSA customers across Europe.

SST can be summarized as follows:

- full coverage of LEO (Low-Earth orbit (below 2000 km altitude)), GEO (Geostationary Earth orbit) and near-circular MEO (Medium Earth orbit) orbits;

- autonomous build-up and maintenance of a catalogue of all observable space objects;

- detection, tracking, orbit determination, target correlation, and physical characterisation for objects in LEO, MEO and GEO with a reliability and sensitivity matching the one of the US Space Surveillance Network (SSN);

- estimation of orbit manoeuvres;

- detection of on-orbit break-up events and correlation with the source object

The SSA-SST Space Surveillance Test and Validation Center (SSTC) is located at ESA/ESAC, Spain. Some main elements are required to ensure that the SST segment can meet critical customer requirements and provide reliable operational services:

- A data catalogue. The core of the SST Segment is the catalogue; this contains information on everything that has been detected in orbit. In order to produce this catalogue, it is necessary to: reconstruct an orbit from the data that is produced by the sensors (orbit determination); check to see if this object has already been seen and is already in the catalogue (correlation); and monitor the data in the catalogue so that sensors can be tasked to update the information when needed.

- A network of sensors to accurately detect objects orbiting the Earth. These sensors are usually either optical or radar systems. They are divided into two groups: surveillance or tracking.

  a Surveillance sensors perform the routine task of ensuring that data in the tracking catalogue is accurate and up-to-date. They typically 'stare' across an area of the sky and register objects passing through their field of view. They can observe multiple objects simultaneously and continually add to the quality of the data in the catalogue.

  b Tracking sensors are used when very high-precision data are needed about a specific object. This happens, for example, if it is predicted that this object will collide with an operational satellite.

Activities in the initial SSA Preparatory Programme (2009-11) are concentrating on the consolidation of requirements and on the architectural study and design of the complete SSA system. The budgetary estimate (based on 2008 economic conditions) for 2009-2011 is 55 MEuro.

Several surveillance concepts for LEO and GEO regions have been studied by SSA in order to obtain a preliminary overview.

A survey of existing sensors, in combination with findings from several ESA studies, has led to the following core recommendations for SSA radar design to cover the LEO region. For the location of the bistatic LEO radar, two sites in Spain are considered: Pico Villuercas in Extremadura for the transmission and the Arenosillo military base in Andalucia for the reception. Spain constitutes a near-optimal deployment location due to sufficiently frequent sensor passes with acceptable observation gap times.

As baseline, for LEO space surveillance, a ground based radar system is under consideration. The radar system will be able to survey all objects above a certain size and up to a specified altitude. The ground based radar system for LEO space surveillance forms a part of an entire surveillance strategy including also detection of objects in other orbits (MEO and GEO) traditionally done with optical telescopes. An alternative approach to deal with LEO space surveillance consists on ground based optical sensor only. SSA for the debris surveillance in LEO regime wants to verify if the LEO space (200-2000 km) can be fully or partially covered by an optical ground based system. Presently the LEO radar is intended to cover the full 200-2000 km LEO region. The upper part of the LEO region might also be surveyed by ground based telescopes, which would significantly reduce the performance requirements for the radar system and could reduce the overall system costs. The goal of the study is to analyse and define a LEO survey telescope system and to show the resulting costs in dependence of the covered part of the LEO region. After several studies for LEO space surveillance, a ground based radar system is considered as baseline by ESA, but a mixed solution with this alternative approach, consisting of a ground based optical sensor observation system, actually limited to MEO, HEO and GEO regions (and to the Near Earth Objects), could have a better performances/costs ratio for what concerns the higher part of the LEO.

For debris observations in GEO region, a first network of sensors could consist of three sites for instance: Tenerife (Spain), Perth (AUS) and the Marquesas Islands (France). Each site would be equipped with a detection and tasking telescope, and with a survey telescope. The total cost of the GEO surveillance system is expected to be 16.2 million EURO, distributed over five years.

2.3.2 Radar observations

The most important debris radar in the world are the US Haystack, Haystack Auxiliary, Goldstone, Cobra Dane and the ESA FGAN/TIRA and EISCAT and they all operate in a staring mode, where the antenna is pointed at a fixed azimuth and elevation while objects pass through the field-of view. This operation mode have proven to be very useful for statistical measurements of the space debris environment. The debris radars situation is now presented for these radars with their positive aspects and their limits. It is important to know that US was the first nation to build radars for debris monitoring and so US has developed during the last years an important

knowledge about debris radar observations. Radars have a limit in observation altitude (they can not observe above a certain altitude), consistent with the $1/range^4$ power law inherent in the radar range equation. That range is the dominant factor in probability of debris detection calculations, although it is not the only factor. Radar stations observe only LEO debris and they are often located at high latitude stations to observe high inclination debris in LEO. During post processing of radar debris observations, the radar cross section (RCS) is determined by the signal strength and the range to the object.

Haystack radar

In the late 1980s, NASA needed a better characterization of the orbital debris environment to sizes as small as 1 cm diameter in order to verify the design of the International Space Station (ISS). For this purpose, NASA began using the Haystack radar in Massachusetts to fill this need [72]. Haystack was primarily used by the USAF for range-Doppler imaging of orbiting satellites. The Haystack radar is a high-power, X-band (3 cm wavelength), monopulse radar with very high sensitivity with a peak power of 400 KW, a frequency of 10 GHz, a beamwidth of 0.05 deg and a diameter antenna of 36 m. To detect debris a pulsed, single frequency waveform is used. NASA began collecting statistical data (detection, but no cataloging) on the orbital debris environment using Haystack in August 1990. Since that time it has been the primary source of knowledge of the debris environment in the critical size range from 1-20 cm. The Haystack radar has accumulated the most debris collection. Observations from this radar want to know the distribution of particles larger than 1 cm at altitudes between 350 km and 2000 km trapped in orbit at inclinations above 28°. At the lowest altitudes (300-500 km) debris as small as 2-3 mm diameter are detected while at the highest altitudes (1700-1900 km) the smallest detection is in the 6-7 mm range. Haystack's availability, along with its very high sensitivity, makes it the primary source of data for characterizing the small debris environment.

The Haystack observations were instrumental also to point out the importance of another unexpected source of space debris, the aluminum oxide (Al_2O_3) particles coming from the burns of the rocket motors with solid propellant and the NaK droplets that are released the Russian ocean surveillance satellites (RORSAT) (see sec. 2.1.1).

HAX radar

After some years it was built HAX (Haystack Auxiliary), which would have less sensitivity than Haystack, but higher imaging resolution and would be available full time. HAX is located in Massachusetts and operates at 16.7 GHz. In return, the NASA would provide debris data from Haystack and HAX. Haystack began successfully collecting statistical orbital debris data in October 1990 and has been NASA's primary source of statistical data on the 1 cm size debris population since that time. HAX collected debris data for the first time in March 1994. Both Haystack and HAX are monostatic radars that measure the range, radial velocity, the principal polarization RCS, the orthogonal polarization RCS, and the position within the radar beam using a monopulse system. The HAX radar has less sensitivity than Haystack, but has a larger beamwidth. Both radars are capable of full-sky pointing. Haystack and HAX observe debris from 350 km to

1800 km. In 1995, the large population of debris between 850 km to 1000 km altitude in an inclination band centered near 65° inclination was identified as small spherical droplets of eutectic NaK coolant with these radars (see sec. 2.1.1).

Goldstone

The Goldstone has an 70 m antenna located in California; when operated as a bi-static radar, Goldstone is capable of detecting 2 mm debris at altitudes below 1000 km. The Goldstone radar played a key role in identifying the NaK debris from the RORSAT (see sec. 2.1.1). The Goldstone radar can measure the range, radial velocity, and principal polarization RCS of debris. Currently, the Goldstone radar can only point toward the zenith for debris observations. For debris observations the antenna is pointed at a specified elevation and azimuth and remains there while debris objects randomly pass through the field of view of the radar beam. The Goldstone radar generally observes objects at altitudes from 300 km to 3200 km with near-zenith pointing.

The unknown debris population, at around 2900 km of altitude, consisting of the so called West Ford Needles has been detected by the powerful Goldstone radar. According to the Goldstone observations, a population of about 40000 such clusters is orbiting between 2400 and 3100 km of altitude.

Cobra Dane

In addition to Haystack and HAX, the US has utilized the Cobra Dane radar in Alaska for some of debris observation campaigns. It is another type of radar dedicated to debris monitoring: the phased array radar, capable of tracking several objects simultaneously. It operates differently from Haystack in that it's electronically steered without physically moving the radar antenna. This means that the antenna beam can be instantaneously moved within some angular limits. What is typically done with phased array radars is to rapidly move the beam in a long, narrow pattern to create a virtual fan beam or fence. These latter radars can track objects from just above the horizon to just short of the zenith over an azimuth of 120 degrees. They can track space objects in excess of 40000 km in range and represent the largest source of information for the catalog, especially in Low and Medium Earth Orbit. Cobra Dane, for example, raised the number of objects in the catalog by about 10% pushing the network to its limits in terms of processing and archiving power, to the point that, at present, the principal limitation to the cataloging capabilities seems to be exactly the processed structure and not the sensors power. Cobra Dane is an L-band (23 cm wavelength) radar and generates 30 MW of peak of radio frequency power.

In figures 2.22 the altitude (or range) debris versus size estimated debris for radar detections used by NASA is shown. Phased array radars have a more complicated detection scheme than that is used at Haystack, but unlike the corresponding Haystack plot, no $1/range^4$ detection limit is apparent because debris observations are from 500 km to 2400 km in range. The lower limit of detection for Cobra Dane is about 4 cm diameter, while for other radars is about 2 mm.
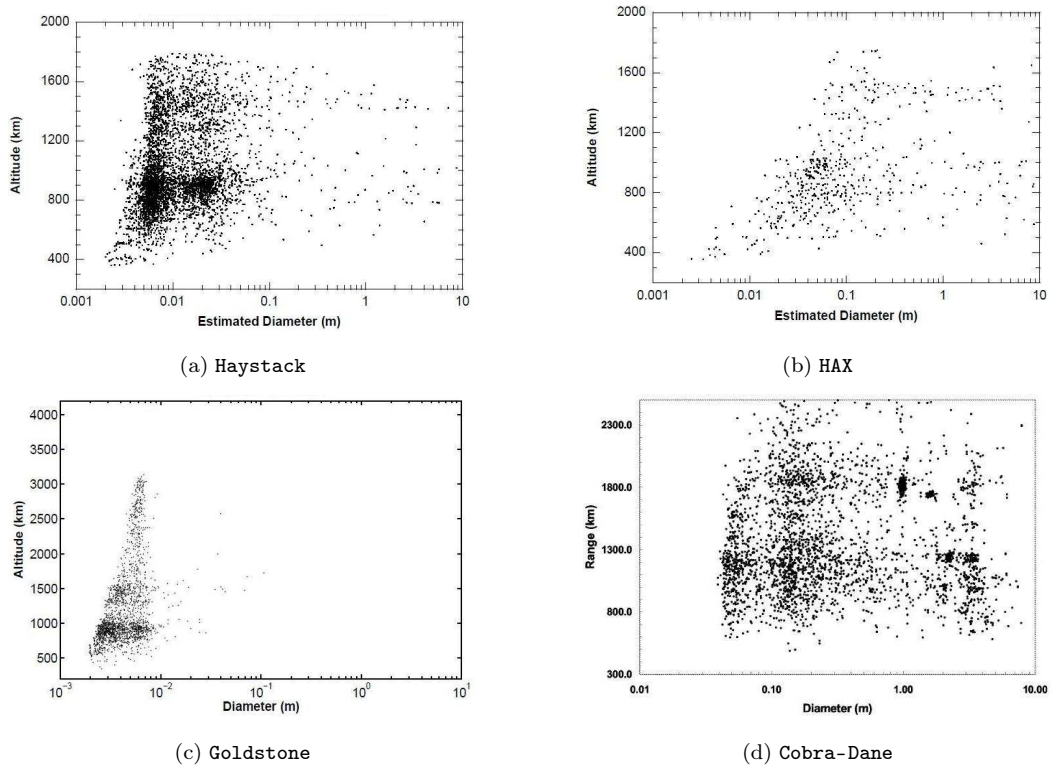
(a) Haystack

(b) HAX

(c) Goldstone

(d) Cobra-Dane

Figure 2.22: Altitude (or range) vs. size estimated for radar detections used by NASA (from [54] [41])

Figure 2.23 shows the four US radars.

(a) `Haystack-HAX`

(b) `Cobra-Dane`

(c) `Goldstone`

Figure 2.23: Radars used by US for debris detection

European radars

Some European radars dedicated to space debris surveillance are now shown. Most of these are used by ESA for SSA. The future SSA radar must be capable of surveying objects down to 5 cm size in all orbits around Earth. While radar technology works most efficiently for the surveillance of objects in low-earth, medium-earth, and highly elliptical orbits (LEO, MEO, HEO), optical surveillance works best for objects in geostationary orbit (GEO). SSA considers as baseline, for LEO space surveillance, a ground based radar system. This system for LEO surveillance forms a part of an entire surveillance strategy including also detection of objects in other orbits (MEO and GEO) traditionally done with optical telescopes. About the SSA radar for LEO debris, location is critical. In fact, factors and requirements that apply to building the SSA radar are similar to those that apply when building a satellite tracking station; possible solution are the ESA's 35 metre deep space antenna stations located at New Norcia, Australia, or Cebreros in Spain and Malargue in Argentina (now under construction). Also the Russian Space Surveillance System (SSS) employs a variety of ground-based radars and electro-optical sensors in and outside of the Russian Federation and maintains a satellite database. Russia is the second country other than the US that operates a significant space surveillance, while ESA is beginning to study an autonomous

space surveillance system.

Fylingdales

The most powerful space surveillance radar sensor in Europe is located in Fylingdales (UK) and it is used by the British armed forces. Most of the activities are geared to the US Space Surveillance Network (SSN) early warning and space surveillance mission. It is a phased array radar operating in the UHF-band. Technical details are not openly available.

TIRA

ESA collaborates primarily with the operators of the German TIRA system (Tracking and Imaging Radar), located at FGAN (Research Establishment for Applied Science), near Bonn, Germany. TIRA has a 34 metre dish antenna operating in L-band for debris detection and tracking (1.333 GHz, 0.45° beam width, at 1 MW peak power) and it is capable of detecting 2 cm debris at a 1000 km slant range. In a bi-static mode, together with the 100 m receiver antenna of the nearby Effelsberg radio telescope, the overall sensitivity increases toward 1 cm objects at 1000 km, with TIRA as transmitter and Effelsberg as receiver. The overlap volume for observations is 600-1400 km altitude.

It was first used for debris measurements in 1996 and has been used in every LEO debris campaign. For debris, it operates in a staring mode very similar to the Haystack radar. The figure 2.24 shows TIRA-Effelsberg radars.
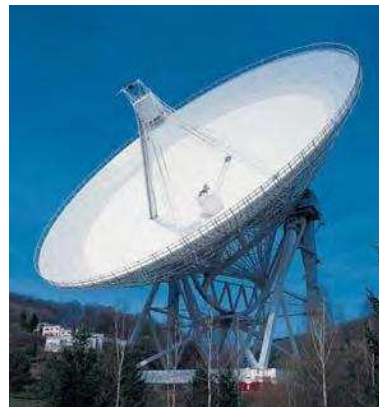
(a) `TIRA`   (b) `Effelsberg`

Figure 2.24: FGAN/TIRA radar (on the left) and Effelsberg radio telescope (on the right)

EISCAT

Beginning in 2000, ESA also began sponsoring the EISCAT (Incoherent Scatter Scientific Association) ionospheric research radars, located near Tromsø, Norway, and on Svalbard, to measure space debris in LEO in parallel with the standard EISCAT ionospheric measurements. The Tromsø radar (32 m antenna) operates at 930 MHz (32 cm wavelength) and can detect objects as small as 2 cm at a 1000 km slant range. The Svalbard radar operates at 500 MHz (60 cm wavelength) and

can detect 2 cm sizes at altitudes of 500 to 1500 km. Since these measurements are insufficient to determine complete orbits, EISCAT is only of limited value for space surveillance. The radar parameters and pointing are not optimized for debris and their location at high latitudes (69° and 79°N) limits the inclinations that the radars can see (high inclination orbits). EISCAT was able to monitor and characterize China's Fengyun 1C debris cloud, generated at 800 km altitude in January 2007, following the worst single fragmentation event in space history. The figure 2.25 shows the EISCAT system.

(a) Svalbard   (b) Tromso

Figure 2.25: EISCAT radar installations in Svalbard (on the left) and Tromso (on the right)

GRAVES

The GRAVES radar is a Frech bi-static, phased array radar. The transmit array is located near Dijon and the receive array is located 380 km away near Apt, France. The GRAVES radar is the basis for the proposed European SSA for low altitude satellite tracking. ESA design studies have proposed a UHF system to be located in Spain, which has a slightly lower latitude than the current French system and could therefore track satellites with lower inclinations. Neither the GRAVES, nor the proposed ESA system, will detect debris smaller than 10 cm. It was the first European installation outside the US SSN that performed a space surveillance in the classical sense. The system produces a *self-starting* catalogue which can be autonomously built up and maintained. The figure 2.26 shows Graves radar.

Figure 2.26: Graves radar

The table 2.3 is an overview of radar characteristics.

Table 2.3: Characteristics of the most important debris radars in the world

Radar	Min. size range threshold	Altitude range (km)
Haystack (US)	1 cm	350 to 2000
	2-3 mm	300 to 500
	4 mm	1000
	6-7 mm	1700 to 1900
	5 mm	ISS altitude (350 km)
HAX (US)	1 cm	350 to 2000
	8 mm	450 to 900
	1-2 cm	ISS altitude (350 km)
Goldstone (US)	2 mm to 2 cm	300 to 3200
	2 mm	1000
	4 mm	2000
	2-3 mm	ISS altitude (350 km)
Cobra Dane (US)	4 cm	500 to 2300
	2 mm	280 to 2000
TIRA-Effelsberg (ESA)	1 cm	1000
EISCAT (ESA)	2 cm	500 to 1500
Graves (ESA)	10 cm	LEO

2.3.3 Optical observations

Above several thousand km of altitude, the radar power is not sufficient to monitor the small space debris, as the returned flux is proportional to the $1/range^4$, and all the space surveillance system use optical sensors for the higher objects. One advantage to using optical measurements is that the telescope can more easily detect debris objects in higher altitudes because rather than a $1/range^4$ detection limitation, optical detection should follow a $1/range^2$ pattern. Until 1987 the

well known Baker-Nunn photographic systems were the primary sources for optical information; they had a limiting magnitude of 14 and used photographic plates, which required long processing. Therefore, after 1987 they were replaced by electro-optical devices, which embrace the Ground-based Electro-Optical Deep Space Surveillance System (GEODSS). This system, combining three telescopes (two primary 1 m telescopes and one 40 cm auxiliary) in each observing site, achieves accurate pointing and a very good sensitivity (limiting magnitude about 16.5). GEODSS telescopes demonstrated the ability to probe for debris not only at GEO, but at LEO and MEO, as well.

As far as the geostationary ring is concerned, dedicated, non-routine, optical observation campaigns have been performed to characterize the environment in this vital region of the circumterrestrial space. The European Space Agency has installed, for this purpose, a 1 meter Schmidt telescope in the Canary Islands, now fully operating and providing an abundance of new data. At near geosynchronous altitudes, CCD detectors are used. In this case, signal to noise ratio (S/N) depends on the sensitivity of the detector, the length of the exposure, the number of pixels the satellite signal is spread over, and how much background light or noise is contained in each pixel. To maximize the S/N, the size of the image should exactly match the pixel size; in practice the signal is typically spread over several pixels. The telescope can be slewed at a selected orbital rate to match the motion of the satellite in order to concentrate all of the light onto a single pixel.

Actually ground-based telescopes can detect GEO debris down to 10 cm in size, ground-based radars can detect LEO debris down to a few mm in size, and in-situ impact detectors can sense objects down to a few micrometres in size. And while telescopes are mainly suited for GEO and high-altitude debris observations, radars are advantageous in the low-Earth orbit (LEO) regime, below 2000 km.

Before explain the most important optical telescopes for debris observation in the world it's possible to see how a debris optical observation is achieved from a telescope, considering two observation approaches: the survey mode and the tasking mode (or tracking mode). In the survey mode the telescope tracking at sideral rate, so stars appear as points while the debris (in LEO, MEO or GEO) streaks to the field. Most optical measurements are taken in survey mode where objects are detected as they go through the FOV of the telescope. By using this method, large sections of the sky can be examined in one night. In addition, objects are in the FOV for a short time and thus, only a small part of the object's orbit is detected. Therefore, a circular orbit assumption is usually made when calculating the orbital parameters of objects detected in survey mode.

When the telescope is in the tasking mode the object appears as a dot, while stars streak through the field. The debris brightness is obtained by comparing its brightness to the brightness of the background stars. In this mode there is no brightness variability in the single image, so the size determination from this exposure is better obtained.

The observation exposure time for these observation methods is about 1 second for objects in LEO, about 10 seconds for objects in MEO and from 20 seconds to 1 minute for objects in GEO.

Figure 2.27 shows a single, 20 second exposure from a Raven telescope during an IADC debris campaign for debris in GEO. The first figure was taken in the survey mode and the second one shows the same object in the tasking mode.

(a) `survey-mode`   (b) `tasking-mode`
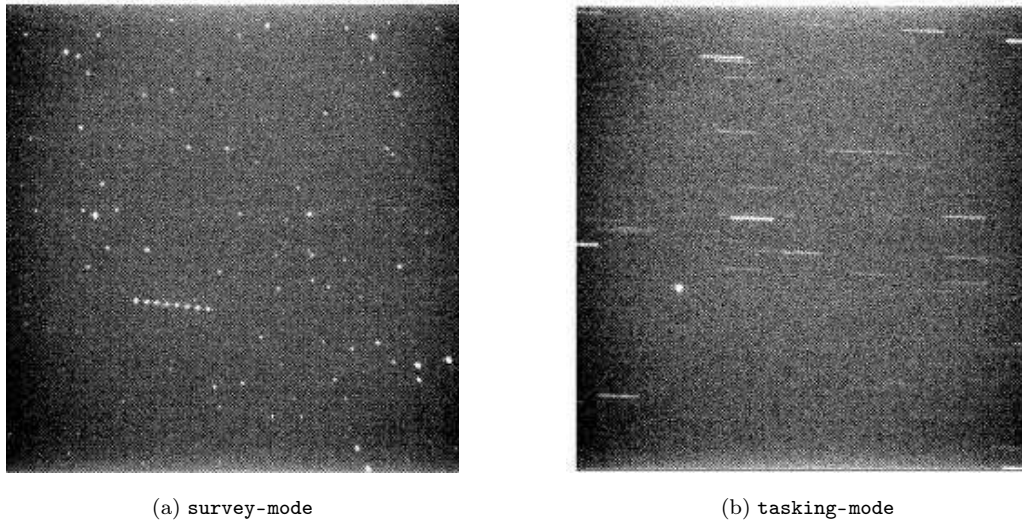
Figure 2.27: Telescope observations during an IADC debris campaign for debris in GEO (from [1])

The figure 2.28 illustrates a debris observation in GEO-tasking mode where GEO objects are two points, while the stars streak through the field.
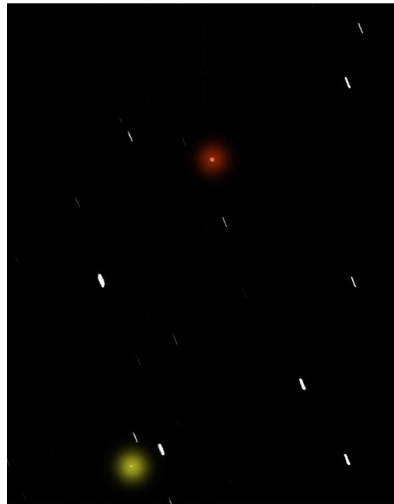
Figure 2.28: Two geostationary objects (marked in red and yellow) detected by the ESA space debris telescope in Tenerife in a tasking mode (stars appear as stripes) (from [68])

The most important telescopes for debris surveillance in the world are now described.

LMT

NASA began LEO optical measurements in 1996 with the construction of the 3 m Liquid Mirror Telescope (LMT) at Cloudcroft, New Mexico [71]. The LMT main mirror is created by spinning

liquid mercury in a parabolic dish. Liquid mirror technology was an extremely cost-effective way of providing a large aperture primary mirror and a relatively large FOV of 0.26 deg. This telescope was built to characterize the optical orbital debris environment, especially in the important, but hard to track, 1 cm to 10 cm size range in LEO. LMT is able to observe 1 cm NaK at 1000 km and 3 cm other debris at 1000 km. LMT operations continued every night until the project termination in 2001. Over 1300 hours of twilight debris observations were acquired, making the LMT dataset one of the most comprehensive optical debris datasets to date.

The LMT was able to detect orbital debris objects as 24 magnitude. Although objects often passed through the FOV of the LMT in just a few tenths of a second, an amazing quantity of information was gleaned. By measuring the object's entry and exit positions and its time to cross the FOV, its altitude and orbital inclination could be calculated. The data reduction software packages produced astrometric positions for all detections. These positions were fitted under the assumption of a circular orbit to produce inferred values for the inclination and range. With this information and its apparent magnitude, the absolute magnitude was calculated and used to estimate an object's size by assuming an albedo (for a better explanation, see sec. 4.2.1). Below 600 km altitude, it is believed that the LMT data still suffers from meteor contamination and is not reliable. The figure 2.29 shows the LMT.

Figure 2.29: US Liquid Mirror Telescope

CDT

In 1992 there was some evidence that debris might be accumulating in GEO. Consequently, the CDT (CCD Debris Telescope), a transportable 32 cm Schmidt telescope began a search for debris near GEO altitudes from Maui, Hawaii. This telescope is part of GEODSS. CDT telescope was developed for measuring the optical properties of known orbital debris particles. In 1997, the CDT was moved to NASA Orbital Debris Observatory (NODO) in New Mexico to join the LMT. The CDT could see objects as faint as 17.1 magnitude with a 30 sec exposure. It could detect approximately 0.8 m diameter objects (assuming an albedo of 0.1) at geosynchronous altitude or an

object size of 0.36 m when a 0.2 albedo with a specular reflection was assumed. Using the CDT, researchers conducted systematic searches of the GEO environment as part of an international measurement campaign under the auspices of the IADC. The objectives for this survey were to determine the extent and character of debris in GEO, specifically by obtaining distributions for the brightness, inclination, RAAN, and mean motion for the debris.

MCAT

NASA and the Air Force Research Laboratory (AFRL) Maui Optical and Supercomputing (AMOS) site are colaborating to place a wide field-of-view (FOV), 1.3 m aperture telescope on Kwajalein Atoll for space debris research. It will be deployed in September 2010 as part of the High Accuracy Network Orbit Determination System (HANDS). The MCAT telescope will have a diagonal FOV of nearly one degree and operate in several different modes. During twilight hours it will sample low inclination, low Earth orbit (LEO) space debris. In the middle of the night, it will perform a conventional geosynchronous orbit (GEO) search. It is co-located with radar installations that enable simultaneous radar and optical observations. With detection sensitivity down to 1 cm diameter at LEO and 10 cm at GEO, MCAT is expected to make a valuable contribution to understand of the space orbital debris environment.

ESA telescope

The IADC has carried out several campaigns to define the GEO orbital debris environment using optical stations. NASA and ESA have been the prime contributors to finding and defining the fainter debris environments. The IADC campaign is to study the high area/mass (A/M) objects that were first detected by Schildknecht (see sec. 2.1.2). Thanks to these campaigns, ESA improved its telescope knowledge [49].

Tenerife telescope

ESA operates a Zeiss telescope of 1 m aperture that is used for the detection and survey of objects near the geostationary ring. The telescope can detect and track near-GEO objects up to magnitudes of 19 to 21 (this corresponds to objects as small as about 10 to 20 cm in size in GEO with 0.1 albedo). With this performance, the ESA telescope is top-ranked worldwide. It operates on the island of Tenerife, about 12 km east of the Teide, which is in Spain's Canary islands. Currently, nearly 50% of the observation time is used to observe space debris. During GEO observation campaigns, typically 75% of all detections are new objects that are not contained in the US Space Surveillance Catalogue because the US catalogue of space objects has a size threshold of 1 m in geosynchronous orbit, so ESA's telescope continuously detects unknown objects. The data provided by the telescope are a major input for space debris environment models, indicating a much larger number of GEO fragmentation events than confirmed so far (a Soviet Ekran 2 satellite explosion in 1978 and a US Titan Transtage break-up in 1992). Observations of highly eccentric orbits passing through GEO led to the discovery of a class of faint, lightweight objects with high area to mass ratio (see sec. 2.1.2).

The telescope has a 0.7° field of view, it uses a 2x2 mosaic of CCDs of 2048 by 2048 pixels each (the figure 2.30 shows the telescope).

Figure 2.30: ESA Space Debris Telescope at Tenerife, Spain

ZIMLAT/ZimSMART

The Astronomical Institute of the University of Bern (AIUB) operates a ZIMLAT telescope. From its location in Zimmerwald, the telescope covers a sector of 100° of the GEO ring. The primary applications of ZIMLAT are astrometry and laser ranging. However, up to 40% of its night-time observations are used for follow-ups of GEO objects discovered by the ESA telescope in Tenerife. ZIMLAT was complemented in 2006 by the 20 cm ZimSMART telescope (Zimmerwald Small Aperture Robotic Telescope). ZIMLAT telescope has an aperture of 1 m and a field of view of 0.5°. A CCD of 2048 by 2048 pixels allows the detection of objects up to visual magnitude 19. The ZimSMART is dedicated to GEO survey, using a CCD of 3056 by 3056 pixels with a field of view of 4.2°. Figure 2.31 shows telescopes.

(a) `ZIMLAT`

(b) `ZimSMART`

Figure 2.31: Telescopes at Zimmerwald, Switzerland (AIUB)

The table 2.4 is an overview of analysed telescopes. It's presented the minimum size range or the minimum magnitude threshold for each analysed telescope.

Table 2.4: Characteristics of the most important debris telescopes in the world

Telescope	Min. size range/magnitude threshold	Region of survey
LMT (US)	1-5 cm / 24 mag	LEO
	1 cm (NaK) and 3 cm (other)	1000 km
CDT (US)	17 mag	GEO
MCAT (US)	1 cm	LEO
	10 cm	GEO
Tenerife (ESA)	10-20 cm / 21 mag	GEO
Zimerwald (ESA)	19 mag	GEO

2.3.4 Debris in situ measurements

Debris optical observations from space are an important in situ measurement. Debris smaller than about 1 mm cannot be detected easily by ground-based radars or optical telescopes. An in situ optical sensor with a large detection area, and long mission duration, is the only means to characterize the particles between a meter and a few millimeters in size. Space-based optical sensors have considerable advantages over their ground-based brethren. Ground-based optical sensors depend upon proper lighting conditions at the sensor site in order to be able to successfully acquire tracking data, including both the time of day lighting (i.e. dusk-to-dawn shooting periods) and an appropriate phase angle (the sun-debris-sensor angle). Ground-based optical sensors' effectiveness is further curtailed by atmospheric effects such as weather conditions (cloud cover and precipitation) and local light pollution. Thus, space-based sensors provide for a greater opportunity of acquiring tracking data on a wider array of targets.

The US MSX spacecraft was launched in 1996 in a near sun-synchronous orbit at altitude 888 km in a circular orbit. It had a 15 cm aperture Space-Based Visible (VSB) telescope. The goal of this mission was to observe cataloged debris and to obtain information about the phase function, albedo and diameter of the debris. It contributed for the 20% of the SSN GEO catalogue.

There is also another debris in situ measurement. All spacecraft collide with very small orbital debris particles and meteoroids; consequently, spacecraft surfaces returned to Earth are found to have many small craters resulting from hypervelocity impacts. In most cases, these craters are too small to have any effect on the operation of the spacecraft. However, by examining them, important clues can be obtained on the sources of orbital debris, and the rate that it is changing. In addition, residual material inside craters on the returned surfaces can be analyzed to obtain the chemical compositions of the impactors.

NASA has a long history of conducting space-based in-situ experiments on micrometeoroids and orbital debris, including instruments on the Explorer and Pegasus satellites in the early 1960's.

Critical surfaces, such as the windows, on the Space Shuttle are examined after every flight.

Other surfaces examined include those from the Solar Max satellite and the Hubble Space Telescope. On average, two Shuttle windows are replaced per mission due to damages caused by micrometeoroid and orbital debris impacts. Impacts on Shuttle windows and radiators are examined after each mission. The analysis results are part of the database NASA scientists use to define the sub-millimeter micrometeoroid and orbital debris environment. Other notable surface examination experiments include the Orbital Debris Collector (ODC), which was part of the Mir Environmental Effects Payload (MEEP) experiment, and the Mir Solar Array Returned Experiment (SARE).

A major milestone for in situ measurements was reached when the LDEF (Long Duration Exposure Facility, in figure 2.32) was launched in 1984 [73]. After a long delay, the facility was retrieved in 1990.

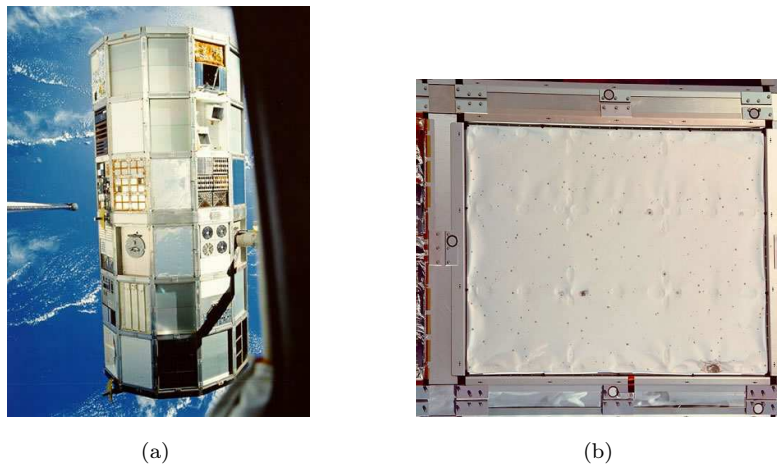

(a)   (b)

Figure 2.32: LDEF: the satellite (on the left) and a surface (on the right) (from [70])

LDEF is a unique data set for several reasons. LDEF had a number of large surfaces that were deliberately designed and calibrated to measure the debris environment. LDEF maintained its orientation throughout its mission, allowing for a detailed analysis of the directionality of the debris and meteoroid impactors. Over 20000 impacts have been documented on LDEF. These measurements have provided NASA scientists important information not only on the micrometeoroid and orbital debris populations, but their orbital distributions as well.

Also aerogel has been used in recent years to capture meteoroids and orbital debris for additional sample-return laboratory analysis (for Mir and ISS). For near-Earth in situ measurements, the utilization of aerogel has the potential to further our understanding of the origin and composition of the meteoroid and orbital debris populations.

In 1996, the ESA Geostationary Orbit Impact Detector (GORID) was launched into GEO. In 2001, a newly designed Debris in-Orbit Evaluator (DEBIE) was launched into LEO on ESA's PROBA-1 satellite. In 2008, DEBIE II was launched together with the Columbus science module, now docked to the International Space Station (ISS). It is now operated via the EUTEF (European

Technology Exposure Facility), one of the external Columbus payloads.

2.4   The hazard posed by space debris

The overcrowding of the space around the Earth makes collisions a serious threat and, as pointed out by some events a reality. To protect the space assets against impacts with small debris multi-wall bumper shields have been devised and installed on some modules of the International Space Station (ISS). Yet, for larger debris the shields are not enough to prevent the penetration of the target or even its complete fragmentation; in this case an avoidance maneuver, if the projectile is trackable from the ground, is the only solution to save the ISS or satellites. Note however that most of the debris between 1 cm and 10 cm are not cataloged. In addition, most of the operational satellites cannot carry the heavy bumper shields so they can rely only on avoidance maneuvers or on their 'good luck' to survive the harsh debris environment. Also the Space Shuttle has already performed several maneuvers to avoid pieces of junk which might have crossed its path.

The figure 2.33 shows the most important collision events happened in LEO orbit. Vertical lines mark the location of some known accidental collisions happened in orbit. The Cerise collision, were a debris of about 10 cm, coming from an explosion of an Ariane upper stage, hit the gravity gradient boom of the French microsatellite Cerise, at a relative velocity of 15 km/s and at altitude of 670 km, on July 24, 1996. The Thor Burner 2A Rocket Body collision, were the US upper stage was hit by a fragment from a Chinese upper stage (previously exploded) on a circular retrograde orbit, on January 17, 2005 at altitude of 885 km. The Cosmos 1934 collision, were a non-functional Russian satellite was hit by piece debris coming from a similar spacecraft (Cosmos 926), on an highly inclined orbit. It need to consider also the Iridium 33-Cosmos 2251 collision between two satellites and the Fengyun-1C explosion (see sec. 2.1.1).
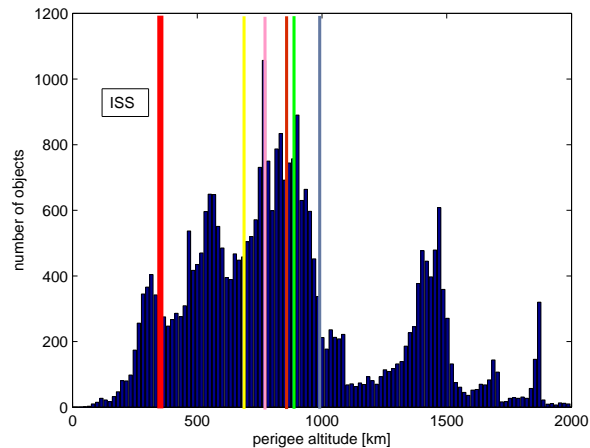

Figure 2.33: Position of the ISS (red line) and the most important collision events happened in LEO (coloured lines from the left: Cerise collision, Iridium 33-Cosmos 2251 collision, FengYun-1C explosion, Thor Burner 2A Rocket Body collision and Cosmos 1934 collision)

It is worth noting that LEO is the region with the highest collision risk for orbiting objects. The only accidental collision ever recorded happened around the high density regions in LEO as pointed out in figure 2.33. The spatial density of debris in LEO is such that, currently, hundreds of close approaches (i.e.,passes within less than 1 km) between catalogued objects occur on a daily basis. This lead the space operators to perform routinely a collision avoidance monitoring for their most important space assets. Currently, close approaches between a satellite and all the crossing catalogued objects are checked every day. Whenever the collision probability between a given satellite and a catalogued object exceeds a pre-defined threshold, a collision avoidance procedure can be activated. At this stage a typical problem arises in the procedure, related to the TLE accuracy, not enough to guarantee an effective and safe collision avoidance (according to the published TLE the Cosmos 2251 and Iridium 33 should have missed each other by about 400 m). And also the opposite problem might occur, i.e. sometimes unnecessary avoidance manoeuvres might be performed on the basis on non-accurate orbits.

In order to better understand the risk posed by space debris, some debris are shown (figure 2.34 and 2.35) with their effects (figure 2.36)

Figure 2.34: A 30 kg titanium pressurant tank from Delta 2 second stage reentered the atmosphere in Texas, US
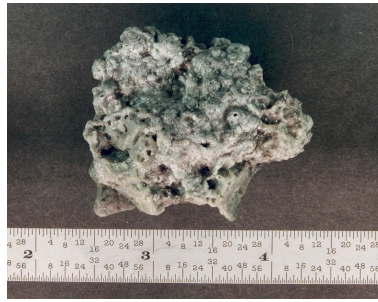
Figure 2.35: Solid rocket motor (SRM)slag. Aluminium oxide slag is a byproduct of SRMs.Orbital SRMs used to boost satellites into higher orbits are a significant source of centimeter sized orbital debris (from [70])
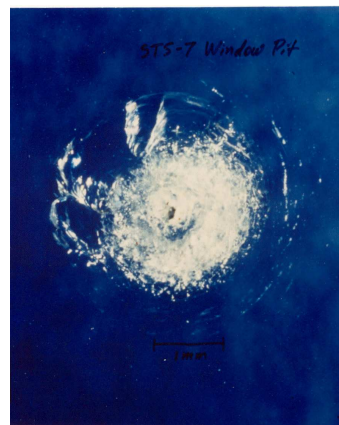

Figure 2.36: Window pit from space debris on STS-007 (from [70])

The consequences of debris impacts on spacecraft can range from small surface pits due to micrometre-size impactors, via clear hole penetrations for millimetre-size objects, to mission-critical damage for projectiles larger than one centimetre. Any impact of a 10 cm catalogue object on a spacecraft or orbital stage will most likely entail a catastrophic disintegration of the target. This destructive energy is a consequence of high impact velocities, which can reach 15 km/s for space debris. Smaller, uncatalogued objects can only be defeated by passive protection techniques, as used with the International Space Station (ISS).

The major concern with debris is that it might hit an operational spacecraft or a larger object such as the International Space Station, with a whole variety of detrimental consequences. The average collision velocity in LEO is greater than in the much higher circular (GEO) orbits and typically ranges between 8 and 12 km/s. In a LEO collision between an operational spacecraft and a catalogued object, it is likely that both would be destroyed and hence many more space-debris fragments would be generated. If these fragments were large enough, they too could generate additional debris through further collisions.

The space agencies and the satellite operators came to realize the urgency of the space debris issue. It is clear that some mitigation measures must be undertaken in the future space activities. More difficult is, as usual, to spread this message outside the space debris field of study and to devise common strategies to mitigate and solve the problem. Currently the most favored mitigation measures include:

- change of the spacecraft design to prevent the release of mission related debris;

- prevent on-orbit explosions: this includes venting the upper stages of the residual fuel to avoid over-pressurization and discharging any power system on board after the end of the operational life;

- de-orbit all the upper stages and the satellites at the end-of-life (either direct or delayed re-entry). If the original orbit is such that a de-orbiting maneuver is too demanding in terms of propellant, than a re-orbiting to a storage orbit above the operative one could be envisaged. The latter might be a short-term solution, that could be abandoned whenever other propulsion methods (e.g., low thrust systems or even electrodynamics tethers) become commonly available on the spacecrafts for de-orbiting purposes.

To protect the operative satellites in GEO, minimizing the collision risk with old non-operational spacecraft, a protected zone was defined at international level by the Inter-Agency Space Debris Coordination Committee (IADC), an inter-governmental panel, including Space Agencies of several countries having assets in orbit, whose aim is to coordinate studies and initiatives on the space debris issue. This protected zone is defined as a toroid centered on the geostationary orbit, extending 200 km above and below the geostationary altitude and 15° in declination. Every spacecraft at end-of-life should be moved to a disposal orbit.

Notwithstanding the wealth of theoretical results and the efforts of these organizations, it must be noted that the actual implementation of the mitigation measures sometimes may collide with technical, political or economical reasons that can slow down and reduce their efficiency. As an example, in the last few years only about 10% of the GEO satellites have followed the de-orbiting procedures recommended by the IADC. In fact the operators often tend to privilege the immediate return of a few more months of operations, performed with the fuel that should be used for the de-orbiting maneuvers, as opposed to the long term benefit of all the space environment.

2.5 Actual mathematical approaches for the debris orbit determination

To produce and maintain a debris catalogue, a large number of optical and radar observations are routinely performed by a space surveillance network (SSN or SSA). To deal with this huge amount of data the interest in the study of orbit determination methods has been renewed, both from the theoretical and the computational point of view. The classical methods of preliminary orbit determination by Laplace and Gauss, that have been often revisited in the last two centuries, are based on the knowledge of at least three observations of a solar system body in three different

nights. Both Laplace and Gauss methods may produce more than one preliminary orbit for the same object. These classical orbit determination methods are today not efficient; in this context the availability of new efficient methods and algorithms for accurate orbit determination is extremely important. The data of the current surveys generally do not provide a single observation for an object in an observing night: in fact the moving objects are distinguished from fixed stars by detecting them a few times in the same night. The sequence of observations usually gives a too short arc on the celestial sphere, such that the data are not enough to compute an orbit for that body. As the number of detected objects per night is very large, it is difficult to decide whether two sequences of observations made in different nights belong to the same object.

The Department of Mathematics of the University of Pisa has developed an important and innovative orbit determination method [12] [31] [32] [33] [34]. This method has been well tested for the optical case with real data from the ESA Optical Ground Station in Tenerife (for GEO debris survey) and for asteroids in simulations of next generation surveys (Pan-STARRS telescope project).

Some aspects of this algorithm is now presented. Given two or more sets of observations, the main problem is how to identify which separate sets of data belong to the same physical object, debris or asteroid (the so-called *correlation* problem for debris and *identification* in the context of asteroid surveys). The problem is the correlation of independently observed *tracklets*, that are sets of astrometric observations over a short time, assembled because they are nearby and aligned, thus believed to belong to the same object (they fit to some smooth curve, typically a low degree polynomial). Two positions taken at the beginning and the end of the exposure forming a tracklet and the exposure time (in a survey or tasking mode) is about 1 second for objects in LEO, about 10 seconds for objects in MEO and from 20 seconds to 1 minute for objects in GEO. The main problem is the correlation of independently observed tracklets, because one tracklet is generally not enough to determine an orbit.

It is important to find two or more tracklets belonging to the same physical object and an orbit fitting all observations. The information contained in a tracklet can be summarized in a 4-dimensional vector called *attributable* (consisting of the angular position and velocity of the body on the celestial sphere at a given time for an optical observation) thus two tracklets are enough for the orbit determination problem to be over-determined (8 parameters from which we can try to compute a 6-elements orbit). Thus the orbit determination problem needs to be solved in two stages: first different sets of observations need to be correlated finding two or more tracklets belonging to the same physical object, then an orbit can be determined; this combined procedure is called *linkage* in the literature.

The Department of Mathematics of the University of Pisa has proposed two algorithms to provide a full preliminary orbit of an Earth-orbiting object with a number of observations lower than classical methods. The first one is the Virtual debris (VD) algorithm, based upon the admissible region, that is the set of the unknown quantities corresponding to possible orbits for objects in Earth orbit. This method can be used to define a preliminary orbits. A similar method has already been successfully used in recent years for the asteroidal case. The second algorithm uses the integrals of the geocentric 2-body motion, which must have the same values at the times

of the different observations for a common orbit to exist. The perturbation of J2 effect, important in LEO debris, is implemented is these methods. Methods are implemented for both optical and radar data.

In the first method the admissible region is a region in the plane defined by the two undetermined quantities for an orbit definition (the main requirement is that the geocentric energy of the object is negative, that is the object is a satellite of the Earth). The region is sampled by an optimal Delaunay triangulation generating a swarm of VD, that is a set of possible, but by no means determined, set of six quantities assigning an orbit. Each virtual debris is then propagated to the epochs for which other tracklets are available, and they are all tested for attribution to the orbit.

The second method was proposed in 1977 by Taff and Hall: they used the angular momentum and the energy integrals to perform orbit determination starting from a data set that corresponds to two attributables of the same observed body. This method is used for simulated debris observations analyses achieved in this thesis. The method is thought for applications to the modern sets of astrometric observations, where often the information contained in observations allows only to compute, by interpolation, two angular positions of the observed body and their time derivatives at a given epoch (attributable). Given two attributables of the same body at two different epochs it is possible to use the energy and angular momentum integrals of the two-body problem to write a system of polynomial equations for the topocentric distance and the radial velocity at the two epochs. It is also possible to compute a covariance matrix, describing the uncertainty of the preliminary orbits which results from the observation error statistics.

Each methods are based on some mathematical concepts. Let (ρ, α, δ) be topocentric spherical coordinates for the position of an Earth debris. The angular coordinates (α, δ) are defined by a topocentric reference system that can be arbitrarily selected. Usually, in applications, α is the right ascension and δ the declination with respect to an equatorial reference system (e.g., J2000). The values of range ρ and range rate $\dot{\rho}$ are not measured. Optical attributable is the vector:

$$A_{opt} = (\alpha, \delta, \dot{\alpha}, \dot{\delta})$$

representing the angular position and velocity of the body at a time in the selected reference frame. Space debris can also be observed by radar: because of the $1/\rho^4$ dependence of the signal to noise for radar observations, range and range- rate are currently measured only for debris in LEO. When a return signal is acquired, the antenna pointing angles are also available. Given the capability of modern radars to scan very rapidly the entire visible sky, radar can be used to discover all the debris above a minimum size while they are visible from an antenna, or a system of antennas. When a radar observation is performed we assume that the measured quantities (all with their own uncertainty) are the range, the range rate, and also the antenna pointing direction, that is the debris apparent position on the celestial sphere, expressed by two angular coordinates such as right ascension α and declination δ. The time derivatives of these angular coordinates, $\dot{\alpha}$ and $\dot{\delta}$, are not measured. Radar attributable is the vector:

$$A_{rad} = (\alpha, \delta, \rho, \dot{\rho})$$

containing the information from a radar observation, at the receive time t.

Given the attributable A, to define an orbit the values of two unknowns quantities (e.g. ρ and $\dot{\rho}$ in the optical case and $\dot{\alpha}$ and $\dot{\delta}$ in the radar case) need to be found at the same instance in time as the attributable. These two quantities, together with A, give us a set of attributable orbital elements:

$$X = (\alpha, \delta, \dot{\alpha}, \dot{\delta}, \rho, \dot{\rho})$$

at a time $\bar{t}$, computed from t taking into account the light-time correction: $\bar{t} = t - \rho/c$. Of course the information on the observer station must be available. The Cartesian position and velocity $(r, \dot{r})$, in a geocentric frame, can be obtained, given the observer geocentric position q at time t, by using the unit vector $\hat{\rho}$ in the direction of the observation:

$$r = q + \rho\hat{\rho} \tag{2.1}$$

These mathematical concepts are the base for the orbit determination method proposed by the Department of Mathematics of the University of Pisa.

The goal of these methods is to obtain an orbit with a smaller number of observations with respect to the classical methods. In the context of space debris surveys, the goal is a full 6-elements orbit from just 2 tracklets, which could be obtained with only 2 exposures.

Another valid orbit determination algorithm is developed in NAPEOS, the ESOC Navigation Package for Earth Observation Satellites. It is a highly portable navigation software system for Earth observation satellite missions providing orbit determination and prediction, manoeuvre planning and parameter estimation capabilities and being able to process a wide variety of observation data.

2.6 Modeling the orbital debris environment

In order to describe the spatial distribution of the debris population (catalogued and not yet catalogued population), mathematical models have been developed. Models are used to take the information obtained by measurements and turn them into useful estimates of the debris population. The idea is to put together as accurate a picture of the past, present, and future environments as possible. Future projections are linked to human activities, launch rates and explosion rates. Heavy-duty modeling tools have been developed to answer these types of questions. The modeling tools require informations on historical launch and explosion behavior, they propagate debris orbits, describe the orbital behavior of breakup clouds, and compute rates of accidental collisions and their effects on the environment.

Most models take the cataloged population as a basis and add fragments from known breakups in the micron to 50 cm size regime to account for the incompleteness of the catalogue. For sizes larger than 50 cm, the breakup model parameters are calibrated such that the theoretical population fits the catalogued population. For the size range between 1 mm and 50 cm, however, observational data are sparse and the uncertainties in the models increase considerably with decreasing object size. However, validation of the models in the size range from a few millimetres

to 50 cm can be achieved with special ground-based measurement campaigns using high performance radar facilities or with space-based measurements. When a new explosion or a new collision happens in the space debris environment, debris models have some problems about their efficiency.

NASA model

The most important model developed by NASA is *ORDEM*. *ORDEM* is a semi-empirical, computer-based orbital-debris model. It approximates the environment with six different inclination bands. Each band has a unique distribution of semi-major axis, for near circular orbits, and a unique perigee distribution, for highly elliptical orbits. In addition, each inclination band has unique size distributions which depend on the source of debris. Collision probability equations are used to relate the distributions of orbital elements to flux on a spacecraft or through the field of view of a ground sensor. The distributions of semi-major axis, perigee, and inclination are consistent with the US Space Command catalogue for sizes larger than about 10 cm, taking the limitations of the sensors into account. For smaller sizes, these distributions are adjusted to be consistent with the flux measured by ground telescopes, the Haystack radar, and the Goldstone radar as well as the flux measured by the LDEF satellite and the Space Shuttle. The current model is the *ORDEM 2000*.

Data sources form the basic database of *ORDEM 2000* are:

- SSN catalog (build the 1 m and 10 cm populations)

- Haystack and Haystack Auxiliary (HAX) radar data (build the 1 cm population)

- Goldstone radar data

- Impact measurements from the Long-Duration Exposure Facility (LDEF) (build the $10\mu m$ and $100\mu m$ populations)

- Hubble Space Telescope Solar Array (HST-SA) impact data

- Space Shuttle window and radiator impact data

- Mir impact data

Major sources are used to build the debris populations, while the other sources are used to verify and validate the model predictions.

Since no direct measurement at 1 mm is available, the 1 mm debris population in the model is based on an interpolation between the 100 μm and 1 cm populations. Goldstone radar data for the 3 mm objects are used to justify the interpolation.

ESA and Russian models

The consolidation of knowledge on all known objects in space is a fundamental condition for the operational support activities of ESA's Space Debris Office. This knowledge is maintained and kept up-to-date through the *DISCOS* database (Database and Information System Characterising Objects in Space). *DISCOS* serves as a single-source reference for information on launch details,

orbit histories, physical properties and mission descriptions for about 33500 objects tracked since Sputnik-1, including 7.4 million orbit records in total. A continuous flow of orbit data for all tracked, unclassified objects is provided by the US Space Surveillance Network (SSN). Today, *DISCOS* constitutes a recognised, reliable and dependable source of space object data that is regularly used by almost 50 customers worldwide. The database has been painstakingly built up through data supplied by USSPACECOM (US Space Command), which operates dedicated tracking radars, and by several European sources. Additional information on objects of sub-catalogue size is provided by ESA's TIRA radar, in Germany, and by ESA's Space Debris Telescope in Tenerife, Spain.

The ESA's most prominent debris and meteoroid risk assessment tool is called *MASTER* (Meteoroid and Space Debris Terrestrial Environment Reference). The *MASTER* model contains the larger objects taken from the TLE (also operative satellites) plus the smaller objects generated with ad-hoc source models. It was first issued in 1995 and has been continuously improved; the current release is *MASTER 2005*, but *MASTER 2009* is under development. *MASTER* uses sophisticated mathematical techniques to determine impact flux (number of impacts per square meter of area and per year) information with high spatial resolution for an object population derived from all known, historic debris generation events. It is an engineering models series in the public domain that have been designed for the same purpose as that of the *ORDEM* model series to provide satellite operators with an accurate and quick estimate of the present and future vulnerability of their vehicles to debris.

The model can be used to assess the debris and meteoroid impact flux that a spacecraft would encounter on any arbitrary Earth orbit. The *MASTER* model covers all debris and meteoroid sizes larger than 1 μm and it describes the man-made and natural particulate environment of the Earth and its incident flux on user-defined target orbits. All relevant meteoroids and debris source terms are also considered.

Apart from spent payloads and upper stages (TLE background), *MASTER 2005* considers fragmentation from on-orbit collisions and explosions, dust and slag from SRM firings, NaK coolant droplets from RORSAT satellites, surface degradation particles (paint flakes), ejecta, and West Ford needles (as part of the TLE population). For each simulated source, a corresponding debris generation model in terms of mass/diameter distribution, additional velocities, and directional spreading has been developed. The *MASTER 2005* model offers a full 3-dimensional description of the terrestrial debris distribution reaching from LEO up to the GEO region.

To support the planning of observation campaigns and the exploitation of data for improved debris environment models, ESA has sponsored the development of the *PROOF* software (Program for Radar and Optical Observations Forecasting). *PROOF 2005* simulates space debris observation campaigns for ground and space-based sensors using available population data from the *MASTER 2005* model.

The russian *SDPA 2000* (Space Debris Prediction and Analysis) model is a semi-analytical, stochastic model, developed by ROSCOSMOS, for the medium and long term forecast of the man-made debris environment (with sizes larger than 1 mm), for construction of spatial density and

velocity distributions in LEO and GEO, as well as for risk evaluation.

It is now possible to compare these models. *ORDEM 2000* is a LEO model only, while both *MASTER 2005* and *SDPA 2000* extend to the GEO region. The main differences between the three model results lie in the flux vs. particle diameter distributions, with *ORDEM* predicting fluxes higher than *MASTER* and *SDPA* for particles smaller than 1 cm with differences of up to one order-of-magnitude. For particle sizes > 1 cm, *ORDEM 2000* produces fluxes similar or somewhat smaller than the other models. For particle sizes > 10 cm, the models are in general agreement. Figure 2.37 shows main differences between debris models.

	ORDEM2000	MASTER 2001	SDPA 2000
Minimum size	10 μm	1μm	1 mm
Upper altitude border	2000 km	37000 km	36200 km
Elliptical debris orbits implemented	Yes (if Ha < 3000 km)	Yes	Yes (if Ha < 3000 km)
Elliptical target orbits possible	Yes (if Ha < 2000 km)	Yes	Yes (if Ha $\leq$ 2000 km)
Source terms	Primarily an empirical fit to data, avoiding source term assumptions as much as possible	TLE breakup frag's paint flakes NA/K SRM slag SRM dust ejecta West-Ford Needles	Sum of all source terms
Modeling approach	Fit to measurement data, populations template define environment around the Earth	Semi deterministic including some measurement data	Semi-analytical, stochastic

Figure 2.37: A comparative survey of debris model characteristics (from [41])

2.7 Considerations about actual debris observation methods

It's possible to make a trade-off between higher performance radars and lower performance radars supplemented with a different observational technique. The main physical difference between radar observations and optical observations is in the type of illumination of the observed object. In the radar sensor the target is actively illuminated by radar signals, an optic sensor is based, on the contrary, on the passive reception of light scattered from the object illuminated by the Sun. The advantage of optical observations is precisely in the possibility of exploiting the abundant radiation provided for free from the Sun. The sensor so detects a signal characterized by an energy density, per unit cross section area, immensely superior to the one achievable even with the most powerful conceivable radar system. A further consideration which leads to a performances advantage is that the intensity of illumination of the receiving surface (hence the signal to noise ratio of debris detections) is inversely proportional to the square of the distance between the target and the optical observer, with a certain advantage of the signal to noise ratio of detections.

On the other hand the radar technology is characterized by a decreasing of the signal which is function of the inverse of the fourth power of the distance. Thus the optical observations have an obvious advantage on radar observations when the distance is larger, and indeed the advantage grows with the square of the distance. For this reason no one has proposed to use radar to observe GEO, and even for MEO the energy required from radar would be too high. The signal to noise ratio (S/N) for an optical observation is proportional to:

$$S/N \approx \frac{d^2 \cdot D^2}{r^2} \tag{2.2}$$

where d is the diameter of the object, D is the diameter of the photon collecting area in the telescope and r is the station-debris distance (or range) [7]. This implies that the minimum observable diameter d is inversely proportional to the distance r, for the same diameter D of the telescope.

The figure 2.38 resumes actual debris observations for all regions around Earth, considering both radar and optical observations.
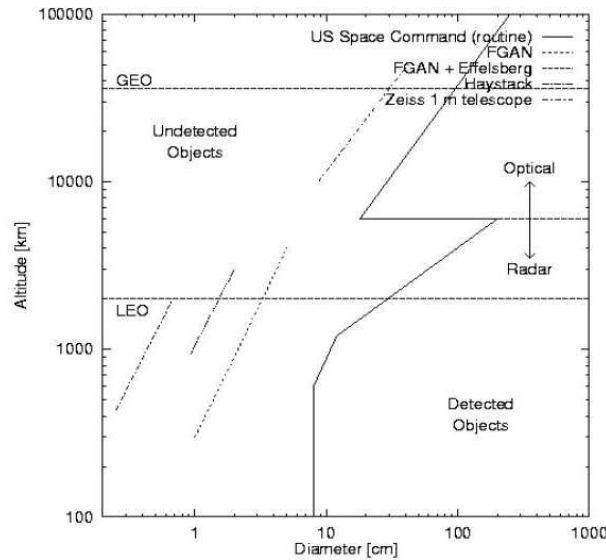

Figure 2.38: Actual debris observation methods (radars and telescopes) for all regions around Earth (from [27])

Optical debris observations from a ground station have also limitations, resulting from the physics of the observation process. Because the source of light illuminating the satellite/debris is the Sun, an essential requirement is that the object is outside the shadow cone of the Earth. Moreover, the optical ground sensor cannot operate unless the ground station is inside the same shadow cone. Last but not least, there are meteorological constraints: a simple cloud cover is sufficient to prevent any optical observation. These limitations must be joined to the effect of the Earth's surface curvature. In summary it is possible to observe an object from an optical station only when:

- the observing station is in shadow

- the debris resides outside of the Earth's shadow (it must be illuminated from the Sun)

- clear sky conditions of the observed sky area are present (no cloud coverage)

Moreover, the object elevation needs to be greater than a fixed value, such as 15 degrees, allowing for a reasonable air mass and avoiding unacceptable seeing values.

After these considerations, the new approach in this thesis is the study of debris observations in LEO using optical telescopes from ground stations. This study wants to show that optical observation in LEO are not only possible, but this new approach would significantly reduce the performance requirements for the radar system and could reduce the overall system costs. The LEO space surveillance consisting on ground based optical sensors only is an alternative approach because optical observations are mainly used for the GEO region. LEO debris have been studied for many years with radar stations: actually the LEO debris radar covers the full 200-2000 km LEO region, but the upper part of the LEO region might also be surveyed by ground based telescopes. The new approach analysed in this thesis also reflects the SSA scope: ESA considers as baseline observations in LEO with radar but it wants to study LEO optical observations possibility.

In order to analyse the feasibility of this new approach for LEO debris, simulated optical observations are required using a software interface and results will be compared with the most powerful telescopes in the world in order to understand the efficiency of the simulated observation system here developed.

Chapter 3

Debris observations from optical ground stations

The previous chapter illustrated advantages and disadvantages for optical debris observations, in particular from a ground station. In this chapter the feasibility of LEO debris optical observations from a ground station is analysed. This work has been developed for a ESA contract in the SSA context [10] in collaboration with the *Carlo Gavazzi Space* that has developed for this purpose the *SARA* project [7]. The study strategy is presented, showing parts of *SARA* project developed by the industry, in which this thesis has an important role because the work presented in this thesis contributes to ESA contract. In fact, in this work a software interface between two tools (STK and Matlab) has been created in order to compute simulated debris observations, used for the debris orbit determination (not analysed in this thesis) and to understand the feasibility and the efficiency of the debris detection system here developed. A lot of study assumptions have been determined by the *Carlo Gavazzi Space*, but the simulated debris observation software interface between STK and Matlab tools and the debris detection analysis program have been developed in this thesis in the *SARA* project context.

3.1   SARA project

SARA (*SYSTEM SUPPORT FOR SSA REQUIREMENTS ANALYSIS*) is a study proposed by *Carlo Gavazzi Space* in July 2009 [7] that replies to the ESA request for System support for SSA requirements analysis [10]. The project goal is to present a study aiming at the definition of an optical ground based system for the debris observation and tracking, in the contest of the European program SSA, to partially cover LEO region, reducing radar system performance requirements and the overall system costs in this important region with a great debris density.

After several studies for LEO space surveillance, a ground based radar system is considered as baseline by the ESA, but a mixed solution with an alternative approach consisting of a ground based radar sensor and a ground based optical sensor observation system, actually limited to MEO, HEO and GEO regions (and to the Near Earth Object), could have a better performances/costs

ratio for what concerns the higher part of the LEO. The advantage of the optical solution comes from several considerations (see sec. 2.7), in particular for MEO and GEO region, but the scope of this study is to show that optical observations for LEO debris are not only possible but it is possible to observe very little objects (few centimeters) reducing system surveillance costs with respect to the radar solution.

The study shows the necessity of a high number of optical stations in order to have the required level of service coverage. This is mainly due to following factors: clouds presence in the sky and limited daily sky observation time (in particular for the equatorial stations).

3.1.1   Study requirements

This section summarizes performance requirements from the ESA document [10] for the SSA feasibility study. These requirements show ESA study characteristics and they are useful to plan analyses developed in this thesis. It is important to underline that this thesis does not satisfy all requirements because most of them are about debris orbit determination (not studied in this thesis); following analysis will show only debris detection study.

Only principal requirements are here described.

a) The ground based telescope system shall be such that a catalogue can be build and maintained, even from a cold start (i.e. no a priori information of any object is available).

b) The ground based telescope system shall survey LEO objects with a perigee altitude (h_p) from h_{pmin} to $2000\,km$. The goal of the study is to find a suitable h_{pmin}, for h_{pmin} between $800\,km$ to $1500\,km$.

c) The main observation goal to be reached is the percentage of objects to be detected as function of its dimension and distance; this requirement rely on the following perigee-altitude-dependent (h_p) diameter envelope (d_{min}):

$$d_{min} = \sqrt{\frac{h_p^4}{h_{ref}^4} d_{ref}^2} \tag{3.1}$$

which is based on an object size-to-altitude dependency according to the standard radar equation and where d_{min} is the minimum object diameter, h_p is the object orbit perigee altitude and h_{ref}, d_{ref} are the altitude and the diameter of reference. The ground based telescope shall guarantee a catalogue coverage of P_{cov} of all LEO resident objects above d_{min} as specified in equation (3.1), where:

- $h_{ref} = 2000\,km$
- $d_{ref} = 32\,cm$ with $P_{cov} = 98\%$

The ground based telescope can also be upgradable to a catalogue coverage of P_{cov} of all LEO resident objects above d_{min} as specified in equation (2.2), where:

- $h_{ref} = 2000\,km$

- $d_{ref} = 20\,cm$ with $P_{cov} = 98\%$

This requirement refers to the whole catalogue and thus just specified a value averaged over all objects of the catalogue. Catalogue coverage, in the context of ESA study, is based on debris orbit determination, while in this thesis only debris detection is studied.

d) Any resident object shall have a probability for coverage in the sense of this service of at least 90%. The service refers to the detection of debris fragmentation events and to the screening process for collision avoidance. This requirement relates to each individual object and should ensure that all regions around Earth in LEO are covered at least with a minimum service quality.

e) The overall system shall be able to catalogue and publish all debris orbits according to the requirements on catalogue coverage within a period of 6 months.

f) The response time to a repeated user request for a high-fidelity screening process for collision avoidance shall be less than 1h after submission of the request.

Considering the requirement *c)* it is possible to produce a graph of the required detectable object for different orbit altitudes. The figure 3.1 shows the object size-to-perigee altitude dependency, in case of ground based telescope system guarantee and upgradable, obtained through formula (3.1).
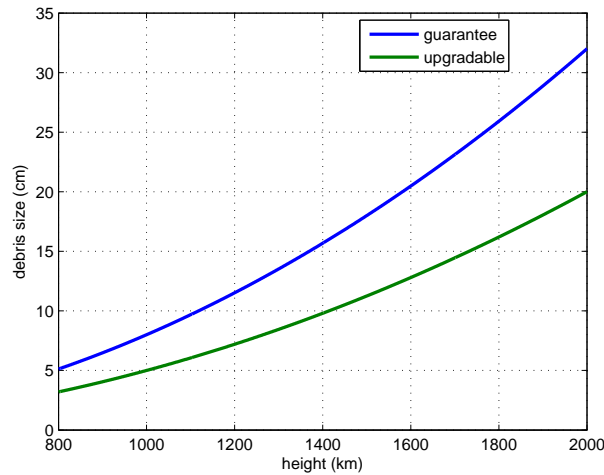

Figure 3.1: Debris size-to-perigee altitude dependency from SSA requirements for the ESA study

The study in this thesis has been performed considering the worst case condition related to the observation requirement. The worst condition is explained by the upgradable requirement. Deeper studies on the debris population distribution (see figure 2.14) show an objects crowding zone around 1400 km of altitude, for these reasons it had been chosen this region like characteristic

case in this study. So the first goal of the study in order to have an early feasibility indicator shall be demonstrate that, observing objects orbiting around 1400 km of altitude, it is possible to catalogue (in the sense of debris detection and not debris orbit determination) the 98% of the objects having the diameter from 10 cm to the bigger ones. Then the study will demonstrate that it is possible to detect objects at 1000 km of altitude having the diameter from 5 cm.

3.2   Study strategy and network observation architecture

The study can be divided in five parts:

- Creation of an optical network architecture specific for LEO debris: it is important to find equatorial and medium latitude stations in a correct position around the world and to set the performance parameters of the optical network.

- Creation of a debris population record in LEO for the analysis.

- Generation of simulated observations from the debris population with ad-hoc software interface considering all optical observations limits for debris. Simulated observations are analysed to define the debris valid observation percentage (considering meteo data for stations and the signal to noise ratio of detections). The thesis concerns this aspect.

- Debris orbit determination from simulated observations.

- Define how meteo data for stations (and the response time) affects the system efficiency.

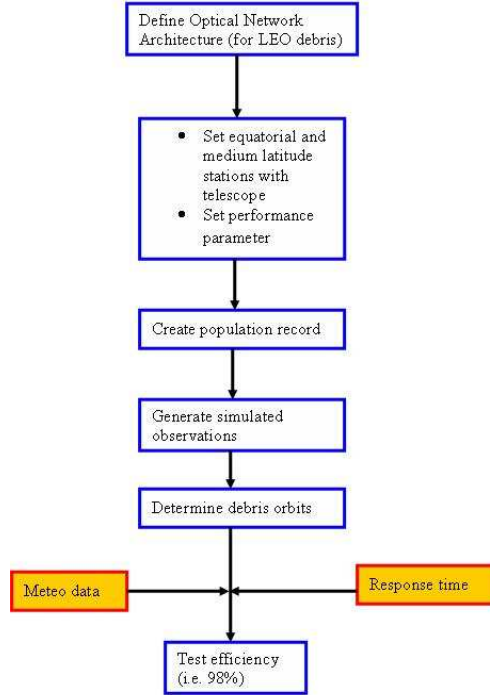The figure 3.2 summarizes study components.

Figure 3.2: Study levels

3.2.1 Observability and requirements analysis

In this section the observation strategy is presented. In this study, for a preliminary debris observation concept, the survey mode for observations is used with an observation exposure time of 1 second (see sec. 2.5 for a better explanation).

It is important to distinguish two important concepts in the debris optical observations: the observability and the detectability.

Observability In order to perform the debris observation some conditions shall verified, a minimum elevation angle, a maximum range, etc. These conditions are strongly dependent on the object orbit parameters, on the observatory station location and on the seasonal factors (relative earth-sun position, weather conditions, etc.). With these conditions a debris is observed.

Detectability Once the above reported conditions are satisfied a detailed analysis of the factors allowing to detect a particular object must be performed in order to assess the effectiveness of the applied optical architecture. The possibility to detect an object and in particular to acquire the object tracklet, allowing for successive orbital data elaboration, is fundamentally dependent on the object apparent magnitude along the trail, on the object speed, and on the sensitivity of the applied optical sensor; all these features are summarized in a critical

signal to noise (S/N) for debris detection. For this study a critical S/N has been chosen: above this value a debris observation is *valid*, that is the debris is detected.

After these considerations, the possibility to observe and to detect an object, by means of optical methodologies, fundamentally relies on:

- the physical characteristics of the observed object (magnitude, speed) and its surrounding (sky albedo)

- the optical and operational characteristics of the optical sensor (telescope diameter, focal length and pixel size, CCD efficiency, exposure time, minimum S/N for debris detection)

- the observation conditions (object illuminated, observatory in shadow, good meteo conditions, elevation $> 15°$ in order to eliminate atmospheric effects)

After that a debris is detected for the first time from the ground telescope and after a preliminary orbit determination, it is possible to make a debris follow-up with the telescope for the following detections of the same debris, increasing the detection accuracy. For all optical characteristics of optical sensor and for the telescope description used in the $SARA$ proposal for debris observations, see [6] and [7].

It is fundamental to understand SSA requirements for the ESA study (sec. 3.1.1) in order to find what parameters are more important and to analyse some observation strategies.

The apparent magnitude of an object ($H_{apparent}$) is a key element to define whether or not the object will be observable by the optical sensor. The apparent object magnitude sets the actual photon flux arriving from the debris and impinging on the optical sensor. This flux is due to the light reflected by the debris surface, when exposed to the Sun illumination, and hence is dependent, beyond the pertinent geometrical factors, on both the object illuminated surface area (approximately proportional to the square of the object diameter) and albedo. In order to observe debris with a low apparent magnitude (high debris brightness) it is important to have a precise observation strategy.

Another limiting factor which must be considered when LEO objects are observed through optical methods is due to their relatively high speed. For example, considering orbits characterized by 1400 km of altitude, the distribution of the objects speeds is expected to span from $300"/s$ to $1000"/s$.

The lower is the orbit of the object, the more reduced are the available observation times: in this view, contrarily to the case of radar techniques, the most stringent conditions for optical observation systems are encountered in the lower part of the LEO altitude range. This analysis shall also consider some statistical aspects, such as the cloud coverage, affecting the observation conditions and depending on the geographical displacement of the observatory network.

The design of stations network takes into account the need for a rapid response (within 1 hour, requirement *f)*) for a refinement of a debris orbit in case of a collision avoidance procedure is set up because collision avoidance is one of the most demanding task faced nowadays by a space surveillance network. This requirement poses strong constraints in the number and the location

of stations inside the network, to overcome problems related to possible meteorological adverse conditions and, mainly, unfavorable orbital geometries.

The overall catalogue (requirement *e)*) should be produced within a time span of 6 months. Once more, though this is of course a function of the available network and therefore an output of the study, the network and the correlation algorithms should allow a fulfillment of this requirement.

It is clear that the verification of the compliance with the requirements on the distribution in time of the observations cannot be obtained with a simple computation, like a scaling law. This is due to the very complex interplay of light, shadow, and clouds in determining the observability of a given object when it is passing above the horizon of a given station. Thus, the only way to assess the compliance with observability requirements is to use simulated observations performed by an orbit propagation tool. The results from such simulation, for a given population model (or segment of it, such as the population between 1000 and 2000 km of altitude) and for a given network of stations, have to be expressed in a statistical form, to be compared with requirements also expressed as a probability of coverage (requirements *c)*).

Optical observations are limited by the physics of the observation process. Because the source of light illuminating the satellite/debris is the Sun, an essential requirement is that the object is outside the shadow cone of the Earth. Moreover, the optical ground sensor cannot operate unless the ground station is inside the same shadow cone. Further, there are meteorological constraints due to the fact that a simple cloud cover is enough to make the observations impossible. These limitations are complicated by the effect of the Earth's surface curvature following the inverse square law, it would be desirable to observe an object while it is sufficiently distant from the observing station (in shadow) in order to be outside of the Earth's shadow, but this may not be possible because an object at a given height above the surface is placed below the horizon if it is beyond a given distance. It will be shown (sec. 4.2.1) that the best time for optical debris observations is only immediately after sunset and immediately before sunrise observing a precise portion of the sky where orbiting objects are fully illuminated in all directions

3.2.2 Network architecture analysis

A nearly equatorial station can operate in theory only about 10 hours per day (namely) because it must respect the requirement that the telescope is in full darkness. Higher latitude stations can operate on the average for a similar time but with huge seasonal changes. However, as the night progresses from sunset to local midnight, the shadow cone grows larger and larger on the portion of the celestial sphere observable from a given station. It must be emphasized that equatorial stations represent the most critical case in terms of effectively available observation time, a restriction which relaxes at medium latitudes, but which is further complicated by the seasonal effects and by the meteorological factors.

Namely, 3 equatorial stations spaced in longitude by about 120 degrees, which are of course necessary for observations of GEO and could be enough for MEO, would still be completely blind over time periods of months to highly inclined objects in LEO with some range of ascending node longitudes (RAAN), such that the sun-synchronous noon-midnight orbit, while the sun-synchronous dawn-dusk orbit are visible. Thus such a network, for the extension to LEO debris,

would need to be complemented by a number of high latitude stations, both in the North and South hemispheres to operate all year round, also spread in longitude. This implies that a network with 14 telescopes spread on 7 stations could have full coverage (each station has 2 telescope for redundancy, see sec. 4.1.2). If it will be required to provide a debris new observations within a small period, to avoid the risk of a collision, it would be necessary to increase the number of network stations. The main difference with radar arises because of the geometry of sunlight. Observation requirements are at least 3:

- the ground station is in darkness, e.g., the Sun must be at least 10-15 degrees below the horizon, that is the sky is dark enough to begin operations, typically about 30-60 minutes after sunset and before sunrise, but it strongly depends on the latitude and the season of the station,

- the orbiting object is in sunlight,

- the atmosphere is clear (no dense clouds).

The meteorological constrain can be handled by having multiple opportunities of observations from stations at different longitudes, far enough to have low meteorological correlation. Multiple stations at low latitude, probably 3 to 4, are required, and also some high latitude stations. Although each high inclination object can be observed by both high latitude N stations and high latitude S stations, the fact is that when N hemisphere is in summer the high latitude stations have almost no dark nights, and vice versa. Thus to guarantee a good coverage in all seasons both N and S high latitude stations are required. The larger the latitude, the smaller the obstruction to observability due to the shadow cone. However, higher latitude (both S and N) implies shorter hours of darkness in summer and worst weather in winter, thus there needs to be a trade off, which would probably favor intermediate latitude stations, somewhere between 50 and 40 degrees both N and S. The most effective observing strategy depends on the location and on the season.

Other elements to be considered in the network design are:

- *Geography*: the network needs to be spread over the world to increase the efficiency of the system, that is to avoid meteorological correlations, to increase the number of detections of an object and to cover all possible inclinations. For oceanic areas, it is important to find islands near the optimum position. The limitations of the European continent implies that sites in minor European islands around the world are needed as well as observing sites in other Countries.

- *Geopolitics*: the land needs to belong to Europe, or to friendly nations. Space debris are military sensible objects then a minimum level of security is required.

- *Logistics*: some essentials like electrical power, water supply, fast and reliable internet access, airports, harbors and road have to be available.

- *Meteo*: the cloud cover can be extremely high, in some geographic areas, and especially in (local) winter. Other meteorological parameters such as humidity, seeing, wind play an

important role. High elevation observing sites over the inversion layer are desirable, but in mid ocean there aren't many high mountains (see sec. 4.2.2).

- *Orography*: to have unobstructed view of the needed sky portions. Usually standard astronomical observatories are not so demanding, especially at the pole direction.

- *Light pollution*: the limiting magnitude is affected also by the sky background, so an observing site with low light pollution is desirable. There is the need to evaluate the impact of near by towns.

These considerations are used to choose the station network in sec. 4.1.2.

3.3   Study implementation methodology

For the complex study based on debris observation analyses it is important to use an observation simulator system, which main components are:

- Population model

- Data simulator

- Orbit determination simulator and efficiency validation

Figure 3.3 shows the study implementation scheme. Rectangles are actions developed by specific softwares, while circles are input or output data for each actions. Blue coloured rectangles are softwares developed in this thesis, the others are developed from the Department of Mathematics (DM) of the University of Pisa. From the LEO population provided by the particular *MASTER 2005* file (see sec. 2.2) a software developed by the DM, selects orbits for the simulation. The STK-Matlab Software Interface developed ad-hoc in this thesis context, generated simulated debris observations (and so simulated tracklets). These observations are filtered by a Matlab program developed for this thesis, considering the minimum S/N for the objects detections and the meteo data in order to obtain valid observations: with this software it's possible to study the debris detectability percentage. Valid tracklets selected by the previous software are used for the correlation and orbit determination with the algorithm developed from DM (see sec. 2.5) in order to obtain an orbit debris catalog. This orbit catalog is compared with selected orbits for the simulation in order to value the efficiency of the orbit determination algorithm. Only blue coloured rectangles are actions developed in this thesis, for other actions and relative softwares it is possible to refer to *SARA* proposal [7].
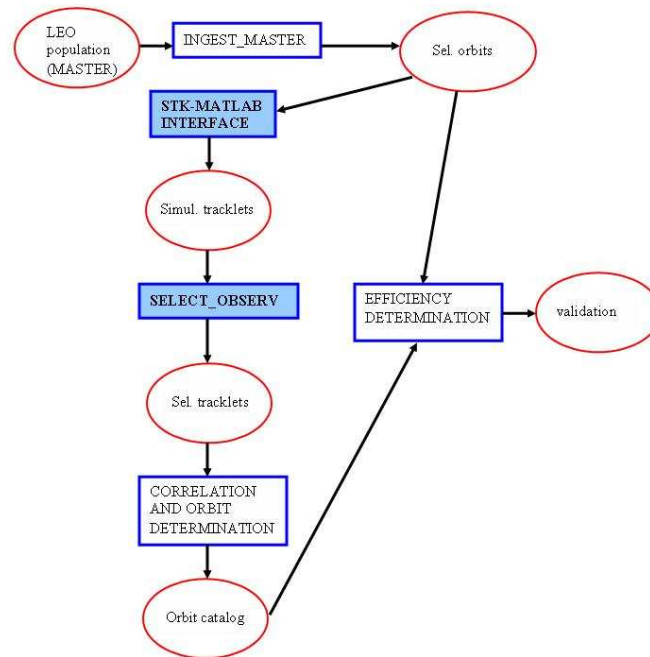
Figure 3.3: Study implementation scheme, considering ad-hoc softwares developed in this thesis and softwares developed from the Department of Mathematics of the University of Pisa

3.3.1 Population model

For *SARA* study, ESOC provided a file with a subset of the *MASTER 2005* population, integrated with the recent in-orbit collisions (Fengyun-1C, Iridium-Cosmos). The file is the same used for the LEO population analysis in sec. 2.2.

Quantities listed in the file for each debris are:

- ID: progressive number

- Factor: sampling factor

- Mass (kg)

- Diameter (m)

- Mass over area (kg/m^2)

- a: orbit semimajor axis (km)

- e: orbit eccentricity

- i: orbit inclination

- RAAN: orbit RAAN

- Aop: orbit argument of perigee

The true anomaly TA is not listed in the file. A true anomaly randomly extracted between 0 and 360 degrees was assigned to each object. For simulation purposes a de-sampled file was produced, where every line corresponds to a single object, adding a different random value for the true anomaly to every de-sampled object. From this population file debris are extracted in order to analyse them with simulated observations.

The debris population chosen for analysis varies from 1000 to 2000 km as the perigee radius, because this study is focused on the peak of LEO population around 1400 km (see figure 2.14), considering the first peak around 800-900 km covered by radar or satellites observations (see cap. 5).

The population file comes with no indication of the albedo of the objects, a quantity that is needed to derive for the debris magnitude valuation. The magnitude is an essential information to simulate the visibility of an object in the sky, but the state-of-the-art knowledge concerning the physical characteristics of the debris population, like albedo and magnitude, is very poor. Therefore an absolute magnitude value was added to each object in the file computed from its debris diameter using an albedo value. From the available literature a commonly accepted value of the albedo debris has been assumed and the realistic magnitude formula used for asteroid is applied (see sec. 4.2.1).

3.3.2 Data simulator

The data simulator runs through all the orbits contained in the population model and checks the observability conditions, for a given network of station. If all the conditions are satisfied, a simulated observation is generated and stored in a file in a standard observation format (*DES* format, see sec. 3.4.4). Data simulator is the aspect of *SARA* project developed in this thesis.

The compliance with observability requirements (elevation, illumination of the object and darkness at the station, limiting magnitude) will be checked using a well tested commercial tool (STK), using the Matlab interface, which will generate the simulated observation. It has been created a STK-Matlab Software Interface using the STK possibility to interface this tool with external tools. The softwares interface and the observations analysis program have been developed in this thesis for the *SARA* study.

The probabilistic meteorological model and the S/N filter used for debris detection are implemented in a separate software program, which values when an observed debris is also a detected debris.

3.3.3 Orbit determination simulator and efficiency validation

The simulated observations computed from STK-Matlab Software Interface are used as input to the correlation and orbit determination software, developed from the Department of Mathematics (DM) of the University of Pisa.

A fundamental requisite for the orbit determination is the availability of an efficient and aggressive orbit determination algorithm, allowing to correlate observations of the same object taken at different times, using just two tracklets for the preliminary orbit determination, which allows

to reduce the times required for catalogue build up. The Keplerian integral method has been used from DM for this purpose (see sec. 2.5). It was already successfully applied to optical observations in the geosynchronous region and it will be tested for the first time for LEO debris. The main difference with the GEO case is the fact that, for LEO debris, it is generally not possible to neglect the nodal precession of the orbit due to the term of the Earth geopotential, J2 (the coefficient of the second zonal spherical harmonic of the Earth gravity field). The method, based on the two-body integrals, produces preliminary orbits starting from two attributables A_1, A_2 of the same object at two epoch times t_1 and t_2. The orbit between t_1 and t_2 should be well approximated by a Keplerian 2-body orbit, with constant energy E and angular momentum vector c, but in this case, considering the J2 effect, it is not possible to use the conservation of angular momentum. The multiple orbits obtained from the solutions of the algebraic problem are just preliminary orbits, solution of a 2-body approximation (as in the classical methods of Laplace and Gauss). Even after confirmation by least squares fit, every linkage of two attributables needs to be confirmed by correlating a third attributable. The process of looking for a third attributable which can also be correlated to the other two is called *attribution*. From the available 2-attributable orbit with covariance it's possible to predict the attributable A_p at the time t_3 of the third attributable, and compare with A_3 computed from the third set of observations.

In this study the survey mode is considered for debris observations, so stars appear as points while the debris streaks to the field. For optical survey in LEO 1 second for the exposure time has been chosen, so a tracklet is here defined as two consecutive observations with 1 second between the first and the second observation.

It is also essential to decompose debris observations into three conceptually different goals: detection, discovery and orbit maintenance. The essential difference between detection and discovery is that a too small data set, although it is enough to claim something is there and has been *detected*, does in general not allow to compute an orbit: e.g., a tracklet provides four constraints and cannot be used by itself to solve for the six parameters of an orbit. Thus discovery, which implies that an orbit becomes available, requires more data than detection, and over a limited time span. On the contrary, for maintenance of an already computed orbit the detections are enough. This implies that the requirements for the quantity of observations are very different for detection, discovery and maintenance, and also strongly dependent upon the orbital period of the object.

3.4 Data simulator: debris observations for the orbit determination

In this section it will be analyzed the data simulator concept and what a simulated debris observation represents for the study. Simulated observations are achieved in order to obtain the debris orbit determination. It will also be studied how a simulated observation is obtained with the creation of ad-hoc software interface between two well tested tools: AGI Tools Kit (STK) and Matlab.

3.4.1 STK software use for debris propagation and interface with Matlab

In this section it will be analyzed the data simulation approach used to run through all the orbits contained in the population model in order to check the observation conditions expected for a given network of stations.

AGI Tools Kit (STK) has been used for simulated debris observations because it's a well tested tool and it performs complex analysis of space assets allowing to define relationship between the different objects integrated into a defined scenario. It has been used STK Version 8.1.3 for simulations, but simulated debris observations have been tested also with STK Version 9.0.1 with the same results of the previous version.

The STK computation produces simulated observations that they are then used by the software developed by the Department of Mathematics (DM) of the University of Pisa for the correlation between different debris observation sets and for the orbit determination. STK and DM softwares are very different orbit propagator tools, created for different studies and used in different ways. So it has been done an important, complex and precise interface work between tools, to obtain the same results in the orbit debris propagator. STK and DM softwares must have the same Earth characteristics (radius, perturbation model, rotation model and gravitational constant); these characteristics are very precise in order to guarantee the perfect interface and compatibility between STK and DM softwares without error.

From the preliminary analysis of the STK capabilities, a whole series of functions has been identified to be developed in an external environment. Matlab was selected to the purpose, as both offering all the necessary mathematical and computational tools required to implement the identified functions, and being already predisposed to be interfaced with the STK using the STK option *Connect*. It has been created a STK-Matlab Software Interface.

The STK receives as input the file describing the debris population. This file, structured as indicated in the `DES ORBIT FORMAT` (see sec. 3.4.4), contains principal orbit parameters for each debris which shall be considered in the simulation. This file has been used by STK to generate debris orbits and to propagate them. The STK simulation produces as report the debris position data, in terms of their right ascension and declination in spherical coordinates with respect to a reference system centered in a selected station. Other information regarding the relative position of the debris are included in the STK output file, in particular the time of the observation, the debris position range, the phase angle and the elevation angle. All these data are generated, and stored in an ASCII *.txt file*, only during the accessibility periods between the ground telescope and the debris.

Matlab is used to process the STK simulated data: the *.txt file* generated by STK is fed to Matlab which utilizes the contained input to check the validity of the observation period and to calculate the apparent magnitude and S/N (applying a random error to RA, the declination and the apparent magnitude). Matlab configures STK to generate a report during a time observation period and then Matlab reads the report and selects parameters of an instant and the instant after 1 second: they are two observation instants with 1 second difference that form a tracklet in LEO (see sec. 2.5). Finally Matlab stores the results in a file, formatted following the

DES DETECTION FORMAT (see sec. 3.4.4), tailored for debris. This file is been used for the debris orbit determination (developed from DM) and for detection analyses (see sec. 4.3)

Figure 3.4 summarizes the STK-Matlab interface with actions performed from relative softwares.
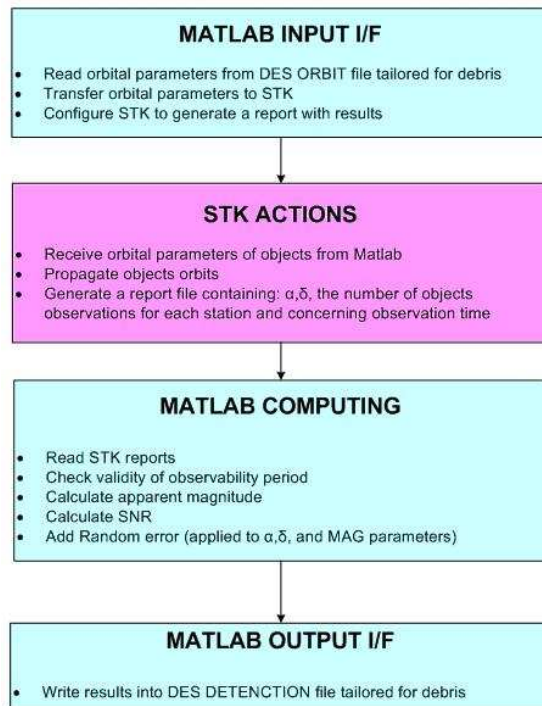

Figure 3.4: STK-Matlab Software Interface actions

3.4.2   STK configuration

Before starting a debris simulation with STK, the first action to be accomplished is to generate an observation scenario inside the program, i.e., by creating predetermined stations, orbital objects and by setting all the necessary constraints and options.

The chosen scenario is composed with 7 ground station (see sec. 4.1.2) and 1 satellite that represents the considered orbital debris. After the scenario creation it is necessary adding to the environment some constraints. The most important station constraint, consists in assuming that the selected station shall be always in umbra when it performs a debris observation. Umbra condition is made considering the Sun angle $10°$ below horizon (this means around 40 minutes after the sunset). Moreover when the observation time is less than 2 minute, the observation is considered as invalid. Another condition, set in the station parameters, which refers to a physical limit of the telescope, is the elevation angle, that is forced to be greater than $15°$ (in order to avoid a significant air mass disturbance in the actually received photon flux). Another condition about station is that the angle from the station between the moon and the debris must be more than $20°$

in order to avoid the light disturbance. The unique orbital debris constraint consists in assuming that it shall be always illuminated from the Sun when the station performs an observation.

To propagate the debris, a series of choices are taken, concerning both the frame of reference and the propagator. In particular:

- the selected frame of reference is the J2000 system

- with regard to the propagator, the only considered disturbance is gravitational (using the EGM96 model),

- moreover, the integration step is fixed at 40 seconds.

The table 3.1 summarizes the above-mentioned conditions. These conditions are important for the debris observability: when all these conditions (considering also weather conditions) are respected the debris is observed but not detected (it need to consider the critical S/N for debris detection, see sec. 4.3).

Table 3.1: Observation and propagation conditions in STK for debris observability

Object	Condition	
Ground optical station	Darkness	Sun 10° below horizon
Ground optical station	Time observation	2 minutes
Telescope	Minimum angle for debris	15° elevation angle from the horizon
		20° from the moon
Debris	Lighting	Illuminated
Debris	Frame of reference	J2000 topocentric
Debris	Propagator	Integration step: 40 sec
		Perturbation: gravitational (model EGM96,ord/deg 2)

Following figures (figure 3.5 and figure 3.6) show the STK debris propagation and its observation constraints (minimum elevation angle of 15°, debris illuminated and station in darkness).

(a) `observation`

(b) `no-observation`
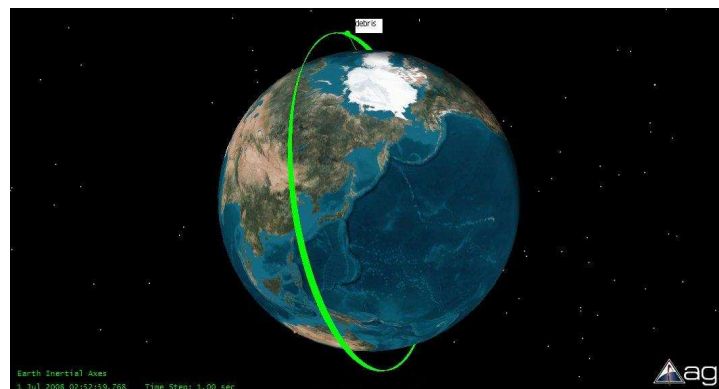
(c) `observation`

Figure 3.5: Ground optical station and debris constraints from STK: debris must be illuminated from the Sun and the station must be in darkness for an observation

Figure 3.6: Telescope constraint from STK: minimum elevation angle for an observation (15°)

For the debris propagation in STK and for the creation of a simulated observation file with the STK-Matlab Software Interface, it has been used a dedicated Processor: Intel® Core2 Duo, 2.13 GHz, 1066 MHz FSB.

3.4.3   Matlab computing

In this section the Matlab interface and Matlab actions developed to generate simulated debris observations are analyzed. Matlab main actions are:

- Check about the time between two consecutive tracklets

- Correction for the aberration of light

- Apparent magnitude calculation

- Check for a better phase angle

- S/N model for trailing pixel

- Error distribution for angles, S/N and apparent magnitude

Actions are now illustrated.

Time between two consecutive tracklets

The time between two consecutive tracklets must be greater than 30 minutes, so in the Matlab interface has been developed this control. This control is important because if the time between two consecutive tracklets is shorter than 30 minutes, the new observation belongs to the last tracklet. Debris can be in the Earth cone shadow for a time period, so two consecutive tracklets are as a matter of fact the same tracklet.

Correction for the aberration of light

The aberration of light is an astronomical phenomenon which produces an apparent motion of celestial objects about their real locations. It depends only to the finite speed of light. At the instant of any observation of an object, the apparent position of the object is displaced from its true position by an amount which depends on the transverse component of the observer velocity, with respect to the vector of the incoming beam of light (i.e., the line actually taken by the light on its path to the observer).

In this study the debris observation time computed from STK is the time when the object emits the signal light (t_{debris}); this signal arrives at the station ($t_{station}$) after a Δ_{time} because the speed of light is finite. The figure 3.7 represents this astronomical phenomenon: red points are two consecutive position of the debris moving on its trajectory, while, in the same time, the observation station (black points) moves around the Earth surface. The signal light from debris to station is represented by the red arrow: the emitted signal from debris in position 1 arrives at the station when it is in position 2.
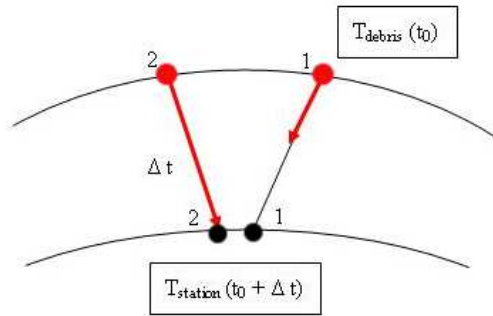
Figure 3.7: Aberration of light phenomenon (red points are the debris and black points are the ground station)

The time computed in Matlab and contained in the `DES DETECTION FILE` (sec. 3.4.4) is the $t_{station}$:

$$t_{station} = t_{debris} + \frac{r}{v} \tag{3.2}$$

where r is the range between station and debris and v is the velocity of the light (about $300000 \, km/s$).

Apparent magnitude calculation

Parameters which are still a matter of debate considering orbital debris, due to the lack of structured experimental data, is represented by albedo and magnitude characteristics.

The apparent magnitude (or relative magnitude, $H_{apparent}$) of a celestial body is a measure of its brightness as seen by an observer on Earth, normalized to the value it would have in the absence of the atmosphere. The brighter the object appears, the lower the value of its magnitude. Magnitude is complicated by the fact that light is not monochromatic. The sensitivity of a light detector varies according to the wavelength of the light, and the way in which it varies depends on the type of light detector. For this reason, it is necessary to specify how the magnitude is measured in order for the value to be meaningful. The V band is chosen for spectral purposes and gives magnitudes closely corresponding to those seen by the light-adapted human eye. In this study typical values for $H_{apparent}$ are from 12 to 27 (the study is focused on debris size about 10-30 cm): in order to make a comparison it's possible to consider that maximum brightness of Jupiter is about -2.9, maximum brightness of Pluto is 13.65 and the faintest objects observable in visible light with 8 m ground-based telescopes is 27.

Absolute magnitude $H_{absolute}$, also known as absolute visual magnitude when measured in the standard V phometric band measures a celestial object's intrinsic brightness. To derive absolute magnitude from the observed apparent magnitude of a celestial object its value is corrected from distance to its observer.

In this study, due to the lack of magnitude model for debris, the asteroid (or minor planet) model and its definition is used for debris: the absolute magnitude is the magnitude an object would have if it were at a standard luminosity distance (1 AU from the Sun and 1 AU from the Earth) away from the observer and with the phase angle = 0. This is an impossible scenario but it is just the definition of $H_{absolute}$. This is different than the absolute magnitude used for stars. From absolute magnitude is possible to calculate the debris diameter using debris albedo (see sec. 4.2.1).

It's fundamental to define now the phase angle (figure 3.8). The phase angle is the angle between the Sun-debris and observer-debris lines (the angle Sun-object-observer). The phase angle varies from 0° to 180°. The value of 0° corresponds to the position where the Sun, the debris and the observer are collinear, with the Sun and the observer on the same side of the object (the observation occurs at opposition). The value of 180° is the position where the object is between the illuminator and the observer. The brightness of an object is also function of the phase angle and it's important, for these reasons, to have a low phase angle value with observations achieved at opposition (see sec. 4.2.1).
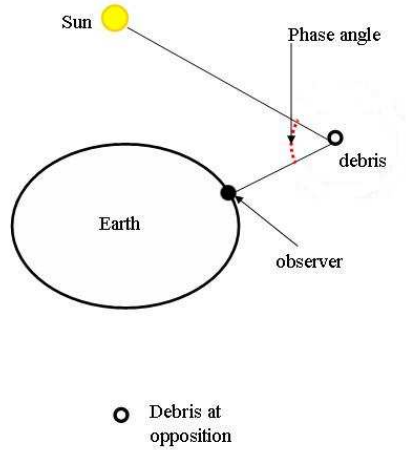
Figure 3.8: Phase angle definition

Hence, for the calculation of the apparent magnitude of the studied population, models applied for asteroids are used [4], because there isn't at now a debris magnitude model. This study and analysis in this thesis want to show that asteroid magnitude model is a good approximation for debris magnitude model.

The orbital object apparent magnitude can be calculated from the following formula (this value is in the `DES DETECTION FILE`, sec. 3.4.4):

$$H_{apparent} = H_{absolute} - 2.5 \, log_{10}[(1-G)\phi_1(\varphi) + G \, \phi_2(\varphi)] + 5 \, log_{10}(r \, \Delta) \qquad (3.3)$$

where:

- $H_{absolute}$ is the debris absolute magnitude calculated from the formula (4.2);

- φ is the phase angle;

- r is the heliocentric distance of the debris in AU;

- Δ is the geocentric distance of the debris in AU;

- G is the slope parameter. Indicative of the gradient of the phase curve, it has been scaled in such a way that $G \approx 0$ for steep phase curve (low-albedo bodies, generally) and $G \approx 1$ for shallow phase curves (high-albedo bodies). It has been assumed G = 0.15 for this study.

and

$$\begin{cases} \phi_i \,=\, exp\left[-A_i \, (tan \, \frac{1}{2} \, \varphi)^{B_i}\right] \\ A_1 = 3.33 \qquad\qquad\qquad A_2 = 1.87 \\ B_1 = 0.63 \qquad\qquad\qquad B_2 = 1.22 \end{cases} \qquad (3.4)$$

ϕ_1 and ϕ_2 are two specified phase functions that are normalized to unity at $\varphi = 0°$. Equations (3.3) is valid for phase angles $0° \leq \varphi \lesssim 120°$ and for $0 \lesssim G \lesssim 1$. This is the IAU recommended

formula for computing the visual magnitude V of a body. This formula implies that the magnitude of a debris becomes fainter as the phase angle increases. The slope parameter (G) controls how the apparent brightness of the object decays with increasing phase angle. Bodies with great slope parameter are brighter than bodies with small slope parameter, for the same value of absolute magnitude, phase angle and range.

Table 3.2 shows some albedo classes and the correspondent G value. An high albedo means an high objects brightness. In this study it has been considered an albedo=0.11 and G=0.15.

Table 3.2: Albedo classes and G values (from cite36)

Mean albedo	G
0.04	0.13
0.055	0.15
0.099	0.18
0.197	0.25
0.462	0.40

Check for a better phase angle

The phase angle for a debris is a very critical observation parameter. The phase angle is defined as the angle between Sun-debris-observer (see figure 3.8). The optical magnitude of an object (generally all Solar System moving objects) depends among other parameters by the phase angle: the smaller the phase angle the brighter the object. For this reason a dynamical telescope must be simulated in the software that chooses, during the observation period, the segment with the minor phase angle (the best condition for observation). The STK-Matlab Software Interface 'filters' the observation period and take the better phase angle. For this purpose the software calculates the phase angle at the beginning and at the end of each observation period of debris from a station; then it divides the observation period into 3 parts and it selects the part with the minor phase angle. See sec. 4.2.1 for better explanation.

S/N model for trailing pixel

The simulation allowed to associate to every object extracted from the population model and successively treated also the signal to noise ratio (S/N), expected at the observatory station performing the observation. S/N is very important for the debris detectability after all observability conditions are satisfied (table 3.1); in fact the application of a strategic image processing tools for automated trail detection allows a more efficient approach in tracklet identification.

The S/N model developed in this thesis refers to the model used in the *SARA* proposal [6] [7] [36]. The model considers the S/N for the trail and the astrometric resolution obtained on the trail by applying the S/N value on the single pixel. The S/N value for a single pixel and for a fixed star (no-trailing object) is calculated as:

$$S/N = \frac{S}{\sqrt{S + N^2}} \tag{3.5}$$

where S is the signal and N^2 is the noise (intended as the sum of the different source contributions). This way for an object trailing T pixels one obtains the following relationship:

$$(S/N)_{pix} = \frac{S/T}{\sqrt{S/T + N^2}} \tag{3.6}$$

From formula (3.6) it is possible to obtain:

$$(S/N)_{pix} = 1.128 \frac{\frac{10^{10-0.4\,H_{atm}}}{N}}{\sqrt{\frac{10^{10-0.4\,H_{atm}}}{N} + 641.825}} \tag{3.7}$$

This S/N value is used for the astrometric uncertainty (or angles accurancy, see sec. 3.4.4).

By integrating along the trail (application of the above referenced method), one obtains for the tracklet the following expression:

$$S/N = \frac{S}{\sqrt{S + TN^2}} \tag{3.8}$$

From formula (3.8) it is possible to obtain:

$$S/N = 1.274 \frac{10^{10-0.4\,H_{atm}}}{\sqrt{1.274 \cdot 10^{10-0.4\,H_{atm}} + 817.772 \cdot N}} \tag{3.9}$$

This S/N value is considered as the actual parameter for determining an object detectability and it's in the `DES DETECTION FILE` (sec. 3.4.4) with its uncertainty. An object tracklet was assessed as detectable for S/N > 6. Numbers in formula 3.7 and 3.9 derive from some optical considerations. Noise is inherent to all electronic image sensors, and a careful control of all noise components, both in the design and the operation of the CCD system, is necessary to ensure that the signal level relative to noise is adequate to allow capture of accurate image information. For any electronic measuring system, S/N characterizes the quality of a measurement and determines the ultimate performance of the system. The noise disturbance registered in a CCD camera, when this is applied for astronomic purposes, arises from different specific contributions (the photon counting uncertainty, the sky background, the read out noise and the dark current) that determine number in equations 3.7 and 3.9.

In equations 3.7 and 3.9, H_{atm} is the apparent magnitude of the observed debris considering the atmospheric disturbance term, calculated from formula:

$$H_{atm} = H_{apparent} + 0.04\,sec(\beta) \tag{3.10}$$

where β is the co-elevation angle from the horizon and 0.04 a coefficient for the atmospheric disturbance. Figure 3.9 represents the atmospheric disturbance effect for simulated observations. It's possible to notice that most observations have low elevation angle.
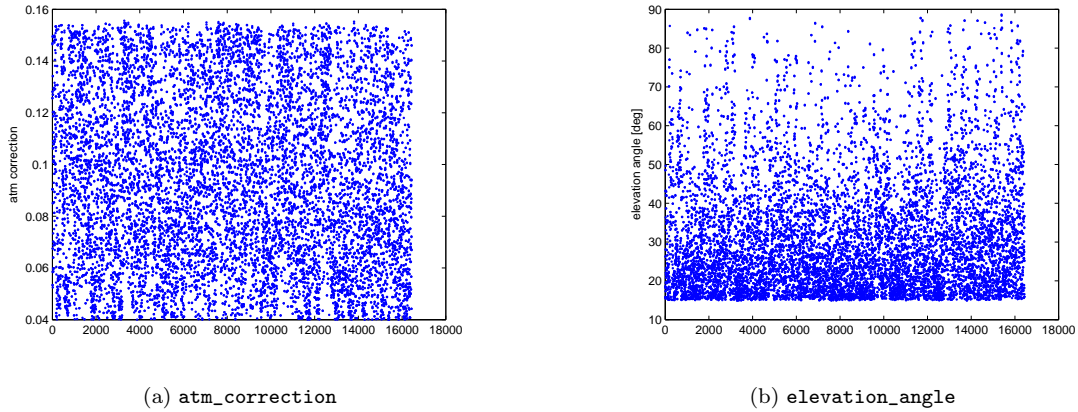
(a) `atm_correction`

(b) `elevation_angle`

Figure 3.9: Atmospheric disturbance effect for an observations sample (the atmospheric correction terms is $0.04\,sec(\beta)$)

It must be clearly remarked that from equation (3.9) it's possible to obtain the S/N of the an object, observed when it trails the camera field at a speed determined by its proper motion. In fact N in formula (3.7) and (3.9) is the number of pixels trailed in the camera field during the exposure time. The calculation of N is carried out by using the spherical coordinates generated by the STK during the orbit propagation, in particular given $\Delta\alpha$ and $\Delta\delta$ the differences in right ascension α and declination δ of the observed object, measured in degrees, respectively, the number of pixels N trailed by the object in the CCD array can be calculated by means of the following equation:

$$\begin{cases} N = \sqrt{\Delta\alpha^2\,cos^2(\delta) + \Delta\delta^2} \\ \Delta\alpha = (\alpha_2 - \alpha_1) * 3600/PS \\ \Delta\delta = (\delta_2 - \delta_1) * 3600/PS \end{cases} \qquad (3.11)$$

Where PS is the pixel size ($PS = 1.547\,arcsec$). Typical values for N come from 0 to 800.

Error distribution

An observation error has been introduced in order to make simulated debris observations more realistic. The error is introduced for the angles measures (astrometric uncertainty for right ascension α and declination δ) and for the S/N (photometric uncertainty). The error has a normalized (or Gaussian) distribution with mean and standard deviation (or uncertainty).

	Mean	**Uncertainty**
Angles	0	astUnc
S/N	0	1

where

$$astUnc = max(0.4, 1.5\,\sqrt{Z})arcsec \qquad (3.12)$$

and

$$Z = \left(\frac{1}{(S/N)_{pix}} \right)^2 \qquad (3.13)$$

Equation 3.12 calculates the astrometric uncertainty for angles that is in the `DES DETECTION FILE` (sec. 3.4.4).

The Gaussian error distribution is represented in figure 3.10.

(a) `Photometric(S/N)`

(b) `Astrometric(angles)`
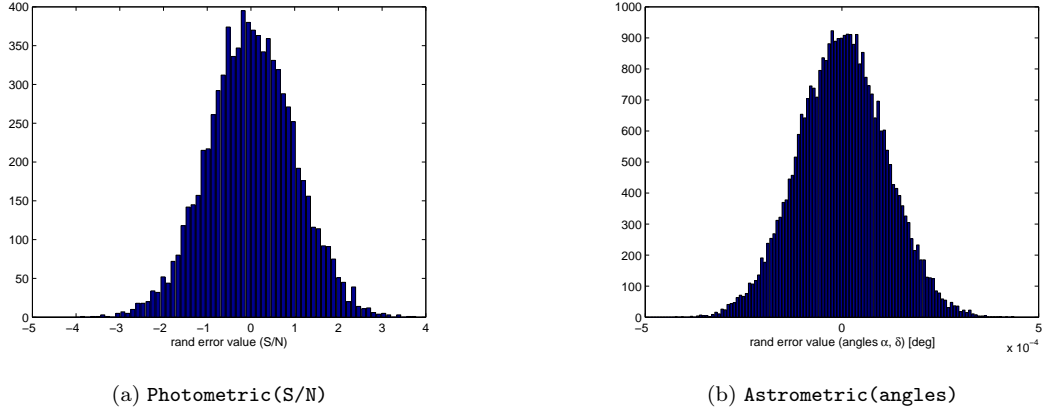
Figure 3.10: Gaussian error distribution for photometric and astrometric uncertainty

The error in the angles measures is supposed to be independent between α and δ and it is also independent between two observations of the same tracklet, while the error in the S/N is supposed to be dependent between two observation of the same tracklet. From the S/N (formula (3.9)) with error (that is in the `DES DETECTION FILE` (sec. 3.4.4)) is calculated the apparent magnitude with an error that derives from the S/N error. The magnitude (or photometric) uncertainty in the `DES DETECTION FILE` (sec. 3.4.4) is the absolute difference between nominal apparent magnitude and apparent magnitude calculated from the S/N with an error:

$$dMag = \left| H_{apparent}^{nominal} - H_{apparent}^{fromS/Nerror} \right| \qquad (3.14)$$

The scheme in figure 3.11 summarizes the calculation using the Matlab interface to obtain S/N, angles and relative uncertainty.
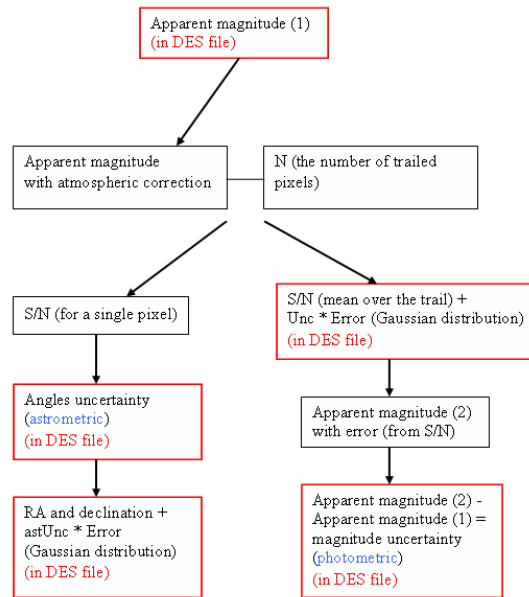
Figure 3.11: Logical flow for S/N, angles and relative uncertainty calculation (red rectangles represents objects that are in the DES DETECTION FILE)

The scheme reported in figure 3.12 summarizes the detailed structures of the Matlab program, developed to support the STK software (STK-Matlab Software Interface).
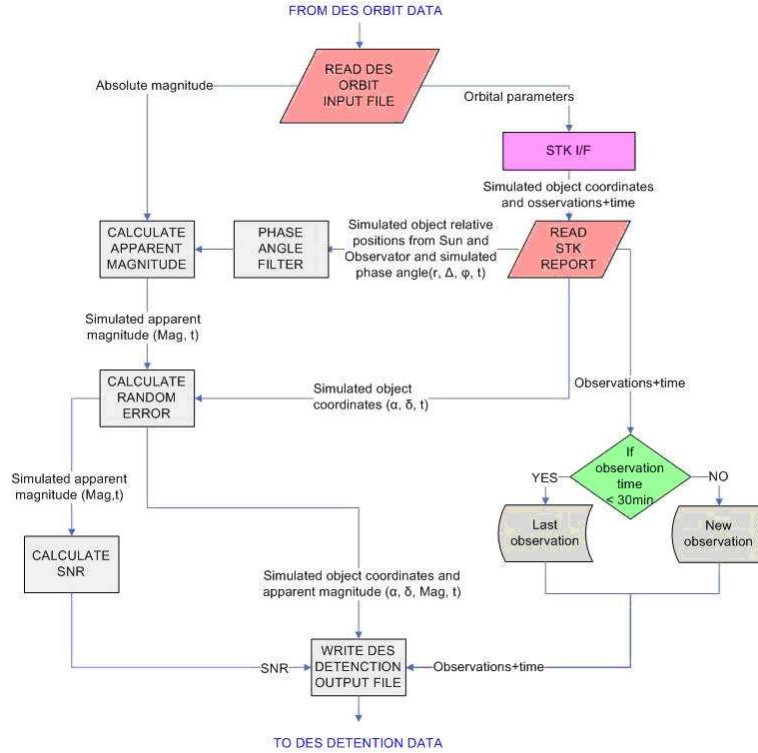
Figure 3.12: Structures of the Matlab program used for the interface with STK

All objects, which must be propagated one-by-one, are contained into the `DES ORBIT FILE`. Matlab reads the input `DES ORBIT FILE` and passes to STK the orbital parameters of each object while the absolute magnitude is used to obtain the apparent magnitude, calculated using the phase angle, and then the S/N. A random error is added to S/N. STK assigns the input values to an object contained in the scenario, that represents the debris, and it propagates the debris around its orbit. Moreover STK produces a report where the simulated object coordinates and the observation time were stored. Matlab reads the STK report and executes a test (time observation < 30 min) to verify if the observation belongs to the last tracklet. Matlab also filters the phase angle: it divides the observation period of debris into 3 parts and it selects the part with the minor phase angle (and so with a good condition for observation). Finally Matlab supplies a `DES DETECTION FILE`, containing for each propagated object the coordinates, the observation times, the apparent magnitude and the S/N (with other parameters), which will be given to detection analysis software or to the orbit determination software.

3.4.4 Interface information of data structure used during simulation

To exchange data between different actors and orbit computers, i.e. STK-Matlab Software Interface and DM software, there is the need of a data format, the *Data Exchange Standard* (DES). A detailed description of a proposed DES is contained in the document [35]. DES standard format was developed by the Department of Mathematics (DM) of the University of Pisa at the beginning for the exchange of data of the next generation asteroid surveys Pan-STARRS and LSST, internally,

between them, and with external data processing centers such as NEODyS and the MPC. This model allows the manipulation of complex data types with informatically simple procedures. The basic idea is that the standard is defined starting from an object oriented approach, in which user defined data types correspond to each data object. For the *SARA* proposal DES format is slightly modified for debris observations, most specifically for LEO debris. Debris orbits has been described by means of a dedicated format, called `DES ORBIT FORMAT` (table 3.3). Orbit parameters are written in a *.txt* file structured as follow:

ORBIT = (ID_OID, COO, ELEMS, H, t_0, INDEX, N_PAR, MOID, COMPCOD)
FORMAT: single line
FILENAME: `chiara_orbit.txt`

Table 3.3: DES ORBIT FORMAT

Id_oid	COO	q(km)	e	I(deg)	Omega(deg)	argperi(deg)
21869	COT	7830.70793000	0.01410000	74.04000000	112.66000000	36.55000000
true_an(deg)	**H**	**t_0(MJD)**	**index**	**n_par**	**moid**	**compcod**
271.03379357	38.23500000	54466.000754444	1	6	1452.571630	2005

- ID_OID - the identification alphanumeric code of debris

- COO - the set of used coordinates, in this case COT (Cometary True Anomaly), that comprises a number with 8 decimal digits; it includes:

  a) q - pericenter (in km)

  b) e - eccentricity

  c) I - inclination (in deg)

  d) Omega - longitude of node (in deg)

  e) argperi - argument of pericenter (in deg)

  f) true_an - true anomaly (in deg)

- H - absolute debris magnitude in the V band (it is required 8 decimal digits)

- t_0 - initial epoch time in MJD TDT in days (it is required 9 digits after the decimal point)

- INDEX - a whole number indicating the order in the list of solutions for the same identification (defaults to 1); i.e. there may be multiple orbit solutions for a list of detections.

- N_PAR - the number of fit orbital parameters: 6 for a nominal orbit (a whole number)

- MOID - for debris, the minimum height defined as $(q - R_{earth})$ in km

- COMPCOD - a code designating the software system used to compute the orbit

The debris orbit propagation allows to evaluate the accesses between the debris and a set of ground telescopes. The data concerning each evaluated access has been reported in a file, written following a dedicated format, called `DES DETECTION FORMAT`, described in table 3.4. Detections belonging to a very short time span are assembled into tracklets by polynomial fitting in such a way that they may belong to the same object.

DETECTION = (OID, TIME, OBS_TYPE, RA, DEC, APPMAG, FILTER, OBSERVATORY, RMS_RA, RMS_DEC, RMS_MAG, S2N, Secret_name)
FORMAT: single line
FILENAME: `osservazioni.txt`

Table 3.4: DES DETECTION FORMAT

OID	time	O	RA[deg]	DEC[deg]	APPMAG	FILT
A00057624	54525.2747107357	O	62.119250332	-65.697056816	15.7825391	V
A00057624	54525.2747223055	O	62.337102721	-65.604833637	15.7774744	V
STA	**Rms_RA**	**Rms_DEC**	**Rms_MAG**	**S2N**	**S_NAME**	
Z11	2.375095	2.375095	0.083025	12.154149	21869	
Z11	2.363722	2.363722	0.083025	12.208493	21869	

- OID - a detection_id that must be unique for each record. It's a 9 character alpha numeric string

- TIME - MJD UTC in days of observations. For space debris, it is required to supply 9 digits after the decimal point.

- OBS_TYPE - the type of observation (O for an optical observation)

- RA, DEC - right ascension and declination (in deg)

- APPMAG - the apparent magnitude in the specified FILTER

- FILTER - the image measurement band (V for visible)

- OBSERVATORY - the 3 character observatory identifier

- RMS_RA, RMS_DEC - the estimated accuracy in RA and RA*cos(DEC), in arcsec

- RMS_MAG - the formal uncertainty in the magnitude (in magnitudes)

- S2N - the signal to noise ratio of the source

- Secret_name - an independent multiple character `ASCII` identifier for the detection; for real data the name of the object could be inserted after a firm attribution

These informations are stored for each debris observations in a *.txt* file.

Chapter 4

Simulation results

In this chapter simulations results of debris observations obtained with the STK-Matlab Software Interface will be analyzed. Results are divided into two aspects: the study of a good and efficient optical stations network for debris observation in LEO and the study of simulated debris observations of debris in LEO considering all of the most important aspects for a realistic optical observation. Optical debris properties are also analysed in order to generate an efficient optical observation; that because the state-of-the-art knowledge concerning the physical characteristics of the debris population (in particular the debris albedo and the debris magnitude model) is very poor.

4.1   Study of the optical stations network architecture

At the beginning the STK-Matlab Software Interface is used for a preliminary study of the optical stations network architecture in order to understand the available observation time (i.g. the time during which the debris lighted from the Sun pass in the telescope cone angle if the ground station is in shadow considering all conditions in table 3.1) for each stations. The software has been used to propagate the generic debris motion in some generic representative orbits: generic orbits are defined from their parameters and, consequently, the observation conditions for different ground based stations will be analyzed. As above mentioned the debris orbit is defined by its parameters, but as it results from the concepts emerged by these preliminary simulations, most critical orbital parameters conditioning the observation strategy and the overall system architecture are the inclination and the RAAN.

Simulations have been run with a constant altitude (800 km because this is the zone with the most debris population in LEO, see figure 2.14) and for some periods in the year, particular for the Earth illumination condition. The orbit propagation period is 10 days. Others orbits parameters are maintained constant (see table 4.1).

Table 4.1: Selected orbital parameters for preliminary debris simulation

Orbital parameters	Magnitude
Altitude	$800\,km$
Eccenticity	0.002
Argument of periapsis	0°
True anomaly	0°
Inclination	from 0° to 110°
RAAN	from 0° to 100°
Initial epoch	1\1\2008, 1\7\2008, 21\3\2008
Propagation	10 days

Constraints imposed in STK on the debris are its illumination from direct sun when the observatory station is in observation conditions (see table 3.1 for constraint conditions).

4.1.1 Available observation time

For a preliminary station network analysis a limited number of stations have been chosen: 3 ground stations, one in the equatorial line (Malindi, Kenya) and two at an intermediary latitude, e.g. 50° (one in the northern (Greenwich, England) and one in the southern (Chile) hemispheres of the Earth) were considered. As it will be clear from the simulation results, the intermediary latitude stations are fundamental for the debris observation in particular orbits, i.e. for orbits with high inclination and a particular RAAN. In fact the observation of debris residing in these particular orbits results impossible from the equatorial ground stations for relatively long periods and only after some weeks it is possible to observe a debris in these orbits, because Earth has changed its position respectively to the Sun (see sec. 3.2.2 for a better explanation).

The available observation time for debris has been then calculated for each stations changing both inclination and the RAAN of the debris orbit (see figures 4.1 and 4.2, obtained with the debris parameters in table 4.1).

(a) Chile

(b) Greenwich

(c) Malindi
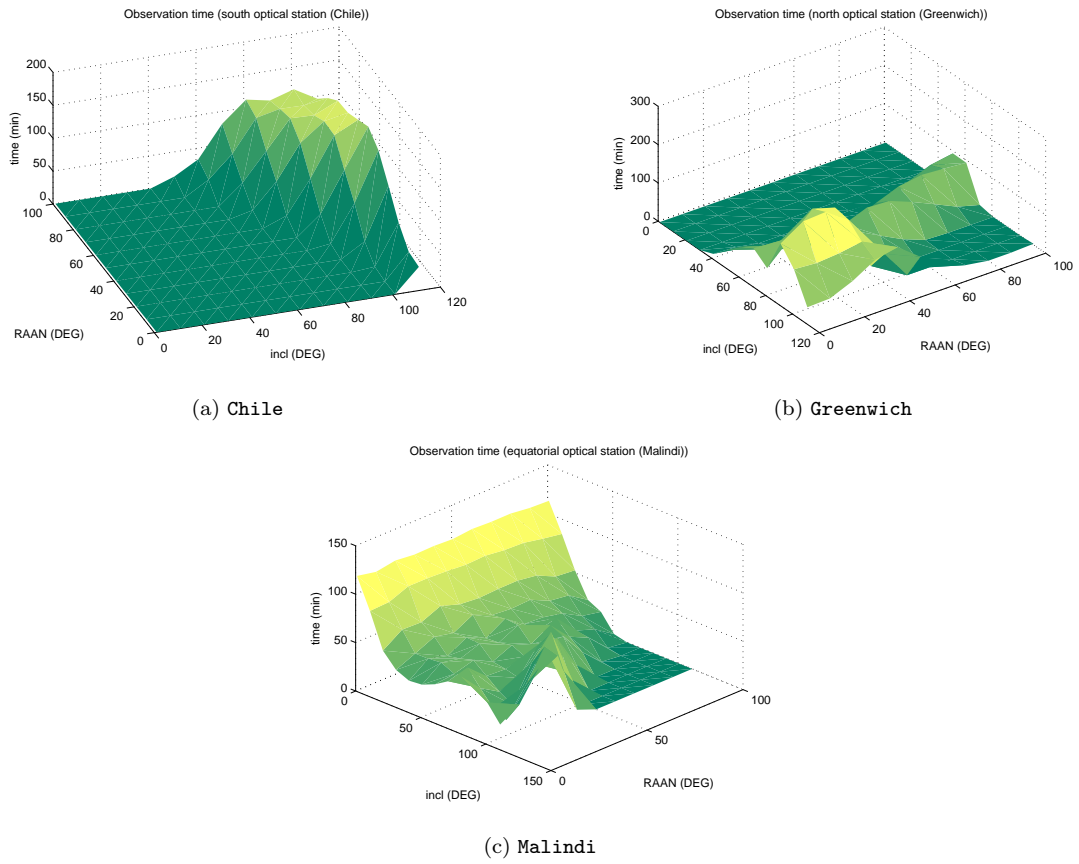
Figure 4.1: Available observation time for two intermediary latitude and one equatorial ground stations at 1\1\2008

(a) Chile

(b) Greenwich

(c) Malindi
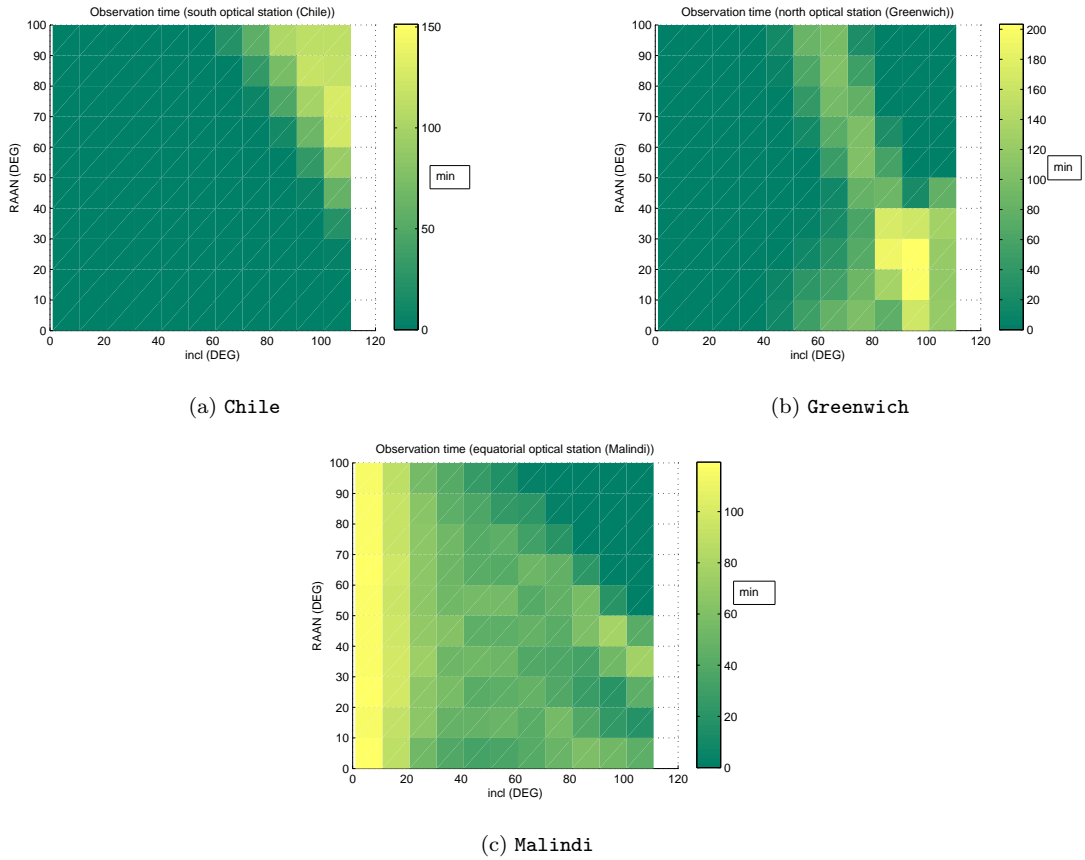
Figure 4.2: Available observation time for two intermediary latitude and one equatorial ground stations at 1\1\2008 in 2D

Figure 4.2 show the observation time for these stations: light-coloured zones represent the inclination and the RAAN for orbits with a high observation time; dark-coloured zones, on the contrary, represent situations in which the ground station is not able to observe or the observation time is very small. From figure 4.2 it is possible to verify that the considered equatorial station is not able to observe within 10 days the debris positioned in high inclination orbits characterized by RAAN higher than 50 degrees, during this year period. In general debris positioned in high inclination orbits are not very visible from an equatorial station in a short observation time period. The immediate consequence is that ground stations with intermediary latitude ($50°$) are needed in order to observe these particular orbits.

From a comparison between the equatorial station and intermediary latitude stations is possible to notice that these stations are complementary: in fact the equatorial telescope is able to observe a lot of orbits, while the other ones are observed from the telescope at $50°$ latitude, that observes less debris orbits than the equatorial one, but it can observe particular orbits with high inclination.

4.1.2 The optical stations network

From considerations in sec. 4.1.1 and sec. 3.2.2 the stations network has been chosen: 7 optical stations (1 equatorial, 3 in the north hemisphere and 3 in the south hemisphere). The figure 4.3 and the table 4.2 show the station network features.
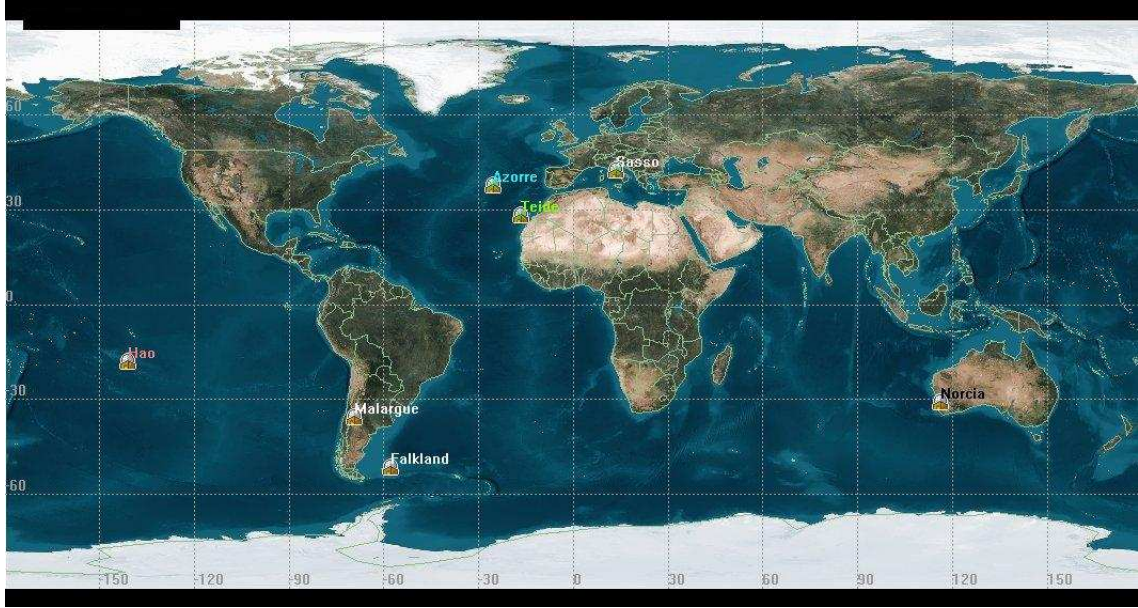
Figure 4.3: Station network for optical debris observations

Table 4.2: Station network coordinates

Station	ID	Geographic Coordinates		
		Latitude [deg]	Longitude [deg]	Height [m]
Teide (Canary Islands)	Z00	$28°18'03''N$	$16°30'42.5''W$	2392
Hao	Z01	$18°08'45''S$	$140°52'54''W$	6
Falkland Island	Z05	$51°42'32''S$	$57°50'27''W$	31
New Norcia (Australia)	Z08	$31°02'54''S$	$116°11'31''E$	245
Malargue (Argentina)	Z09	$35°46'24''S$	$69°23'59''W$	1517
Gran Sasso (Italy)	Z10	$42°29'60''N$	$13°33'04''E$	1447
Pico de Vara (Azorre Islands)	Z11	$37°47'48''N$	$25°13'10''W$	582

For each stations a brief description is presented, considering station characteristics explained in sec. 3.2.2.

Teide is an high volcano (3718 m of elevation) in Canary Island (Spain); midway up the mountain are the telescopes of the Observatorio del Teide, one of the first major international

astronomical observatories, attracting telescopes from different countries around the world for its good astronomical seeing conditions. In this place there are solar telescopes, nocturnal telescopes and radio telescopes. It's a perfect place for the optical telescope because it has all the necessary infrastructures.

Hao is an atoll in the central part of the Tuamotu Archipelago in French Polynesia; there is an old military base with a military airfield, which was the support base for the nuclear testing on nearby Mururoa atoll. In Hao there are also some support facilities, including the electrical and desalinization plants and the hospital.

Falkland Islands are an archipelago in the South Atlantic Ocean and they are a self-governing Overseas of the United Kingdom. Surrounded by cool South Atlantic waters, the Islands have a maritime subarctic climate which is very much influenced by the ocean by having a narrow annual temperature range. East Falkland is generally wetter than West Falkland; humidity and winds are constantly high and gales are very frequent, particularly in the long and severe winter. The Islands are self sufficient for economy and infrastructures, with an hospital and a modern telecommunications network. The Islands have two airports with paved runways.

New Norcia is a town in Western Australia with a ESA ground station located 8 km south of the town. The station has a 35 m radio antenna for communication with spacecraft in deep space. For this reason all necessary infrastructures are present for a ESA telescope building.

Malargue is a city in the south Argentina, located in a semi-desertic area but with some touristic infrastructures. Malargue is also the home to the southern site of the 'Pierre Auger Observatory', an international physics experiment searching for ultra-high energy cosmic rays.

Gran Sasso is a mountain in the middle Italy where in the place called Campo Imperatore there is already an observatory with a Smith telescope ($90\,cm$) now used for the NEO astronomical survey.

Pico Island is an island in the Central Group of the Portuguese Azores noted for its volcano, the highest mountain in the Azores Islands. The climate in the archipelago is tepid, oceanic and subtropical and the average annual rainfall increases from east to west (for this reason Pico Island is not a good choice). Each of the nine Azores Islands has a small airport.

Figures 4.4, 4.5 and 4.6 (obtained with the debris parameters in table 4.1) show the available debris observation time for the optical station network in some representative year periods. It is possible to notice that intermediary latitude stations (Falkland or Gran Sasso) are complementary to equatorial ones (Hao or Teide) and the observation time changes with seasons.
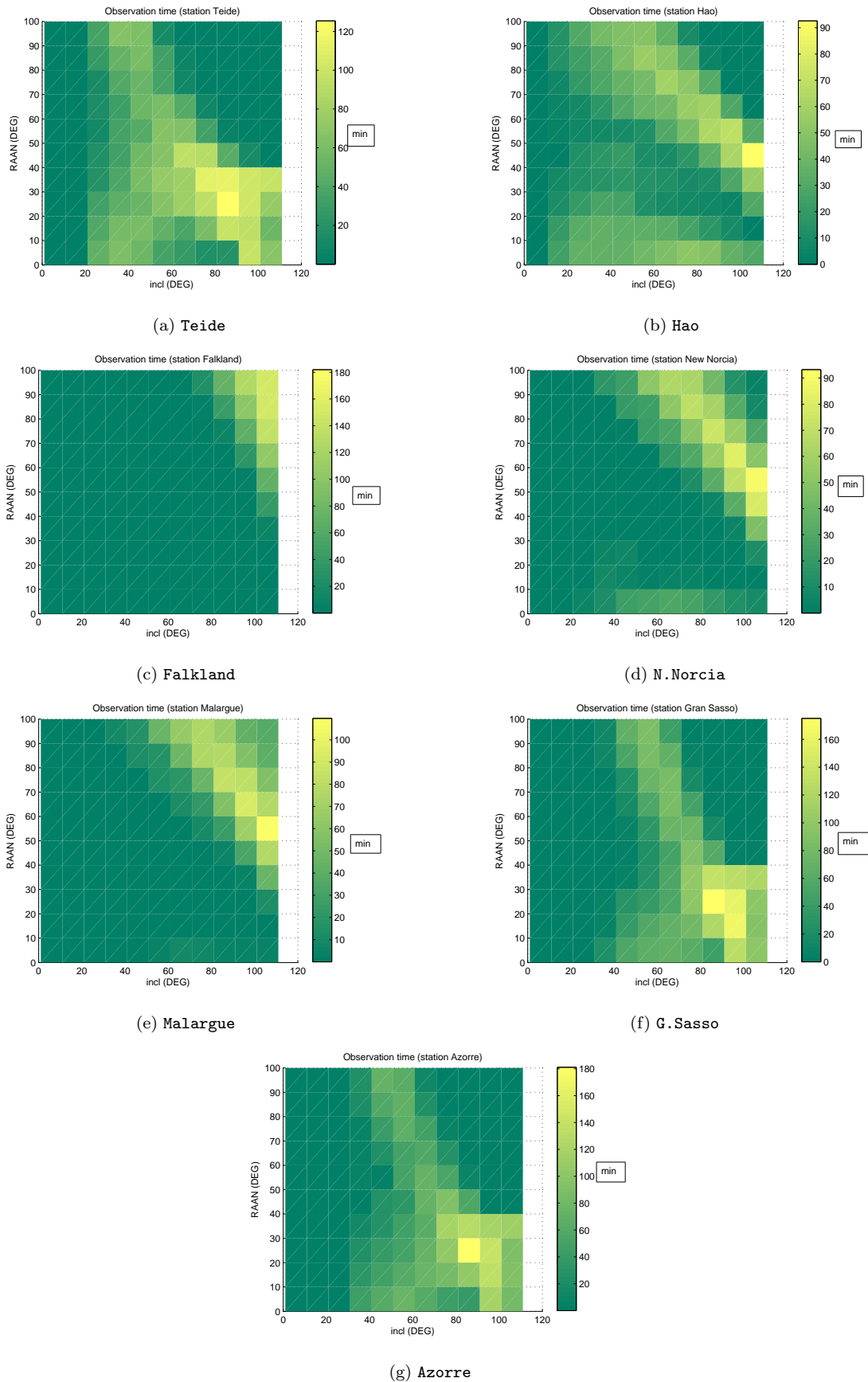
(a) Teide

(b) Hao

(c) Falkland

(d) N.Norcia

(e) Malargue

(f) G.Sasso

(g) Azorre

Figure 4.4: Observation time for the optical stations network at 1\1\2008

(a) `Teide`

(b) `Hao`

(c) `Falkland`

(d) `N.Norcia`

(e) `Malargue`

(f) `G.Sasso`

(g) `Azorre`
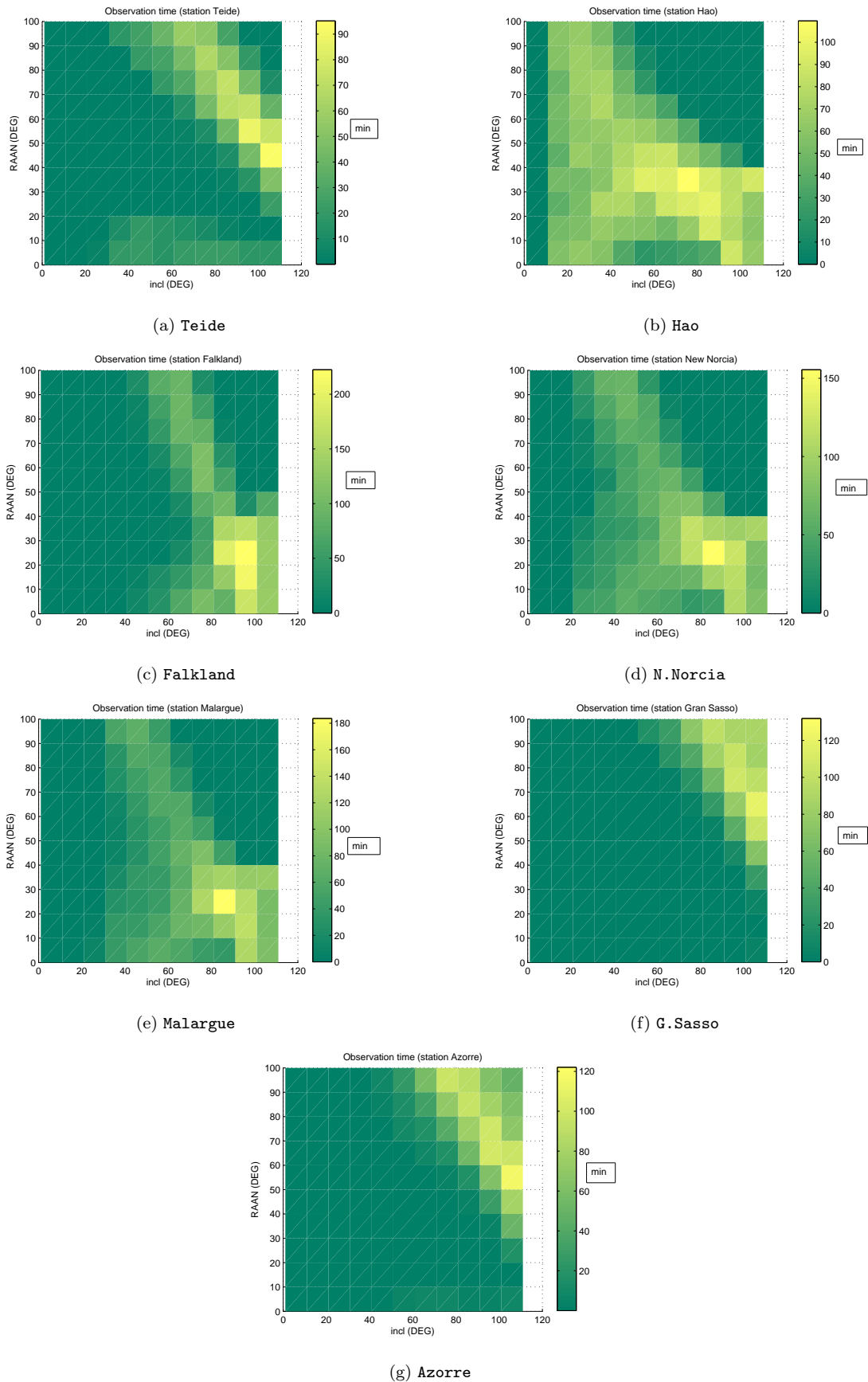
Figure 4.5: Observation time for the optical stations network at 1\7\2008

(a) `Teide`

(b) `Hao`

(c) `Falkland`

(d) `N.Norcia`

(e) `Malargue`

(f) `G.Sasso`

(g) `Azorre`
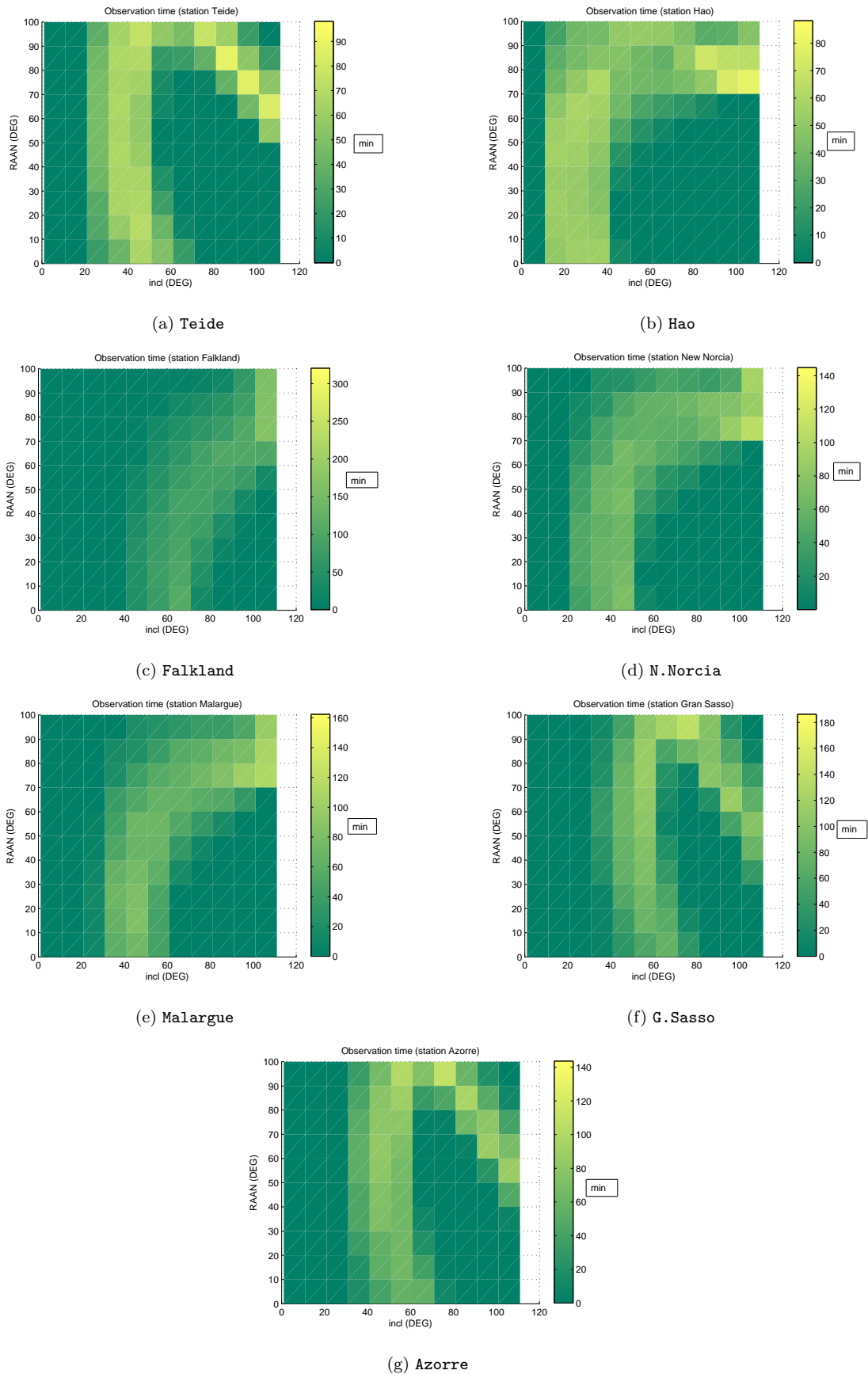
Figure 4.6: Observation time for the optical stations network at 21\3\2008

4.2   Simulated observations parameters

With the STK-Matlab Software Interface it is possible to obtained debris simulated observations considering all possible characteristic parameters of a realistic debris observation in LEO, including meteo data and debris albedo.

4.2.1   Debris albedo and magnitude study and the phase angle effect on the object observability

The state of art about debris albedo studies is now presented. Debris albedo is important to find absolute magnitude (a fundamental parameters for debris optical observations) from debris diameter. It has been shown (sec. 3.4.3) that for debris apparent magnitude calculation, an asteroid model is used and the same things is for the equation that relates absolute magnitude with the debris diameter. This thesis wants to understand the precision of asteroids formula used in the debris magnitude context and wants to find a correct debris albedo to obtain realistic simulated observations.

The albedo of an object is a measure of how strongly it reflects light from light sources such as the Sun. The range of possible values is from 0 (dark) to 1 (bright). The debris albedo depends from debris properties, so it's fundamental to know debris materials. The study of albedo, their dependence on wavelength, phase angle, and variation in time comprises a major part of the astronomical field of photometry.

Optical measurements use reflected solar radiation for observations where the shape and orientation of an object are important, but it have to consider also the surface electrical properties of the debris material (i.e., the surface albedo). The debris-station range combined with the apparent magnitude, can be used to estimate an *absolute* brightness (scaled to a fixed range and phase angle). This absolute magnitude is what is used to estimate debris size in a real observation, while in this study (with simulated debris observations) from the debris diameter of the *MASTER 2005* population file the absolute magnitude is estimated. For these estimations it's fundamental to know the debris albedo distribution that relates object size to absolute magnitude.

Two important studies about debris albedo are now summarizes with their results. They are the most important researches in the state of art context about debris albedo.

The first study [39] considers that ground-based measurements of the orbital debris environment are made using both radar and optical observations in order to gain a more complete understanding of the environment. Comparing the results of the two methods is problematic, however, since methods do not directly measures the size of the object. For radar, the radar cross section (RCS) is a complex function of size, shape, material composition and wavelength of the radar. Converting optical brightness to actual object size for both known and unknown objects is a real challenge for the optical debris community. Optical brightness are complex functions of the shape, size, surface material composition and albedo of the object's surfaces. Adding to these complexities is the fact that the objects change orientation during the observing periods due to the real or apparent rotation of the objects. Similar to radar, the brightness is also a function of the orientation of the object, not only with respect to the observing station, but also with respect

to the illumination source, the Sun. Debris have also complex irregular shapes that produce time varying amounts of shadowing which complicate the interpretation of the photometric signatures and the resulting size estimations.

Measurements acquired by the LMT telescope (see sec. 2.3.3) of a large subset of tracked debris objects with sizes estimated from their radar cross sections (RCS) indicate that the random variations in the albedo (obtained by factoring RCS from brightness) follow a log-normal distribution. In addition, this distribution appears to be independent of object size over a considerable range in size. With the absolute magnitude, it is possible, via optical measurements alone, to estimate the size distribution of debris objects by appropriate choice of a single albedo value. If an albedo for the object is assumed, the photometric brightness of the object can be converted into an optical cross section. It is possible to say that the size distribution of debris obeys a simple power-law and the distribution of debris albedos is observed to be log-normal. There exists a unique global albedo that when applied to an observed brightness distribution recovers the debris size distribution. For the orbital debris population a significant overestimate of the number of objects at a given size results if the canonical 0.1 (a commonly assumed albedo for low Earth orbit objects) albedo is employed. This disproportionately transforms intrinsically smaller objects to larger sizes resulting in a skewed and overestimated size distribution. The choice of albedo is critical over estimating the population at a given size if the choice is too low, underestimating if too high. It was determined that a transformational albedo of 0.13 applied to the observed brightness distribution fully recovered the intrinsic size distribution of the debris population. It's important to consider if after a debris fragmentation, involved debris change their albedo like for asteroid fragmentation.

Another important study about debris albedo is now presented [19]. When transforming number as a function of observed orbital debris brightness into number as a function of orbital debris diameter, the proper average albedo not only depends on the physical characteristics of the debris and the albedo distribution, but on the relative number of small debris to large debris. When the relative number of small debris to large debris is as great as has been measured for debris (that is, that there is a much larger number of small debris as compared to large debris), the frequency of specular reflections was found to increase the proper average albedo significantly.

For any given number of objects, there would be both a corresponding radar diameter and an optical magnitude. The LMT data sets represent the best data sets for obtaining an average albedo. When the LMT detects an object, its maximum brightness is measured and recorded. If the object is 'known' and an average radar cross-section is available, this average is converted to a radar diameter. The maximum visual brightness while the object was in the telescope's field of view was measured and then converted to absolute magnitude, where absolute magnitude is defined as an object's maximum brightness in visual magnitude when observed at a range of 1000 km. The radar cross-sections of 236 of these objects were known and were converted to radar diameter using the NASA size determination model originally developed to analyze the Haystack radar data. Figure 4.7 is a scatter plot of that data, where the absolute magnitude and radar diameter of each object is plotted in terms of these derived parameters. Since absolute magnitude is proportional to the log of visual brightness, which is also proportional to the log of optical

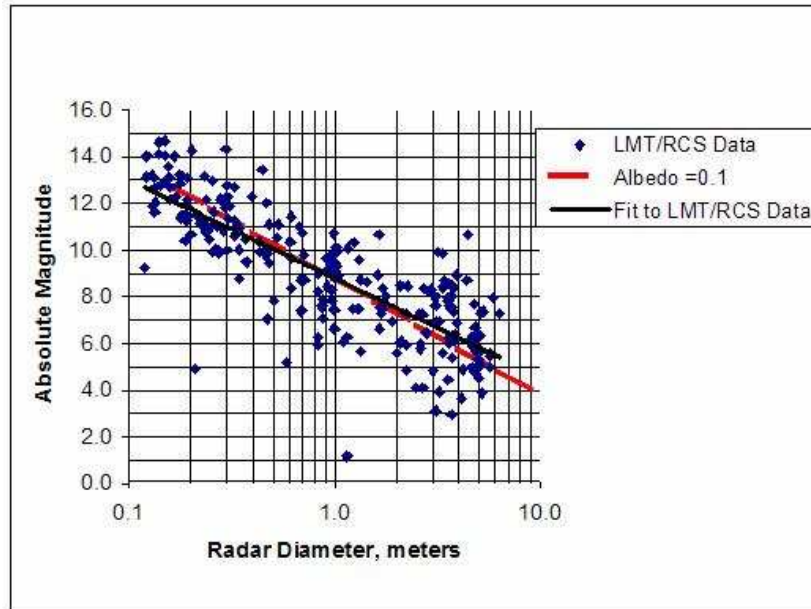diameter, this plot has the same characteristics as a log optical diameter vs. log radar diameter plot.

Figure 4.7: Catalogued objects detected during the LMT 1999-2000 viewing season considering radar diameter from radar detections and absolute magnitude from LMT optical observations (from [19])

The dashed line in figure represents the theoretical relationship between absolute magnitude and radar diameter for a spherical object with an albedo of 0.1 that scatters light equally in all directions. Note that this line seems to fit the data well. The solid line is a least square fit to the data and illustrates a trend of increasing albedo with decreasing size, where objects smaller than about 1 meter will have an albedo greater than 0.1 and objects larger than about 1 meter will have an albedo less than 0.1.

It would also show that in the debris population analysed in this study [19], only 10% of the objects have an albedo greater than 0.5, and another 4% have an albedo greater than 1.0, including two objects with an albedo just over 80. The results indicate that an average albedo of 0.1 is the proper average only for the smaller catalogued objects. The distribution of objects that are too small to be catalogued, yet might be detected optically, is expected to have larger values of average albedo that might be more than 30 times larger than the average for smaller catalogued objects.

From the above theoretical predictions, if an albedo of 0.1 is assumed and used to predict the 'optical diameter' for the optically detected catalogued objects, then a plot of resulting number vs. 'optical diameter' and a plot of number vs. radar diameter should compare favorably, at least for the smaller catalogued objects. For larger sizes the study suggests a larger albedo is necessary to obtain agreement.

In LEO a slightly larger albedo of about 0.25 might be appropriate for sizes between 0.2 m and 1 m, and a much smaller albedo would be required for the few large fragments; however, 0.18 works fairly well for the whole distribution. This study has also shown that the proper average albedo for objects smaller than 20 cm is greater than 0.18 (albedo for these smaller debris should be between 0.23 and 0.36).

The conclusion of these studies about debris albedo, important for the relation between absolute magnitude and debris diameter, is that the debris albedo varies with the debris size, but it's possible to estimate an average albedo for all debris population (0.13 for [39] and 0.18 for [19], considering that 0.1 is the value for the smaller catalogued objects). In this thesis it has been assumed an albedo of 0.11 for all debris population, a correct value because the study is focused only on small debris, but this value is very conservative.

The debris population file used for analysis in this thesis comes with no indication of the albedo or magnitude of the objects (see sec. 3.3.1) because the state of art knowledge concerning the physical characteristics of the debris population, like albedo and magnitude, is very poor. An albedo-absolute magnitude realistic model from asteroids, considering the previous debris albedo study, has been used in this thesis.

The common formula used for the correlation between absolute magnitude, albedo and diameter of asteroids (but now used for debris) is [4]:

$$log_{10}\, p = 6.259 - 2\, log_{10}\, d - 0.4\, H_{absolute} \tag{4.1}$$

where p is the debris albedo and d the debris diameter in km (because this formula derives from asteroid studies). Considering from previous studies that a commonly accepted value of the albedo for a generic debris is between 0.1 and 0.2, an albedo $p = 0.11$ for each object has been chosen. This is a very conservative value equivalent to cut a 0.75 magnitude factor when compared to the more relaxed 0.2 value. Then, the absolute magnitude was derived according to the equation (4.1) considering $p = 0.11$, as:

$$H_{absolute} = 33 - 5\, log_{10}\, D \tag{4.2}$$

where d is the debris diameter in meters.

The figure 4.8 shows the absolute magnitude distribution of the debris population in LEO from the *MASTER 2005* population file (sec. 2.2).
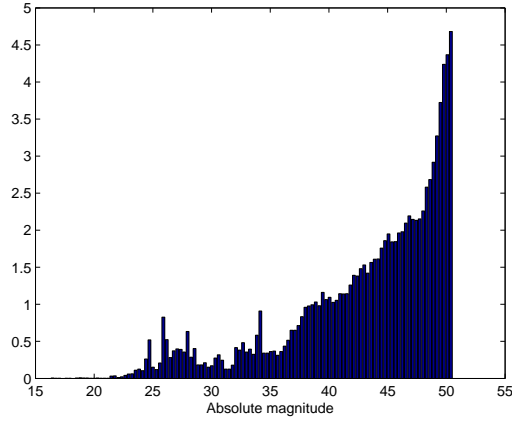
Figure 4.8: The absolute magnitude distribution of the debris population in LEO

Figure 4.9 represents the absolute and apparent magnitude of a debris varying the slope parameter G (see sec. 3.4.3) and the debris albedo. The first figure derives from equation 4.1, considering albedo classes in table 3.2, while the second figure comes from equation 3.3, where the absolute magnitude, range and Δ are fixed.
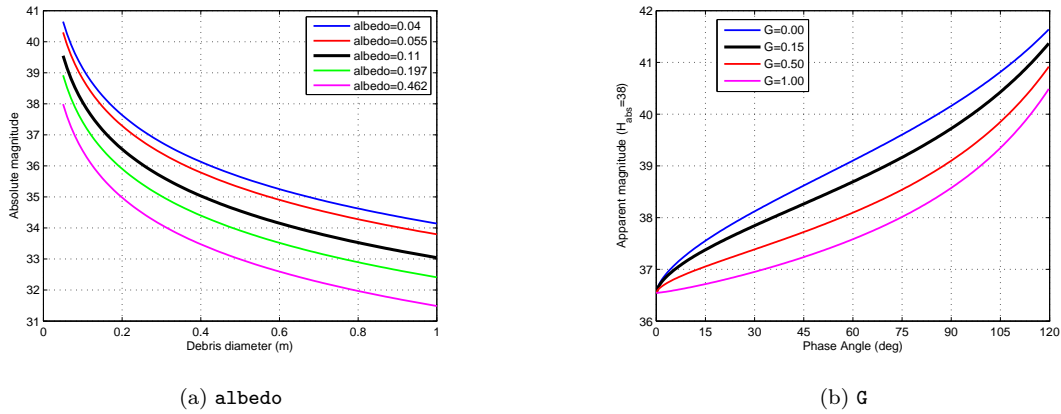

(a) `albedo`

(b) `G`

Figure 4.9: Absolute and apparent magnitude of a debris varying the slope parameter G and the debris albedo (black lines represent values used in this study: albedo=0.11 and G=0.15)

There is another formula for the correlation between absolute magnitude, albedo and diameter of asteroids or minor planets (but now used for debris) [66]:

$$d = \frac{1329}{\sqrt{p}} 10^{-0.2 H_{absolute}} \tag{4.3}$$

where p is the debris albedo and d the debris diameter in km. This equation is very similar to equation (4.1) (see in the figure 4.10 for the fixed albedo value used in this study), but is not used in this thesis.
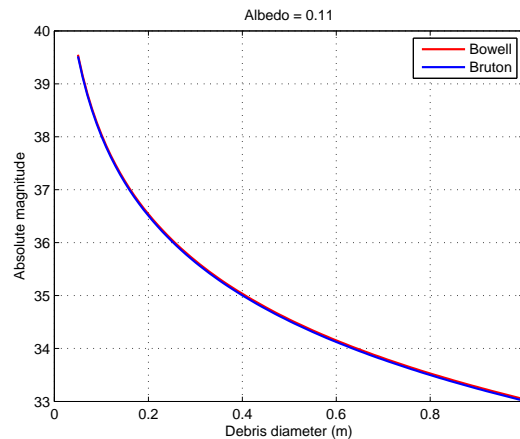
Figure 4.10: Comparison between formula (4.1) and (4.3) for the fixed albedo value

Apparent magnitude strongly depends from the phase angle, the angle between Sun-object-observer. A small phase angle means a small apparent magnitude (see figure 3.8), so a perfect condition for the debris observation with a brighter debris. The observation condition is quite restrictive: the orbiting objects are fully illuminated in all directions and with a small phase angles (so debris have a small apparent magnitude) only immediately after sunset and immediately before sunrise and debris has to be seen in the east direction after the sunset and in the west direction before the sunrise. In fact, in these regions of the sky phase angles are smaller, but in the same regions it's not possible to observe debris because they are in the Earth shadow. For these reasons regions in the sky where observations are possible are very close to the Earth shadow border. Very small objects, down to some centimeters, are detectable only when they pass very close to the Earth shadow border and during the small observability window after sunset or before sunrise. It is very critical to begin operations as soon as the sky is dark enough to avoid background saturation of the images and, conversely, to stop operations as far as possible.

It has been considered a dynamical telescope in the STK-Matlab Software Interface, that 'filters' the observation period. The software calculates the phase angle at the beginning and at the end of each debris observation period from a station, then it divides the observation period into 3 parts and it selects the part with the minor phase angle (and so with a good condition for observation) (see sec. 3.4.3).

Figure 4.11 shows that typical phase angle functions are monotonically decreasing or increasing in magnitude. The red point is the phase angle value chosen after the STK-Matlab filter during the debris observation period.

(a)

(b)

(c)
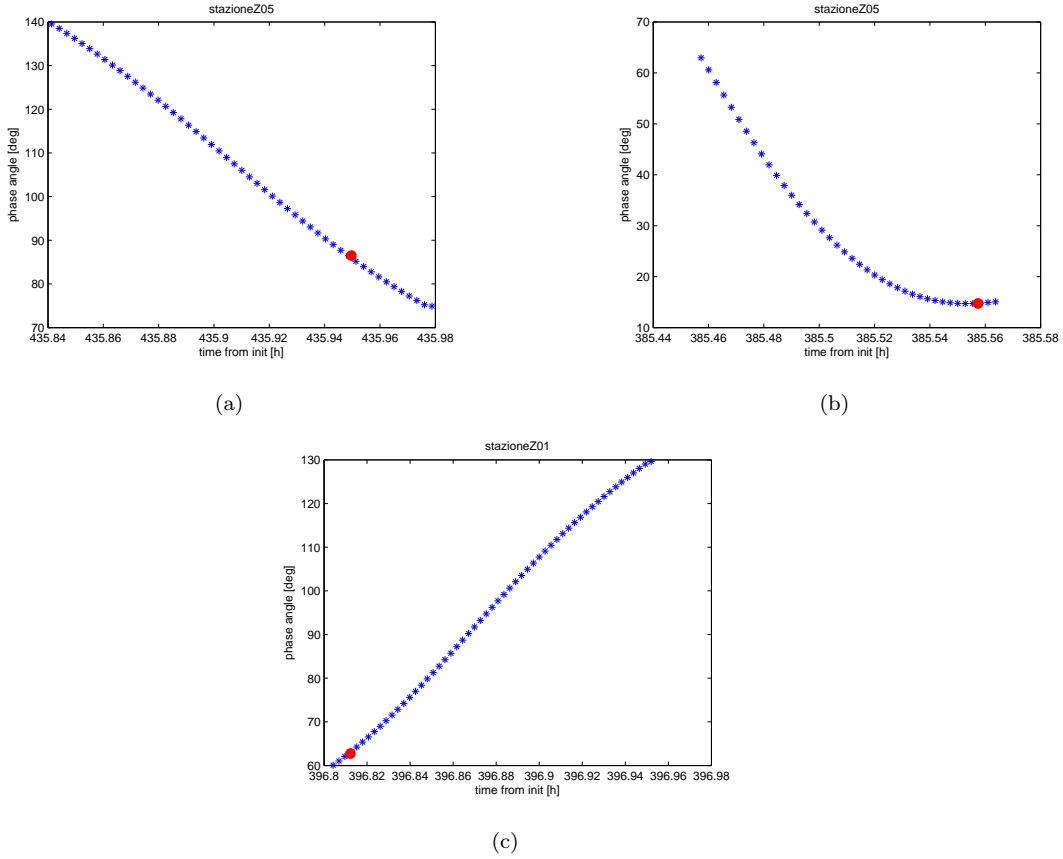
Figure 4.11: Phase angle values during a debris observation period from a station (time on x-axis refers to initial propagation time of debris)

It's possible that phase angle functions are not always monotonically decreasing (or increasing) in brightness and in this case it's possible that the chosen value (red point) is not in the part with the minor phase angle.

Following figures represent all observations of a particular debris with H = 37.5 (a 12.5 cm debris size) from all stations, propagated for 20 days and considering the phase angle filter to improve the observation quality. In these figures each points represent a debris observation. Figure 4.12 shows the debris apparent magnitude and the debris S/N as function of the distance between stations and debris (the range). Circles represent debris observations whereas black lines fit to the data and it is possible to notice the correct S/N and $H_{apparent}$ behaviour of the debris when the range increases. There is a little separated population of observations with high range values because this analysed debris is a TLEO object and so these particular observations are achieved near debris orbit apogee.
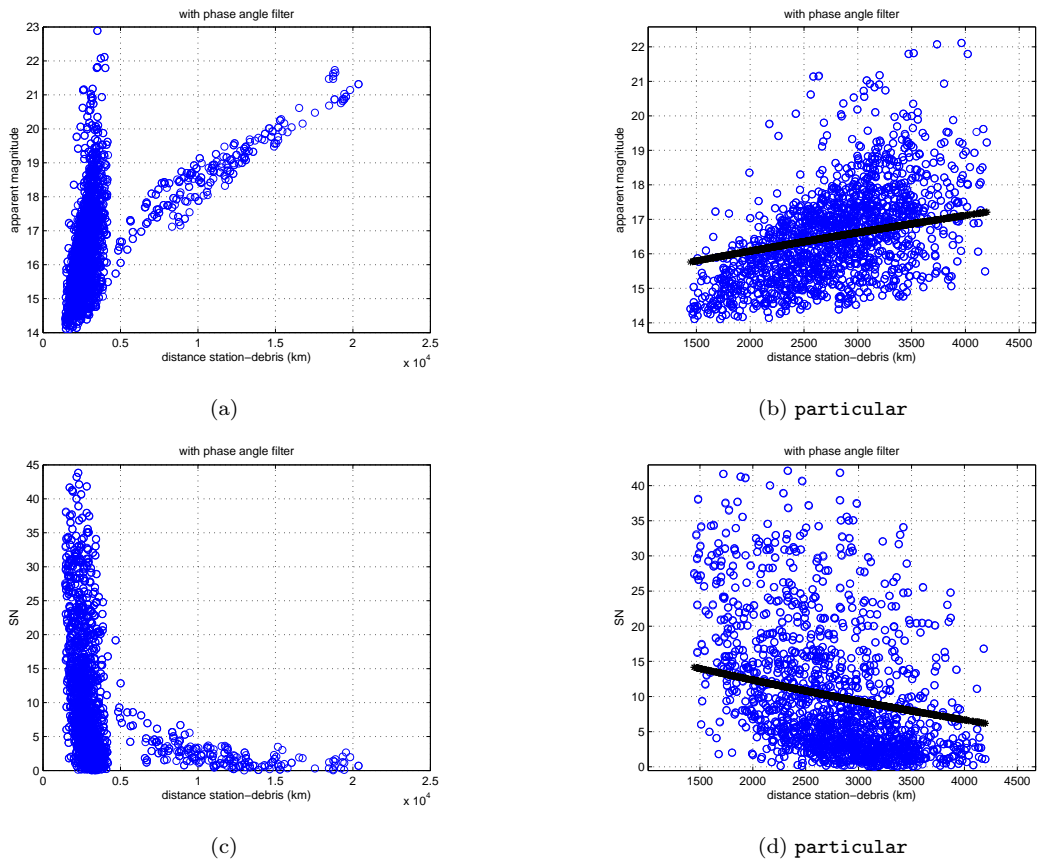
Figure 4.12: Debris apparent magnitude and the S/N as function of the distance between stations and debris (figure b) and figure d) are zoom of figures a) and c))

The figure 4.13 shows the debris apparent magnitude as function of the observation elevation angle considering observations with and without the atmospheric disturbance term. It's possible to notice that a lot of observations have low elevation angles.
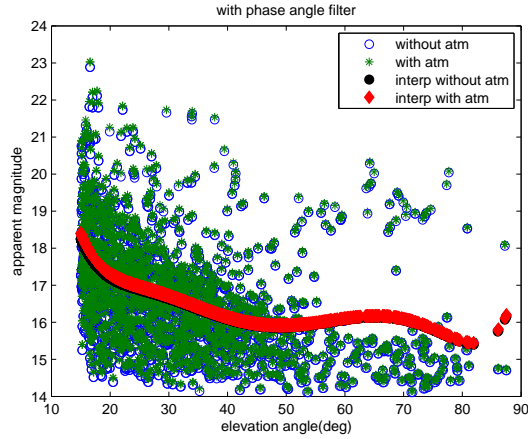
Figure 4.13: The debris apparent magnitude as function of the observation elevation angle (red and black lines fit to the data)

Figure 4.14 represents the $H_{apparent}$ as function of phase angle with and without the phase angle filter implemented in the STK-Matlab Software Interface. All circles (observations) are interpolated and it is possible to notice the phase angle filter effect: most of observations show a phase angle below $100°$, so the apparent magnitude is smaller (with good observation conditions) than those computed in the condition without phase angle filter.

(a)

(b)
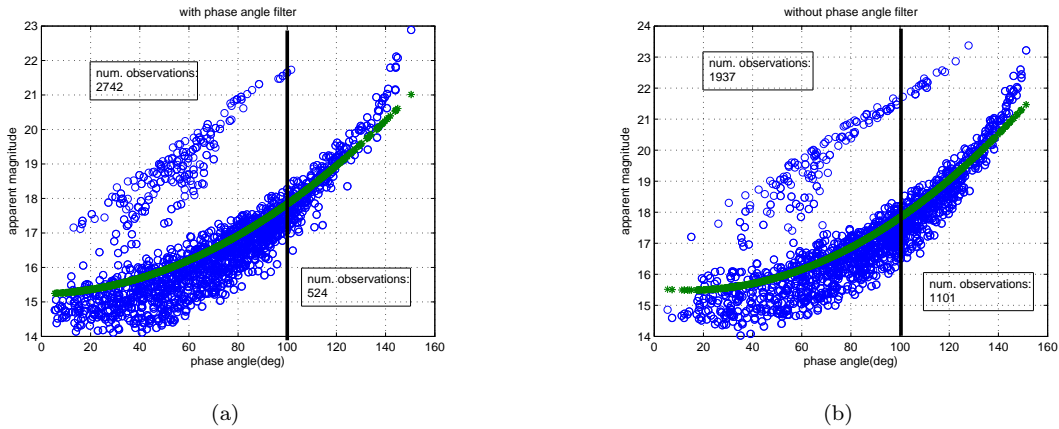
Figure 4.14: $H_{apparent}$ as function of phase angle with and without the phase angle filter

4.2.2 Mean monthly cloud coverage data

A statistical factor which must be considered in the definition of the optical network architecture is represented by the mean meteorological conditions registered at the observatory station: one of the most relevant parameters affecting the possibility to operate the observatory is represented by the cloud coverage. Considering meteorological conditions debris observation is more realistic. In this view some meteorological data bases have been inquired by the *Carlo Gavazzi Space* for the *SARA* study in order to obtain the monthly average *total cloud amount*, defined as

the percentage of cloud coverage of the sky. Another important consideration resides in the fact that the actual interesting data are those concerning not the whole diurnal period but particularly the night, during which observations are effectively possible. In fact, particularly for low latitude stations, the cloud coverage registered during daytime can differ from the corresponding coverage registered during nighttime.

In order to obtain an estimate of the effective nocturnal mean monthly total cloud amount, the ISCCP (NASA) database was inquired by the *Carlo Gavazzi Space* for the *SARA* proposal and the data concerning daily atmospheric data were accessed and processed by the *Carlo Gavazzi Space*. The applied data allow to obtain, in particular, the monthly cloud coverage, averaged over the period spanning from July 1983 to June 2008 for all the Earth surface. Data are collected from the suite of weather satellites operated by several nations and processed by several groups in government agencies, laboratories, and universities.

This datum was calculated for each day of year 2003, 2004, 2005, 2006 and 2007 years: the five year periods were selected principally due to the better quality of the data contained in the corresponding data files (mainly due to an enhanced sensor technology available in that period with respect to the previous year periods) and to limit the analysis to a data set enough significant.

A detailed set of daily nocturnal data was generated allowing the acquisition of statistical tables reporting for each selected observatory station in table 4.2 and for each year between 2003-2007 period, 2 columns:

- a first column containing the progressive day of the year (1-365)

- second column containing the corresponding calculated nocturnal cloud coverage percentage

The meteo filter computation developed in a Matlab program created for debris analysis detection in this thesis context (see results in sec. 4.3) is based on a statistical method: a random number between 0-100 is generated and if the number is greater than the nocturnal cloud coverage percentage the debris is observed while if the number is littler than the coverage percentage the debris is not observed.

Table 4.3 summarizes the nocturnal cloud coverage percentage for the station network for each year considered in this study.

Table 4.3: Nocturnal cloud coverage percentage for the station network

Station	**2007**	**2006**	**2005**	**2004**	**2003**
Teide	39.629	46.874	46.305	44.095	43.265
Hao	51.083	46.348	55.173	49.726	55.383
Falkland	72.797	72.168	70.887	70.114	72.467
New Norcia	34.063	30.404	37.859	34.374	34.566
Malargue	43.933	44.805	48.599	50.751	49.491
Gran Sasso	46.620	48.628	51.397	52.735	49.492
Azorre	67.173	69.134	68.027	72.742	67.793

The generated tables with meteo data are stored in ASCII format files (from the *Carlo Gavazzi Space* for the *SARA* proposal) which are provided to the observation simulator (the Matlab program created in this thesis context) in order to take into account the statistical atmospheric factor; for these analyses the year 2007 has been chosen. The figure 4.15 shows the nocturnal cloud coverage percentage for the network station during the 2007.
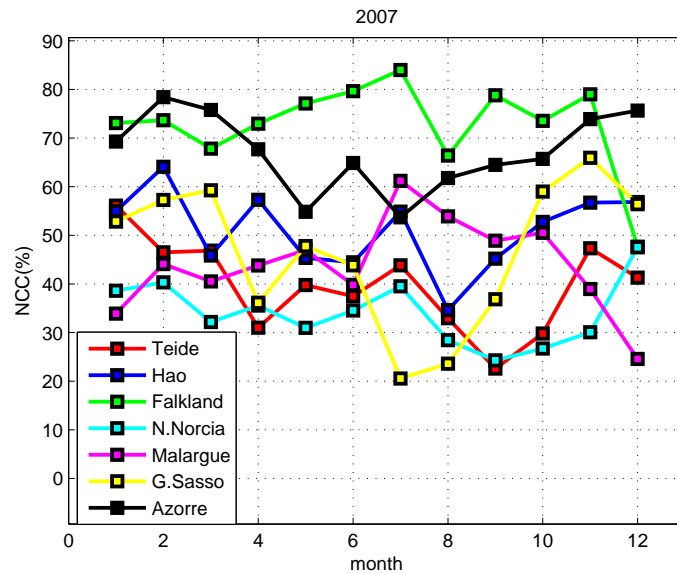

Figure 4.15: Nocturnal cloud coverage (NCC) percentage for the network station during the 2007

The figure 4.16 illustrates the nocturnal cloud coverage percentage for a station (Azorre station) during a month (December) for each year.
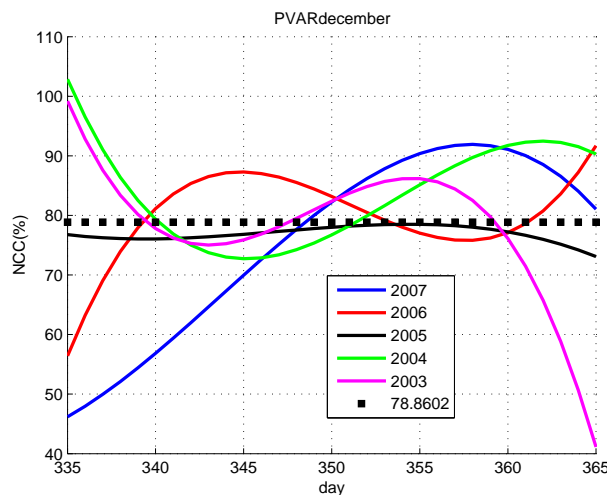
Figure 4.16: Nocturnal cloud coverage (NCC) percentage for Azorre at December (black point represents the monthly mean value during years)

4.3   Simulated observation results

In this section debris observation results from simulations are presented. Simulated observations computed from the STK-Matlab Software Interface are now analysed with ad-hoc Matlab program created in thesis context in order to understand debris detectability. Same simulated observation results are also used for the orbit determination developed from the Department of Mathematics of the University of Pisa. It is important to remind that in this thesis debris detection is study, whereas the debris orbit determination is studied by the Department of Mathematics of the University of Pisa.

Table 4.4 summarizes study assumptions for debris observability and detectability. These assumptions has been decided by the *Carlo Gavazzi Space* for *SARA* study (for better explanation see previous chapters), but the debris observation analysis Matlab program has been developed only for this thesis.

Table 4.4: Observability and detectability conditions for a *valid debris observation*

Object	Observability condition	
Ground optical station	Darkness	Sun 10° below horizon
Ground optical station	Time observation	2 minutes
Ground optical station	Meteo	Nocturnal cloud coverage percentage during 2007
Ground optical station	Station network	7 stations (figure 4.3)
Telescope	Minimum angle for debris	15° elevation angle from the horizon
		20° from the moon
Debris	Lighting	Illuminated
Debris	Albedo	0.11
Debris	Slope parameter G	0.15
Debris	Magnitude model	IAU magnitude model for asteroids
	Detectability condition	
Debris	S/N critical	6

It is important to remind that a debris is *observable* when all the observability conditions are satisfied. After the application of meteo data with the Matlab program, debris is *observed* if there is good meteo conditions. An observed debris is also *detected* when $(S/N)_{tracklet} > 6$ (this condition is computed with the Matlab program). In this case the debris observation is considered a *valid observation*.

The LEO debris population from the particular *MASTER 2005* file (see sec. 2.2) has been divided into two sub-populations in order to perform two complementary analysis.

- Simulation 1: debris with a perigee altitude between 1300 km and 2000 km (debris diameter from 8 to 26 cm)

- Simulation 2: debris with a perigee altitude between 1000 km and 1300 km (debris diameter from 5 to 25 cm)

Different debris diameters chosen for simulations respect study requirements (they refers to ESA requirements for this study, from figure 3.1). These simulations are achieved only for small debris (under 26 cm diameter) because analysis will show that debris over 15-20 cm are easily detected because they have a lot of observations, so it's unnecessary to study over 26 cm. The simulation period is 2 months, January and February 2008, but analysis considering different seasons has been implemented.

The figure 4.17 shows debris populations chosen for simulations as functions of the perigee altitude.
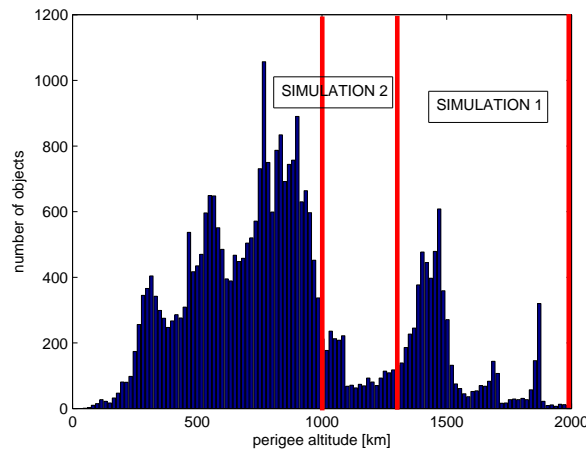
Figure 4.17: Debris population for simulations (the debris population for analysis varies from 1000 to 2000 km as perigee radius)

The debris population analysis in LEO (see sec. 2.2), has been shown that there are a lot of objects with a great eccentricity and apogee radius (HEO debris) that include GTO debris and Molniya debris; it's very difficult to detect these objects because at apogee they are too far for a detection, while at perigee they move quickly. They have been considered like a sub-population of TLEO objects and they are very important because they include GTO debris, a risk for most important launchers that operate in GTO. Figure 4.18 shows debris population considering HEO objects: it's possible to notice that a lot of HEO objects are GTO or Molniya debris (see considerations for LEO population distribution in sec. 2.2).

(a)   (b)
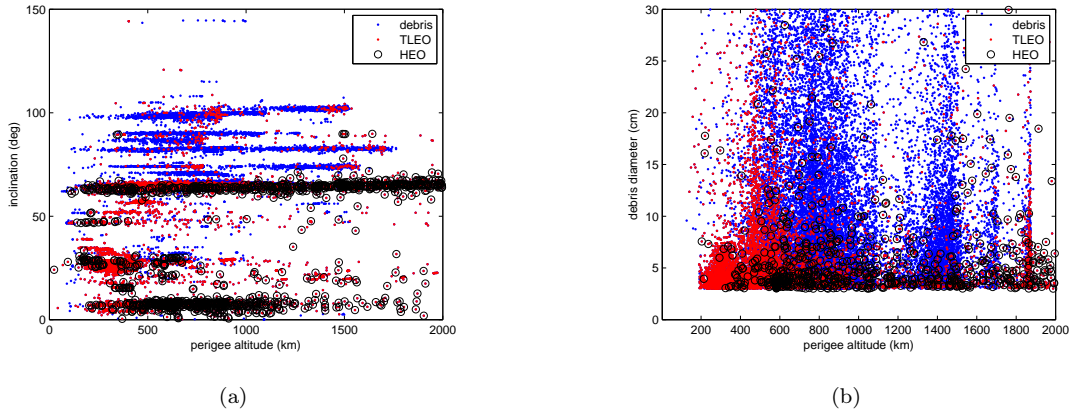
Figure 4.18: Debris population considering resident LEO debris (blue dots), TLEO debris (red dots) and HEO debris (black circles)

The table 4.5 shows characteristics of debris population in LEO, considering all debris, TLEO debris and HEO debris (the analysed population is the same in sec. 2.2) selected for simulations.

Table 4.5: Characteristics of the population model considering TLEO objects and HEO debris like a sub-population of TLEO debris

	Total number	$h_p > 1000 km$ $d > 5cm$	**Simulation 1** (sampled debris 1:2)	**Simulation 2** (sampled debris 1:1)
All debris	31682	6333 (19.9% of pop.)	1821 (5.7% of pop.)	1104 (3.5% of pop.)
TLEO debris	8709 (27.4% of pop.)	796 (9.1% of TLEO obj.)	184 (2.11% of TLEO obj.)	109 (1.25% of TLEO obj.)
HEO debris	1116 (3.52% of pop.)	274 (24.55% of HEO obj.)	34 (3% of HEO obj.)	39 (3.5% of HEO obj.)

Results for debris with $2000\,km > h_p > 1300\,km$

The first simulation for 912 debris is achieved with the following parameters. In this simulation objects are sampled 1:2. The figure 4.19 shows the debris distribution used for simulated observations. Most of TLEO debris are in a stripe at 1870 km of perigee altitude.
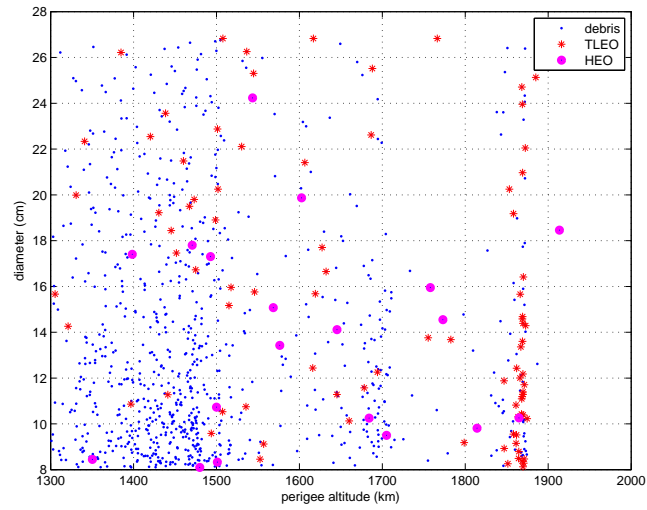
Figure 4.19: Debris distribution for the simulation 1

The figure 4.20 shows the S/N as function of the apparent magnitude for all debris simulated observations. The first figure is in a semi-logarithmic scale and it's important to notice the scattering in apparent magnitude for low S/N values (under 1).

(a)

(b)
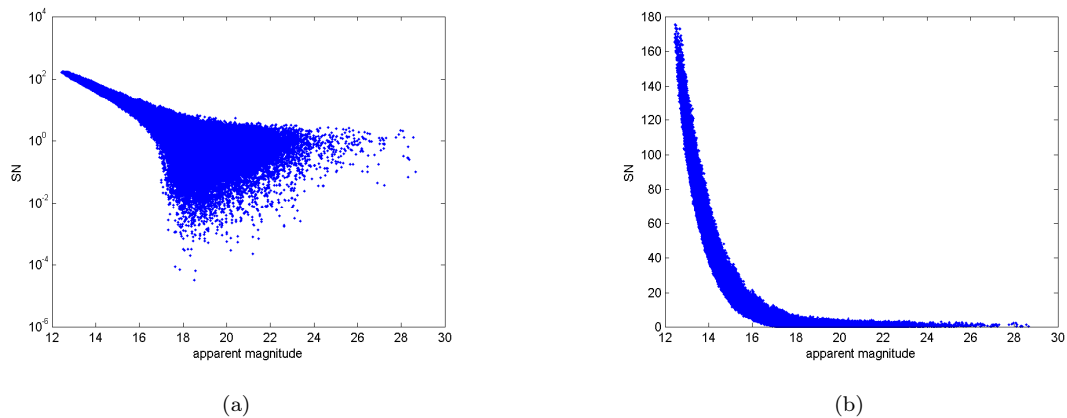
Figure 4.20: S/N as function of the apparent magnitude for all debris simulated observations (figure *a)* is in a semi-logarithmic scale)

The figure 4.21 shows the astrometric and photometric uncertainty histogram and apparent magnitude histogram.

(a)

(b)

(c)
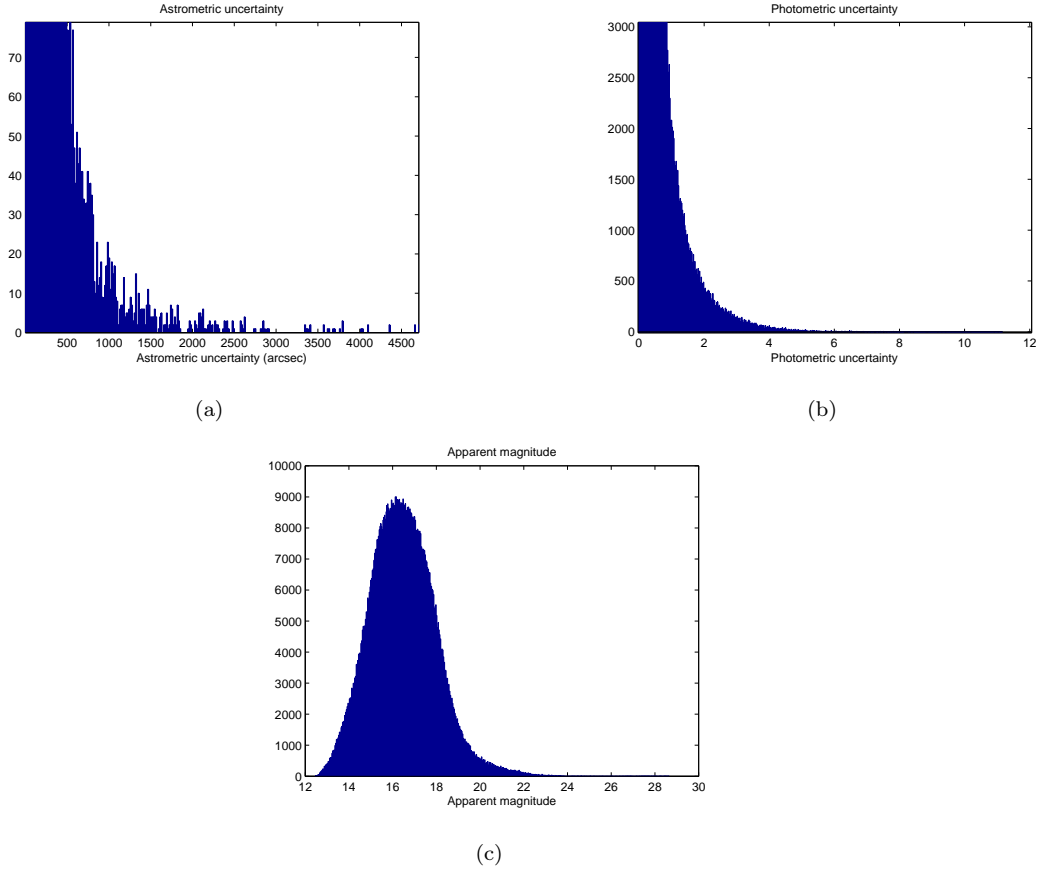
Figure 4.21: Astrometric (figure *a)*) and photometric uncertainty (figure *b)*) histogram and apparent magnitude histogram (figure *c)*)

The simulation has the following parameters (table 4.6).

Table 4.6: Debris population parameters used for simulation 1

Debris number	912
Sampled debris	1:2
Perigee altitude	from 1301.023 to 1913.482 km
Absolute magnitude	from 35.857 to 38.458
Diameter	from 8.098 to 26.828 cm
Debris always in LEO	806
Debris in TLEO (considering debris in HEO)	106 (11.62%)
Debris in HEO	19 (2.08%)
Simulation period	60 days (January and February 2008)
Number of ground optical stations	7

Following figures (figure 4.22 and figure 4.23) represent the percentage of valid observations

from all the observations for each debris as a function of perigee altitude and debris diameter. It is possible to notice the TLEO/HEO debris (in red) and the never detectable debris (black square): 11 after 28 days and 7 after 60 days. Blue points are the debris.

(a)   (b)
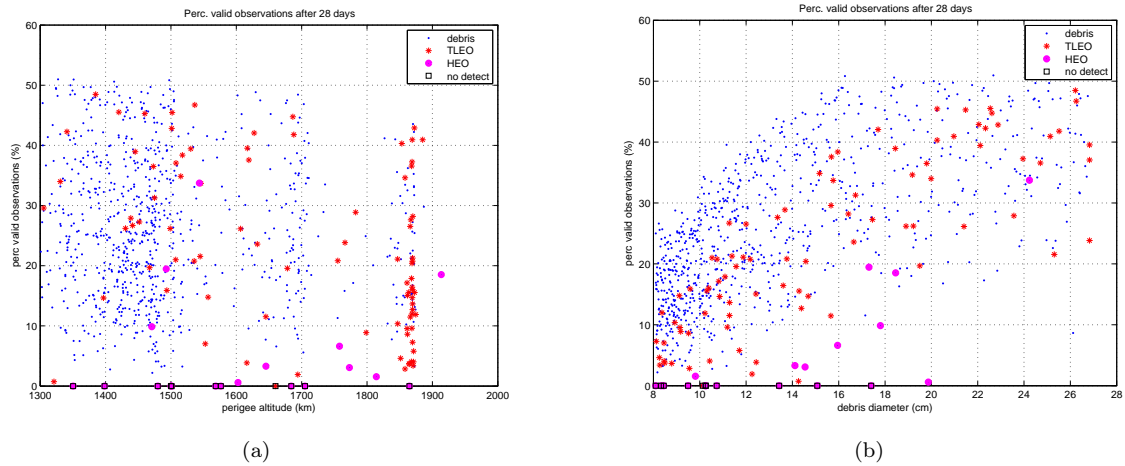
Figure 4.22: Percentage of valid observations for each debris as a function of perigee altitude and debris diameter after a 28 days for the simulation 1
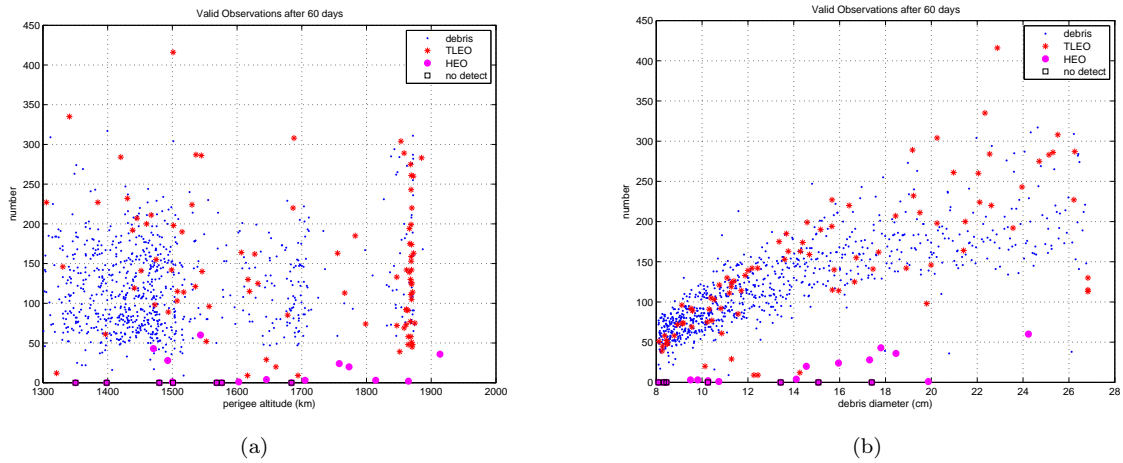

(a)   (b)
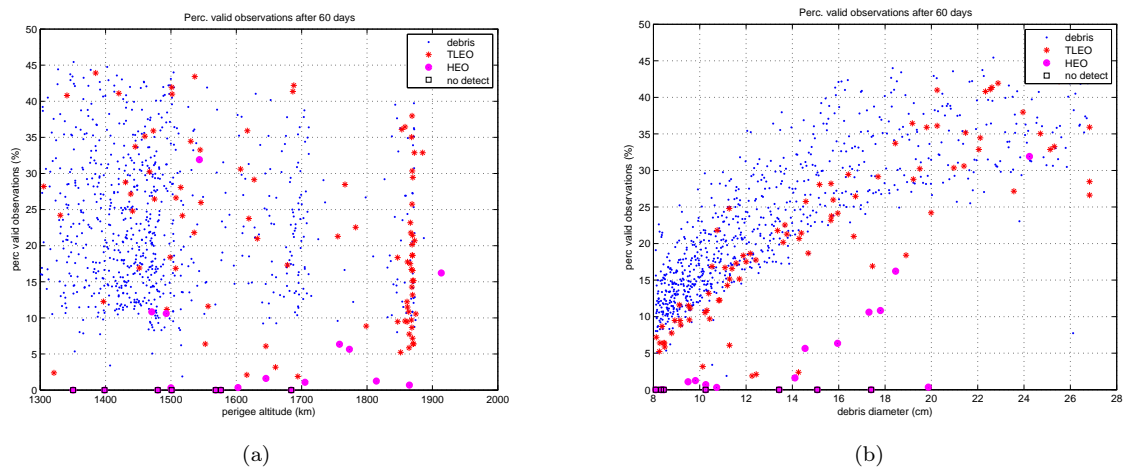
Figure 4.23: Percentage of valid observations for each debris as a function of perigee altitude and debris diameter after a 60 days for the simulation 1

The following figures (figure 4.24 and figure 4.25) represent the total number of valid observations as a function of perigee altitude and debris diameter.
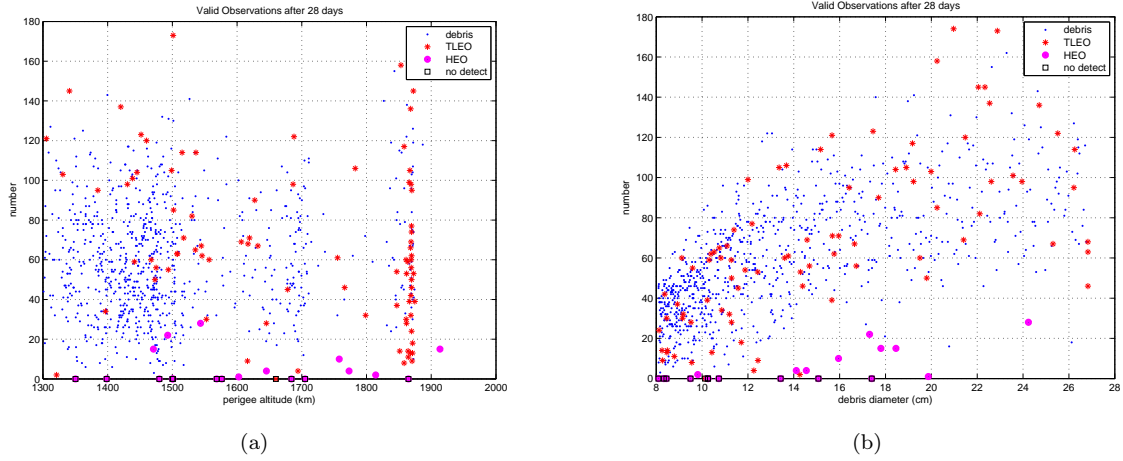
Figure 4.24: Total number of valid observations for each debris as a function of perigee altitude and debris diameter after a 28 days for the simulation 1

Figure 4.25: Total number of valid observations for each debris as a function of perigee altitude and debris diameter after a 60 days for the simulation 1

The figure 4.26 represents the debris analyzed population (in term of perigee altitude and debris diameter) after 28 days and 60 days; blue points represent debris, red points are TLEO/HEO debris and black square are never detected debris. Two curves are the system requirements, guarantee and upgradable, for LEO resident objects (see sec. 3.1.1 for more details). ESA requirements for the SSA study are analysed in this thesis only for debris detection and not for debris orbit determination.
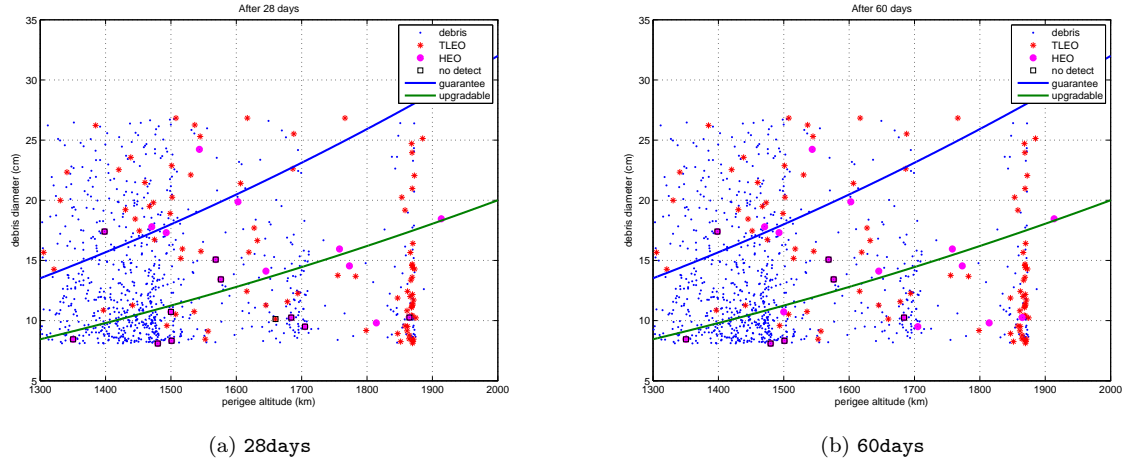
(a) 28days
(b) 60days

Figure 4.26: Debris detection results after 28 days and 60 days for simulation 1

From figures 4.26 it is possible to notice that the never detectable debris are only TLEO or HEO debris (after 60 days only HEO debris are never detected), so for the LEO resident population all requirements are satisfied for the debris detectability. It's possible to notice also that we have a lot of debris with valid observations under the upgradable curve requirements. HEO debris need particular and dedicated observations where debris is observed at apogee. In the regions around the apogees the objects also move slowest and thus stay there for most of the time. There is a disadvantage of searching objects near the apogees of their orbits: the distances are largest in these regions, and thus the apparent magnitudes are faintest. It can, however, be shown that the advantage of the small changes in apparent angular velocity outperforms the disadvantage of large distances.

Results for debris with $1300\,km > h_p > 1000\,km$

The second simulation for 1104 debris is achieved with the following parameters. In this simulation objects are sampled 1:1, so all debris in this region are studied. The figure 4.27 shows the debris distribution used for the simulated observations. Most of HEO debris have a diameter under 10 cm.
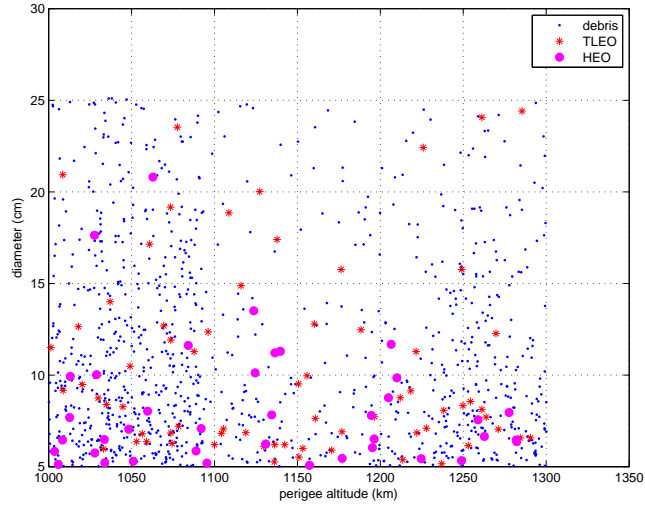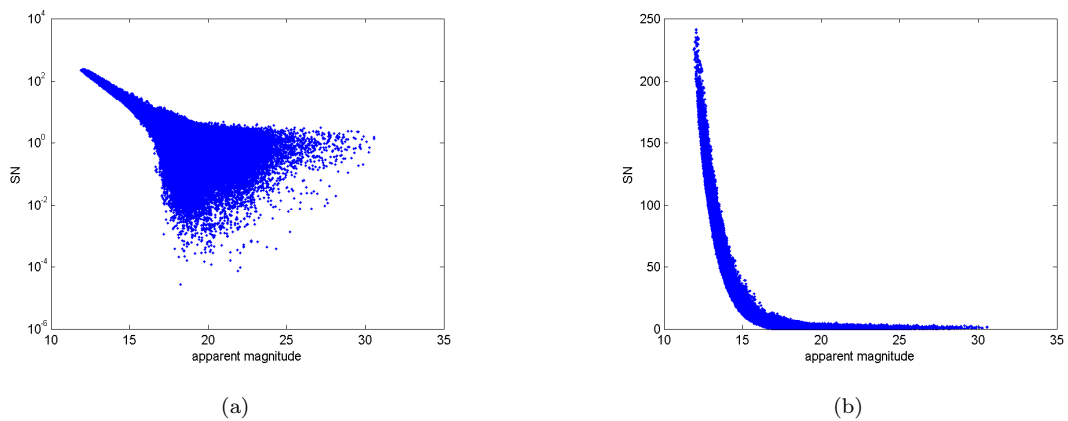
Figure 4.27: Debris distribution for the simulation 2

The figure 4.28 shows the S/N as function of the apparent magnitude for all debris simulated observations. The first figure is in a semi-logarithmic scale and it's important to notice the scattering in apparent magnitude for low S/N values (under 1). There are two main difference between the this simulation and the precedent simulation: simulated observations are achieved for smaller objects (5 cm, so the apparent magnitude should be greater than the first simulation and the S/N should be lower than the previous simulation) and for lower altitudes (1000 km, so the apparent magnitude should be lower than the first simulation and the S/N should be greater than the previous simulation). For these reasons S/N and apparent magnitude values are greater than values in figure 4.20 ($S/N_{max} \sim 170$ and $H_{apparentmax} \sim 28$ for the first simulation and $S/N_{max} \sim 240$ and $H_{apparentmax} \sim 30$ for the second one).

(a)

(b)

Figure 4.28: S/N as function of the apparent magnitude for all debris simulated observations (figure a) is in a semi-logarithmic scale)

The figure 4.29 shows the astrometric and photometric uncertainty histogram and apparent

magnitude histogram. In this simulation astrometric uncertainty values for angles are greater than the precedent simulation because observed debris are smaller.
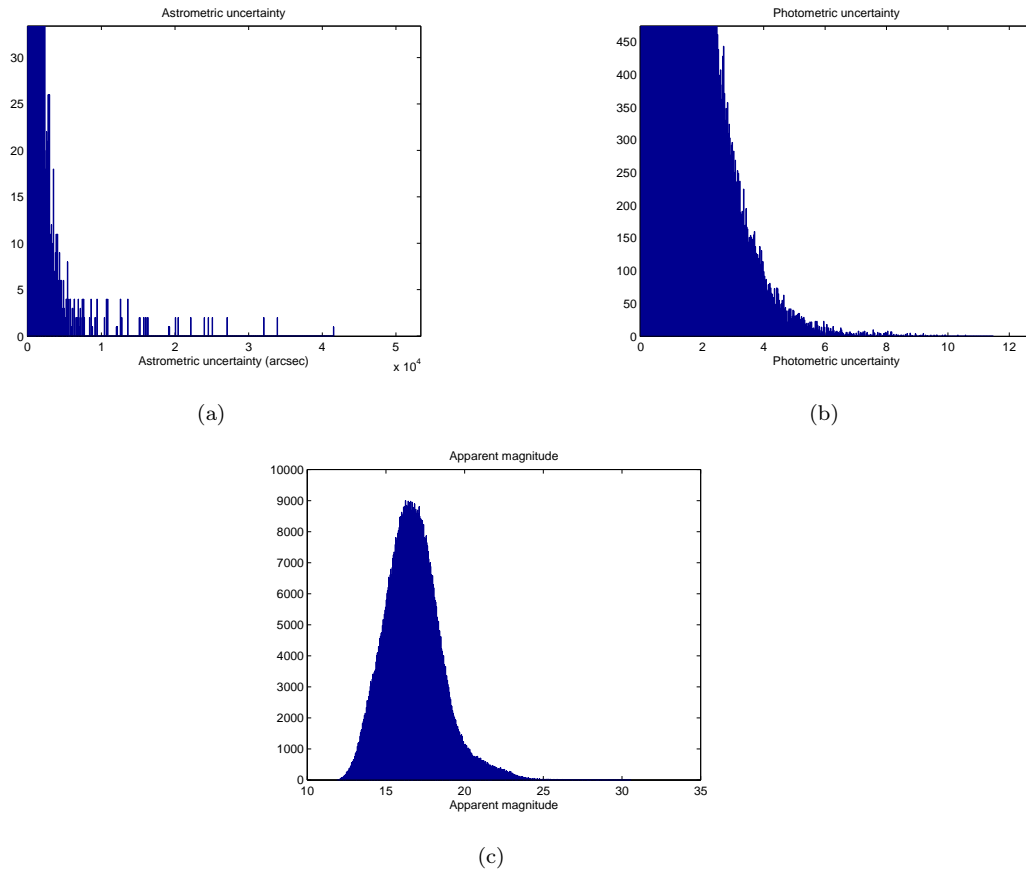

(a)

(b)

(c)

Figure 4.29: Astrometric (figure *a)*) and photometric uncertainty (figure *b)*) histogram and apparent magnitude histogram (figure *c)*)

The simulation has the following parameters (table 4.7).

Table 4.7: Debris population parameters used for simulation 2

Debris number	1104
Sampled debris	1:1
Perigee altitude	from 1000.26 to 1300.104 km
Absolute magnitude	from 36 to 39.5
Diameter	from 5.011 to 25.09 cm
Debris always in LEO	996
Debris in TLEO (considering debris in HEO)	108 (9.78%)
Debris in HEO	39 (3.53%)
Simulation period	60 days (January and February 2008)
Number of ground optical stations	7

The following figures (figure 4.30 and figure 4.31) represent the percentage of valid observations from all the observations for each debris as a function of perigee altitude and debris diameter. It is possible to notice the TLEO/HEO debris (in red) and the never detectable debris (black square): 56 after 28 days and 46 after 60 days. Blue points are the debris.

(a)   (b)
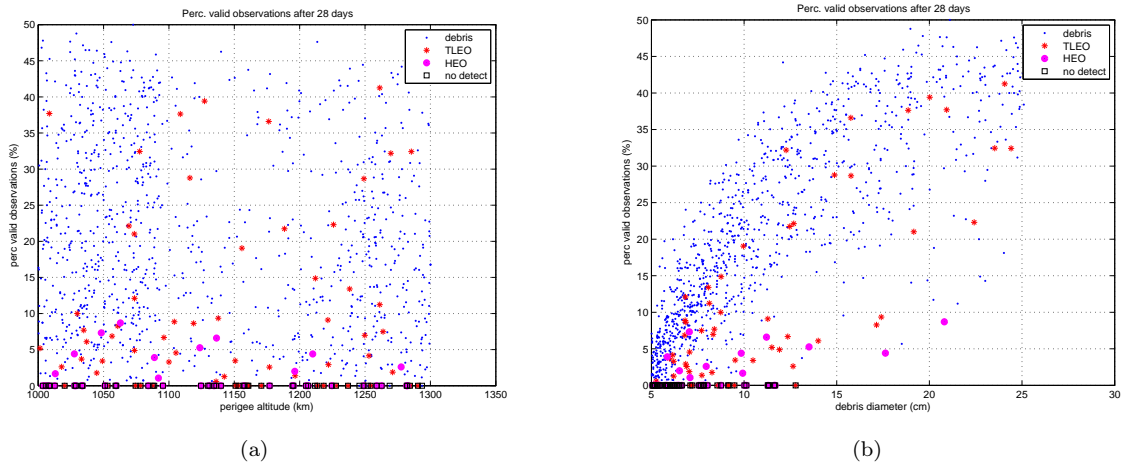
Figure 4.30: Percentage of valid observations for each debris as a function of perigee altitude and debris diameter after a 28 days for the simulation 2
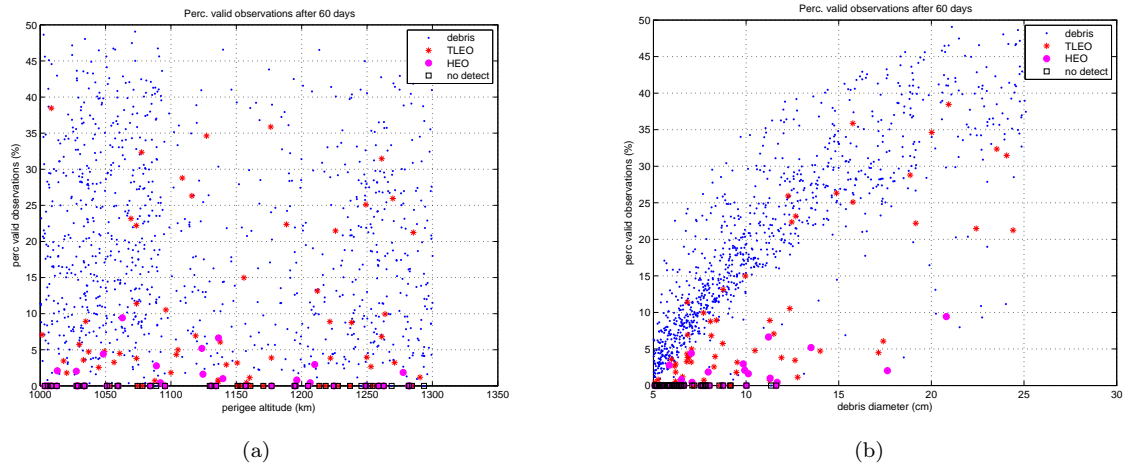
(a)

(b)

Figure 4.31: Percentage of valid observations for each debris as a function of perigee altitude and debris diameter after a 60 days for the simulation 2

The following figures (figure 4.32 and figure 4.33) represent the total number of valid observations as a function of perigee altitude and debris diameter.
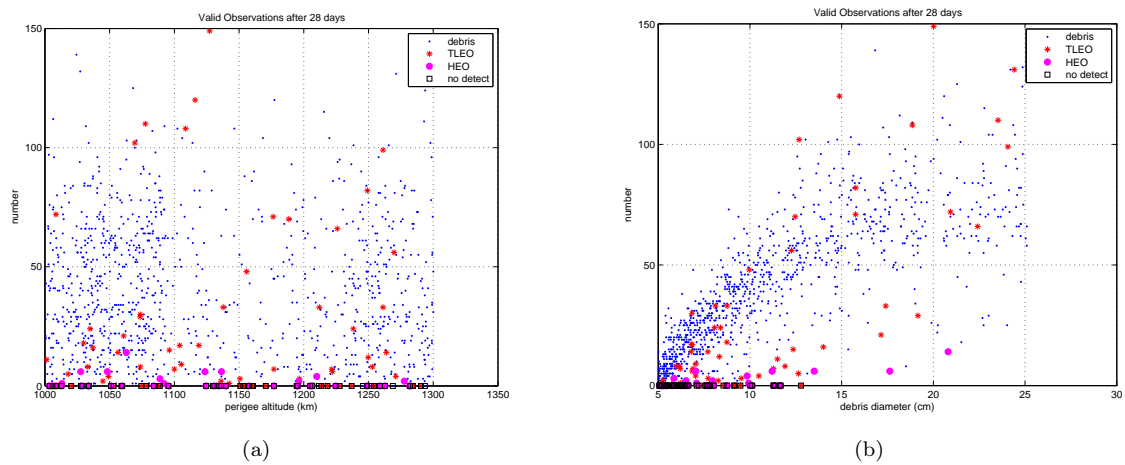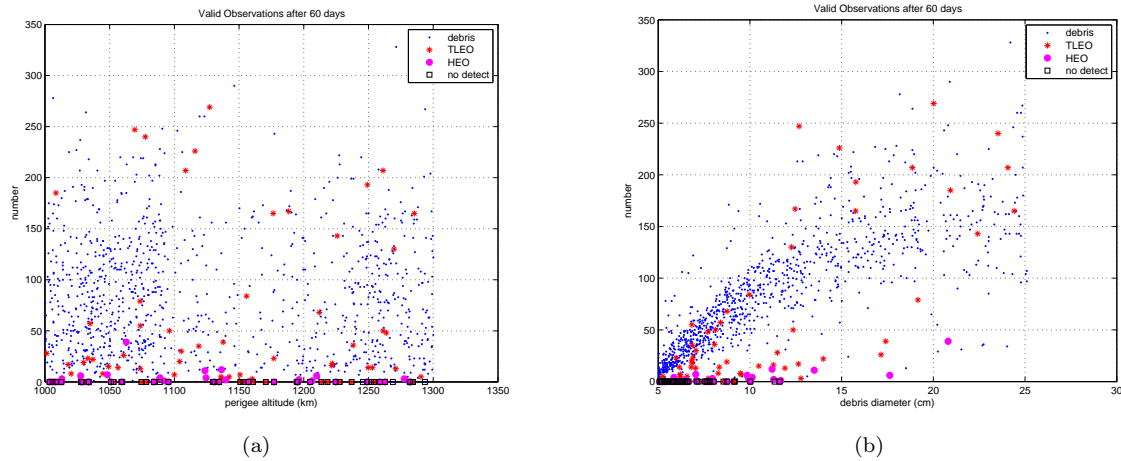

(a)

(b)

Figure 4.32: Total number of valid observations for each debris as a function of perigee altitude and debris diameter after a 28 days for the simulation 2

(a)   (b)

Figure 4.33: Total number of valid observations for each debris as a function of perigee altitude and debris diameter after a 60 days for the simulation 2

The figure 4.34 represent the debris analyzed population (in term of perigee altitude and debris diameter) after 28 days and 60 days; blue points represent debris, red points are TLEO/HEO debris and black square are never detected debris. Two curves are the system requirements, guarantee and upgradable, for LEO resident objects.

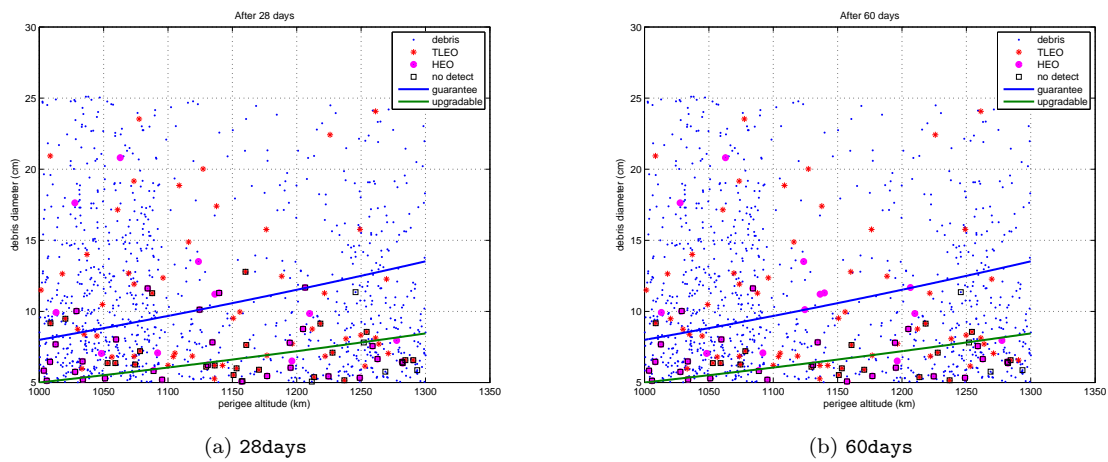(a) 28days   (b) 60days

Figure 4.34: Debris detection results after 28 days and 60 days for simulation 2

From figure 4.34 it is possible to notice that the never detectable debris are not only TLEO or HEO debris, but there are some LEO resident debris never detected (6 after 28 days and 5 after 60 days). Most of never detected debris are HEO objects: HEO debris need particular and dedicated observations where debris is observed at apogee (see previous considerations for HEO observability). It's possible to conclude that the debris system observation here studied is able to

detect a lot of resident debris in LEO as far as 5 cm.

In order to verify the statistical results emerged from these simulation runs a detailed assessment was performed on 3 objects selected as representatives from the debris population used for simulations and used as sample case for their dimensions, considering every days in the simulation period (60 days). The result of the detailed analysis performed on the sample objects is reported in figure 4.35. The figure top caption reports the debris size whereas the two numbers in the box are the number of valid debris observation in 60 days and the mean daily observation number (upper and lower, respectively).
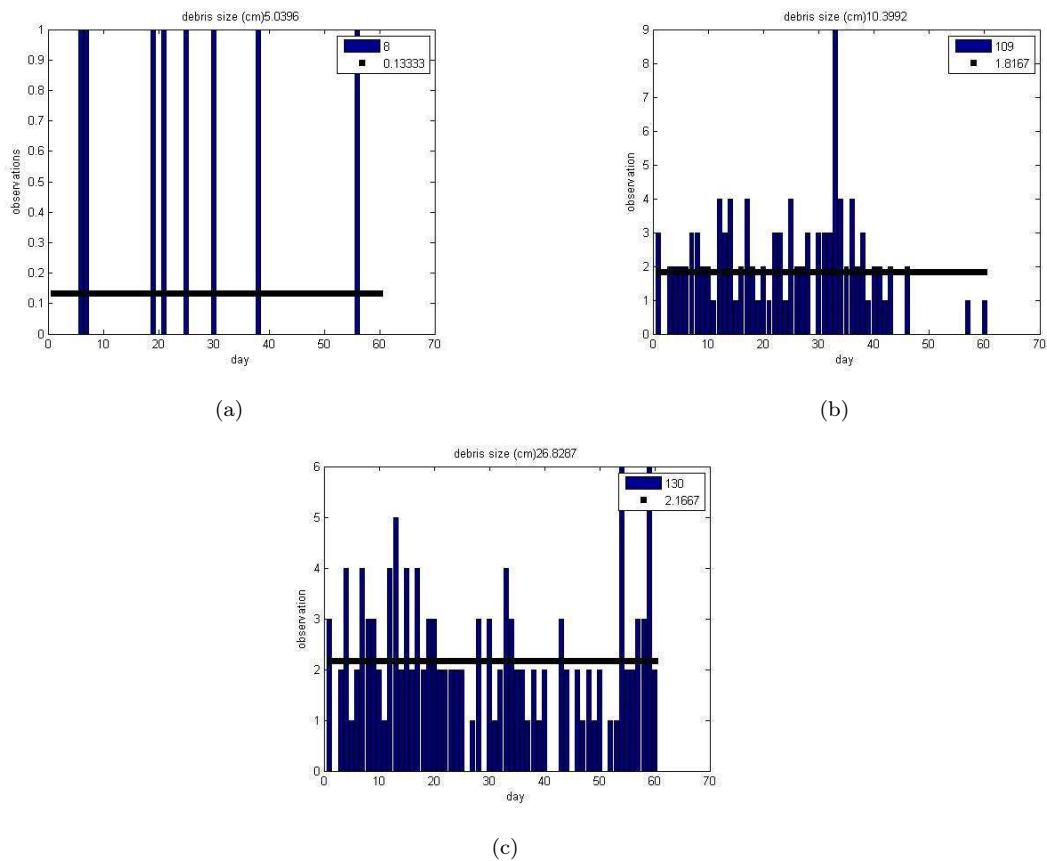

Figure 4.35: Number of debris valid observations for every days in the simulation period (60 days)

System efficiency

It's now presented the system efficiency as function of the simulation period (60 days). The system efficiency here studied refer to debris detection and not to debris orbit determination (analysed in the *SARA* project by the Department of Mathematics of the University of Pisa). Tables 4.8 and 4.9 summarize detection percentages of debris population considering all debris, resident LEO debris, TLEO debris and HEO debris.

Table 4.8: Simulation 1: detection percentage of all debris, only resident LEO debris, only TLEO debris (in TLEO debris HEO debris are also considered) and only HEO debris. There is also the never detected debris percentage

Day	detected	detect.(LEO)	detect.(TLEO)	detect.(HEO)	never detected(LEO,TLEO,HEO)
1 day	810 (88.81%)	90.94%	72.64%	10.52%	102 (73,29,17)
3 days	854 (93.64%)	95.16%	82.07%	21.05%	58 (39,19,15)
7 days	874 (95.83%)	97.51%	83.01%	21.05%	38 (20,18,15)
14 days	893 (97.91%)	99.5%	85.84%	31.57%	19 (4,15,13)
28 days	901 (98.79%)	100%	89.62%	47.36%	11 (0,11,10)
40 days	903 (99.01%)	100%	91.5%	52.63%	9 (0,9,9)
50 days	904 (99.12%)	100%	92.45%	57.89%	8 (0,8,8)
60 days	905 (99.23%)	100%	93.39%	63.15%	7 (0,7,7)

Table 4.9: Simulation 2: detection percentage of all debris, only resident LEO debris, only TLEO debris (in TLEO debris HEO debris are also considered) and only HEO debris. There is also the never detected debris percentage

Day	detected	detect.(LEO)	detect.(TLEO)	detect.(GTO)	never detected(LEO,TLEO,GTO)
1 day	786 (71.19%)	76.1%	25.92%	7.69%	318 (238,80,36)
3 days	879 (79.61%)	84.63%	33.33%	7.69%	225 (153,72,36)
7 days	971 (87.95%)	92.67%	44.44%	23.07%	133 (73,60,30)
14 days	1025 (92.84%)	97.48%	50%	28.2%	79 (25,54,28)
28 days	1048 (94.92%)	99.39%	53.7%	28.2%	56 (6,50,28)
40 days	1050 (95.1%)	99.39%	55.55%	28.2%	54 (6,48,28)
50 days	1054 (95.47%)	99.39%	59.25%	30.76%	50 (6,44,27)
60 days	1058 (95.83%)	99.49%	62.03%	35.89%	46 (5,41,25)

Figure 4.36 shows the detection debris percentage reported in tables 4.8 and 4.9. It's possible to notice the difficult to detect some HEO debris during 60 days: in order to detect these debris it's possible to observe debris for 6 months or to use different observation techniques.
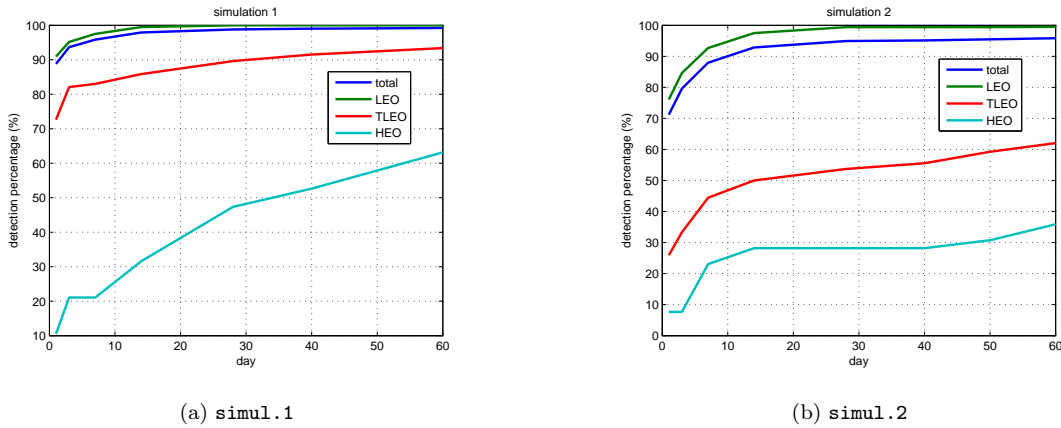
(a) `simul.1`   (b) `simul.2`

Figure 4.36: Detection debris percentage for simulations during the observation period

Figure 4.37 shows the detection debris percentage considering the observation of the same population debris achieved in a different season: June and July 2008. The scope of this analysis is to study how illumination conditions and meteo data in a different season could be change the debris detection. For the first simulation, no evident effects are presented, while for the second simulation it's possible to observe an improvement when observations are achieved in June/July respect to January/February.

(a) `simul.1`   (b) `simul.2`
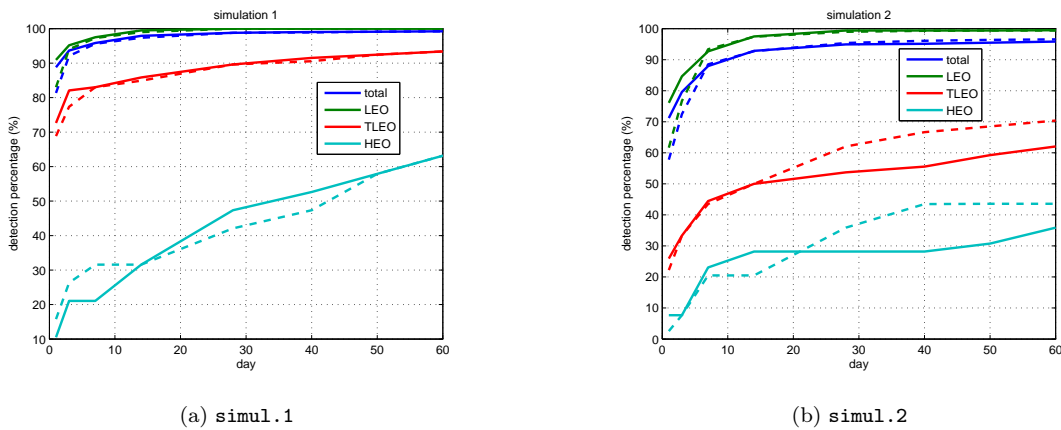
Figure 4.37: Detection debris percentage for simulations during the observation period considering the a different season for observation (solid lines represent observation achieved in the period January/February, while dashed lines represent observation achieved in the period June/July)

It's possible to compare these results for optical simulated observations with the sensitivity of the most powerful telescopes in the world for LEO debris observations: the US LMT and the US MCAT (see table 2.4). Study shows that resident debris in LEO with 5 cm diameter are

easily detectable and it's possible to suppose that debris with 2-3 cm diameter are also detectable. For this reason the simulated observations system developed for this thesis gives good results, considering that a lot of assumptions are conservative. It's possible to compare these results with radar stations performances in LEO (see table 2.3): US radar stations can observe millimeters debris, while actual ESA radars are able to observe 1-2 cm size debris, so ESA radars performances are not very different from optical detection results of this thesis.

Chapter 5

Debris optical observations from a satellites constellation

In this chapter the debris optical observation from space concept is study.

The design of a space-based infrastructures is in complement to the overall SSA ground-based infrastructure (radars and telescopes). It's important to identify potential shortcomings in the catalogue coverage of space objects when using a network of ground-based telescopes alone. As space-based assets are at least an order of magnitude more expensive compared to a ground-based ones, so it is important to identify the minimum number of satellites required in optimised orbits of a realistic constellation that will enhance the debris observability coverage performance of the combined (ground and space-based) network.

It's important to underline the potential gain of adding a space-based infrastructure by comparing it with the number of required additional ground based assets and their distribution around the globe. It will be defined the observation strategy to be used from satellites in a selected orbits to optimise debris observability.

5.1 Space based telescope requirements

The most important consideration on the space-based component is that it can be considered as complementary to and competitive with the ground components. First at all it is identified some portion of the debris surveillance work which either cannot be done from the ground, or is very difficult and expensive from the ground. Second, it is identified a feasible space mission with a small constellation of satellites which can achieve the goal which is difficult from the ground and at a cost which is comparable to, if possible lower than, the one of an equivalent upgrade of the ground system. The goals of a space surveillance system for Earth orbiting objects can be classified by the debris orbit type. The space mission must give a significant contribution to LEO debris discovery. Satellites need to be identical and to be low mass to contain the cost; because of the launch cost, it is much better to have satellites with the same inclination and at least initially the same longitude of node. The problem which has to be solved is the debris detection and the

subsequent orbit determination in a reasonable time. It's important to have enough satellites to allow for re-detection of the same object within a comparatively short time span from another satellite.

The main constraint for detection is the relationship between diameter of the sensor, distance from the sensor to the object and diameter of the object (see equation 2.2). For an optical sensor the relationship between diameter of the telescope (more exactly, of the photon collecting area) and diameter of the object is a direct proportionality. The relationship between diameter of the object which can be detected (at a given S/N) and distance is also a direct proportionality. Thus a sensor of 20 cm diameter at 4000 km distance and a 2.2 m diameter telescope at 40000 km distance can see objects of the same diameter. This is enough to exclude the possibility of using a space based component to discover GEO, because a 2.2 m telescope (for that matter even a 4.4 m telescope) costs much less than a satellite with a 20 cm telescope. (The corrective factor 1.1 is used to take into account atmospheric absorption, which decreases by 20% the S/N for a ground sensor with respect to one above the atmosphere). The same argument applies to MEO: there is no advantage in a space component because the volume of space in which the orbits can be is too large to be kept under surveillance from a distance much smaller than the one from the ground. Thus the portion of interest for a space component is the LEO region.

The approach used for space observation concept is similar the previous analysis, in particular a STK-Matlab Software Interface has been used for simulated observations results (the software is the same used in previous chapters).

5.2   Space observation concept

The observation concept is based on the fact that the atomic unit of observational information to be processed contains 4 scalar quantities (an attributable, see sec. 2.5). For the relative velocities typical of observations of LEO from LEO, with the most common value at $1 degree/sec$, one object can stay in the field of view 5-10 seconds (depending upon the field of view). A sequence of 2 or 3 attributables obtained from consecutive image frames (as an example 1 second exposure every 3 seconds) provides more information, but not enough to compute a full orbit, because the information is not independent. Thus the only possibility is to have attributables from different sensors. The concept is to have two satellites, on a common orbit but somewhat out of phase (or true anomaly), at a distance in the along track direction, with wide field telescopes, pointed in such a way that cones containing the observed object intersect in the region of interest. This would lead to detections almost simultaneous (within few seconds) of the same object, not always but very often for objects in the region of interest. These detections can be used from a well tested algorithms for orbit determination (see sec. 2.5), taking into account that correlation is easy given the time interval of a few seconds.

To define the region of interest it's important to take into account the performance of the ground based sensors, such as the optical one but also the radar one. Because of the radar law, by which S/N scales with the inverse fourth power of distance, it is obvious that optical observations need to be used above a given altitude, radar only below (see figure 2.38 and sec. 2.7). If the S/N

is not enough from the debris of the size specified in the requirements, for optical systems there is little which can be done besides increasing the diameter of the telescope (although aggressive image processing, reducing the trailing loss, can also contribute). For radar systems, it is possible to increase the energy of the emitted signal. Both solutions are very expensive.

Taking into account the population models in LEO (figure 2.14), there are two important peaks: objects between altitudes from 500 to 1000 km and around 1400 km. The second peak is well covered by the ground optical system analysed in previous chapters: system performances coverage are between 1000 and 2000 km. The first peak represents a problem for ESA actual survey; in this case radars are used for low altitude, but ESA radars coverage are good as far as 600-700 km (the ISS region), while the altitude between 700-800 and 1000 km is a problem: study for future ESA radars shows that the coverage of debris about 5-10 cm in this altitude (around 700-800 km) is very expensive (about 300 MEuro). So in the region between 700-800 and 1000 km the possibility of an optical observation is fundamental. Debris observation in this region from a given optical ground station becomes quite a rare event, also because of the shadow of the Earth. Thus there appears to be a region where the trade off is essentially between radar and a space-based system, where, after cost considerations, a spaced-based system is better. The figure **??** summarizes regions of LEO debris population considering different observations methods proposed in this study.
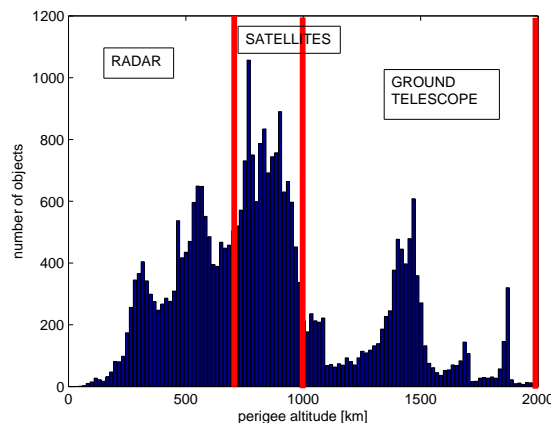

Figure 5.1: Different observations methods for the LEO debris population

Thus the two identical spacecrafts should orbit below the region of interest, at 500 to 600 Km of altitude, and look somewhat up, avoiding as much as possible stray-light from the Earth: a Sun-synchronous orbit could be used to make the problem easier. The direction of observation should be selected in such a way that the intersection of the observed cones cover as much as possible of the 700 to 1000 km altitude shell. The exact direction of observation needs to be adjusted, taking into account both technical consideration on the spacecraft and telescope, and the simulation results. These satellites can also observe all the region (GEO, MEO and all LEO over 700 km).

5.3   Observation strategy definition and simulations

On the basis of debris population in the region of interest, satellite configuration and selected orbit are established. An orbit propagation tool (STK with the STK-Matlab Software Interface) is required to run debris in order to simulate the observed objects tracklets. It has been supposed that the time between the two observations forming a tracklet was 1 second (like the observations in LEO from the ground station, see sec. 2.5). Further, simulated tracklets should be associated with a corresponding magnitude, defined as a function of the observation solar phase angle. As already outlined for the altitudes between 700 km and 1000 km the space based optical observation of space debris has been identified as beneficial and it has been supposed to use the minimum number of satellites (2) to cover this region. Therefore, a basic concept has been developed and some simulations have been performed to assess critical mission aspects. These aspects are observation geometry, the distance between debris and satellite and associated crossing times of the telescope field of view.

First of all the satellites orbit must be chosen. The sun-synchronous (dawn-dusk) orbit allows observation throughout the whole orbit. This orbit combines altitude and inclination in such a way that an object on that orbit ascends or descends over any given point of the Earth's surface at the same local mean solar time. The surface illumination angle will be nearly the same every time and in a dawn-dusk orbit the local mean solar time of passage for equatorial longitudes is around sunrise or sunset, so that the satellite rides the terminator between day and night providing a maximum of sun periods for power generation. This is achieved by having the osculating orbital plane precess (rotate) approximately one degree each day with respect to the celestial sphere, eastward, to keep pace with the Earth's revolution around the Sun.

The figure 5.2 shows altitude vs inclination for a sun-synchronous circular orbit. The red point represents the orbit chosen in this study (at 500 km altitude).
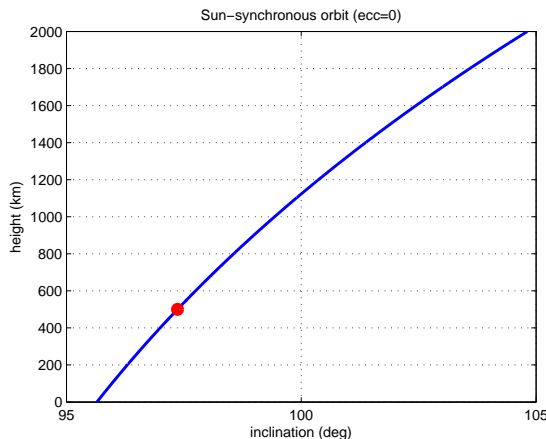

Figure 5.2: Altitude as function of inclination for a sun-synchronous circular orbit

The table 5.1 summarizes the orbital elements for the two identical satellites. They have same elements, a part for the argument of periapsis.

Table 5.1:

Sun-synchronous orbit parameter	Value
altitude	500 km
inclination	97.36°
eccentricity	0 (circular orbit)
true anomaly	0°
RAAN	90° at 21 March (dawn-dusk orbit)

The orbit altitude 500 km of the satellites provides reasonable detection areas for observation in altitudes between 700 km and 1000 km.

To propagate the debris and 2 satellites in the STK tool, a series of choices are taken, concerning both the frame of reference and the propagator. In particular:

- the selected frame of reference is the J2000 system, centered in the Earth,

- with regard to the propagator, the gravitational disturbance (using the EGM96 model with ord.2 and degr.2) and the atmospheric disturbance (with the Jacchia-Roberts method) are considered; the second disturbance is important because satellites are propagate in a very low orbit.

- moreover, the integration step is fixed at 40 seconds.

The unique orbital debris constraint consists in assuming that it shall be always illuminated from the Sun when satellites perform observations.

5.3.1 Trade off between some observation strategies

A trade off between some observation strategies has been achieved in order to analyse the most important differences between these configurations. The angle between the sun direction and the sensor boresight (BS) needs to be greater than or equal 90° in order to provide sun reflectance for debris detection and to prevent the Sun illumination in telescope FOV of satellites. Whit these aspects, 3 observation configurations have been analysed:
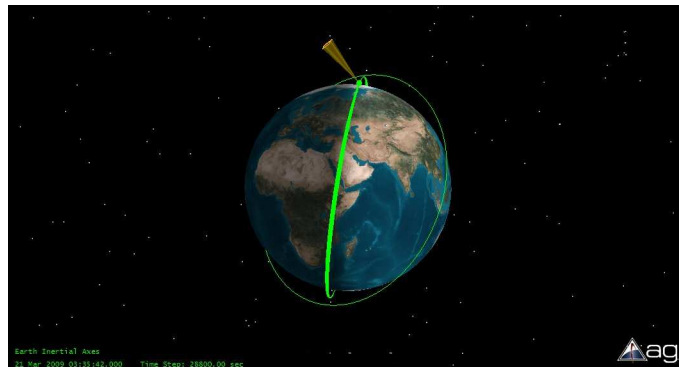
- Configuration 1: observations for Zenith angle pointing
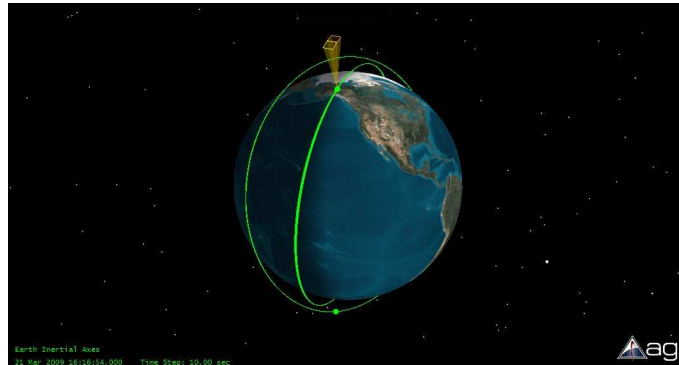
- Configuration 2: observations for 90° Off-Zenith angle pointing
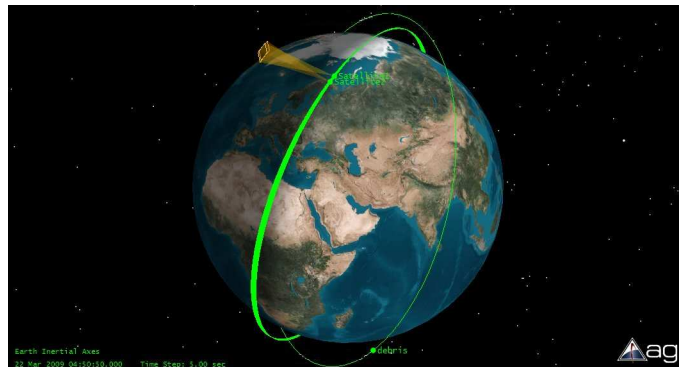
- Configuration 3: observations for 45° Off-Zenith angle pointing

Following features are used for the 3 configurations (table 5.2).

Table 5.2: Observation characteristics for each satellites configuration

	config.1	**config.2**	**config.3**
sensor FOV	10°x10° (rectangular)	10°x10° (rectangular)	10°x10° (rectangular)
Pointing type	fixed	fixed	fixed
Orientation method	Euler angles	Az-elev	Az-elev
Sensor angle (α)	6°	4°	6°
Satellite relative distance (in ω)	0.485° (58.31 km)	2.595° (311.6 km)	0.485° (58.31 km)

Satellites intersected cones are fixed with the attitude satellites, while satellites rotates with the same angular velocity of the Earth (nadir pointing).

The figure 5.3 illustrates the observation strategy from satellites, showing two intersected view cones, where the red arrow indicates the common detection area. A debris is observed when it is in the FOV the satellite, while for debris orbit determination is important to have debris in the common detection area of the two satellites view cones. Black points are two satellites and

the angle α is the sensor angle in table 5.2. This figure represent the observation strategy for all analysed configurations (when satellites observe at the zenith and when they observe at 90° Off-Zenith angle pointing) and for all debris (when debris is in the same orbit plane respect satellites and when it is in a perpendicular orbit plane).
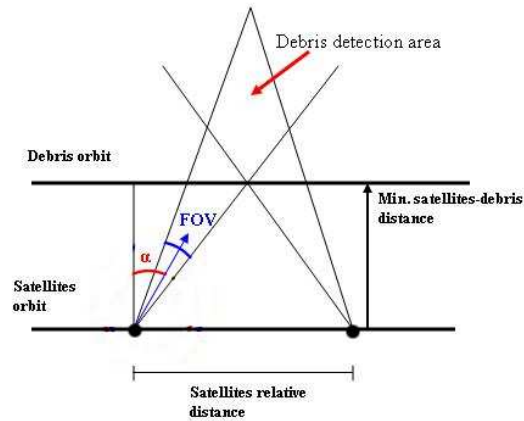

Figure 5.3: Observation strategy from satellites, showing two intersected view cones

Figure 5.4 shows some considerations about satellites relative distance, sensor angle α and observation distance between satellites and debris. All these considerations comes from simple trigonometric calculations. Minimum (represented in figure 5.3) and maximum distance are the minimum and the maximum possible observation distance between satellites and debris (i.e. when debris is the common detection area of the two satellites fields of views).
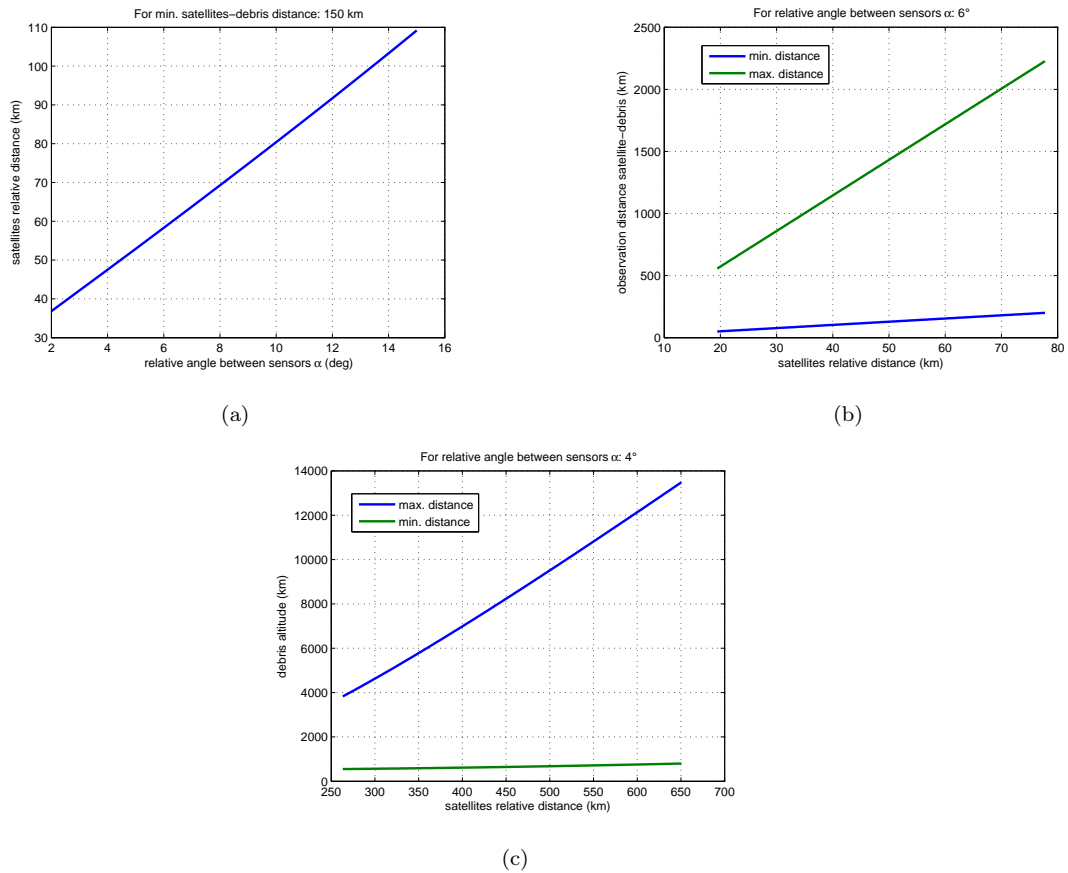
(a)

(b)

(c)

Figure 5.4: Considerations about satellites relative distance, sensor angle α and observation distance between satellites and debris

Figures 5.5 and 5.6 show the overlap of the two fields of views, which determines the area where detection is possible for two configurations (configuration 1 and configuration 2). The possible overlap for observation in altitudes between 700 km and 1000 km depends on the parameters field of view, relative distance of the satellites and the telescope inclination (α angle). When observations are at zenith or at 45° (configuration 1 and configuration 3) it is possible to observe debris with altitudes from 650 km to 2170 km; when observation are opposite to the Sun (configuration 2) it is possible to observe debris with altitudes from 570 km to 4870 km.
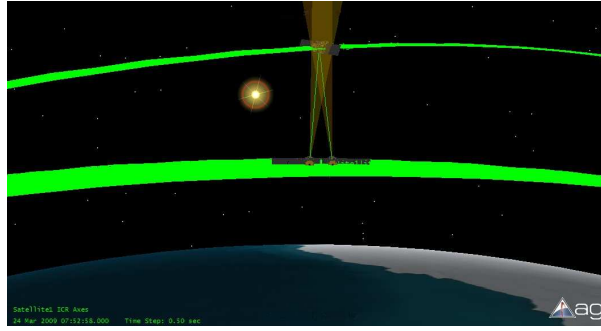
Figure 5.5: The overlap of the two satellites fields of views when observations are at the zenith
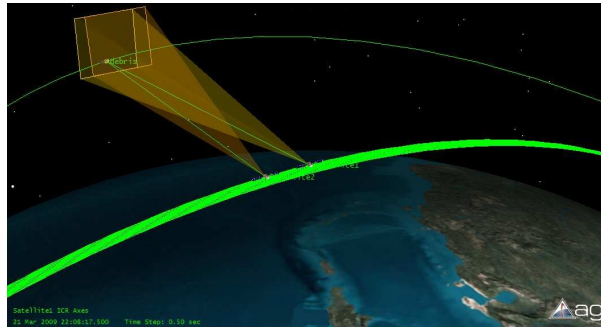

Figure 5.6: The overlap of the two satellites fields of views when observations are opposite to the Sun

The data reported in the following figures allow preliminarily analyzing the trade off between different configurations of debris observation, using simple trigonometric relations. The figure 5.7 shows a schematic representation of debris observations from satellites for the 3 configurations. Satellites are at 500 km of altitude ($r = R_{Earth} + 500\,km$), b is the satellites-debris greater distance when the debris is over satellites (configuration 1), while c is the satellites-debris greater distance for each configuration (it is a variable distance). R is the debris distance from the Earth center, while it's possible to consider x not like a curve line if α angle is little. β angle varies from $0°$ when the observation is at zenith (configuration 1) to $21.21°$ when the observation is at $90°$ (configuration 2). The greater distance satellites-debris (when debris are at 1000 km of altitude) is obviously 500 km for configuration 1 and 2669 km for configuration 2.
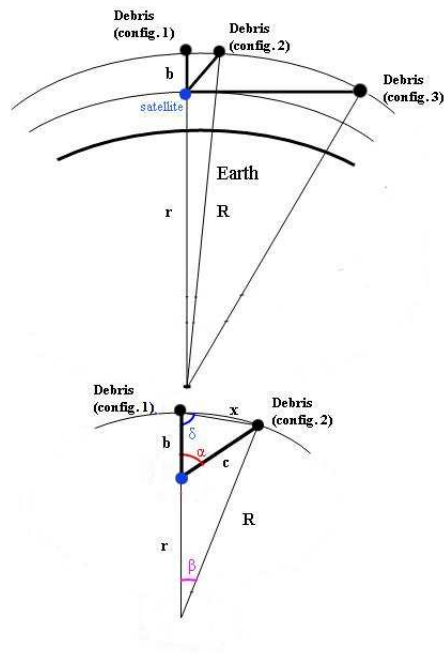
Figure 5.7: Scheme for the observation configurations
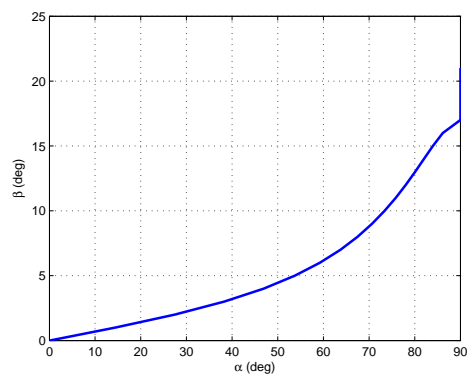
The figure 5.8 shows α (see figure 5.3) and β angles.

Figure 5.8: α and β angles

Figure 5.9 represents the greater distance satellites-debris (the variable distance c) as function of the debris altitude for zenith (configuration 1) and 90° configuration (configuration 2).
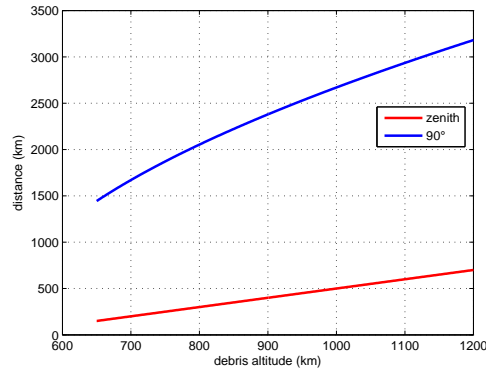
Figure 5.9: Greater satellite-debris distance as function of the debris altitude for configuration 1 and configuration 2

Figure 5.10 represents the greater satellite-debris distance as function of the observation angle α for some debris altitudes, located between 700 and 1000 km.
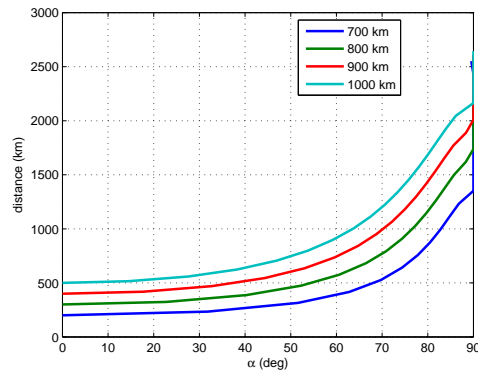

Figure 5.10: Greater satellite-debris distance as function of the observation angle α for some debris altitudes, located between 700 and 1000 km

Simulations have finally been performed with the STK-Matlab Software Interface and the times evaluated, in which space debris objects cross the overlap of the two fields of views. Debris orbits used in the simulation are a representative sample of debris population between 700 and 1000 km (a lot of these orbits are high inclination orbits); 110 debris have been simulated over a period of 15 days from 21/3/2009.

The distance between the satellites and the debris, the observation frequency and observation duration has been analysed. A main concept emerged is that if the debris observation is at zenith the maximum distance is around 500 km (very short), but the observation frequency is very small (some debris are never observed before a time period of two weeks) and the observation duration is too short (between 1 and 20 sec, but often 1 or 2 sec). On the other hand, if the debris observation is opposite to the sun (configuration 2) the maxima distance is about 2000-2600 km (too large for the small telescope), but there are a lot of debris observations in a short time period and the typical

observation duration is between 20 and 50 sec (in some case the duration is about some minutes). The debris observation with an angle of 45° is a configuration near the configuration 1 with maxima distance around 700 km, but the observation frequency and the observation duration are better than those registered for Zenith configuration. Figures 5.11 and 5.12 resume the simulation results for the debris sample population as function of orbit perigee altitude and orbit inclination.
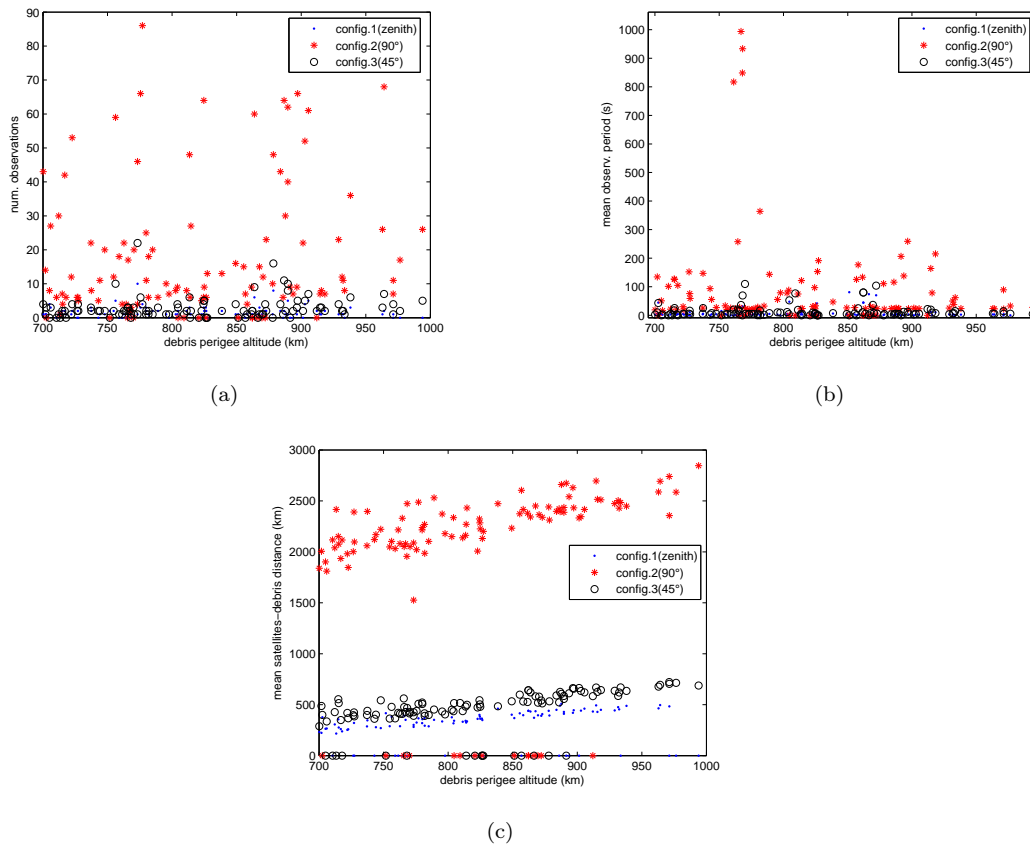

(a)

(b)

(c)

Figure 5.11: Simulation results as function of orbit perigee altitude
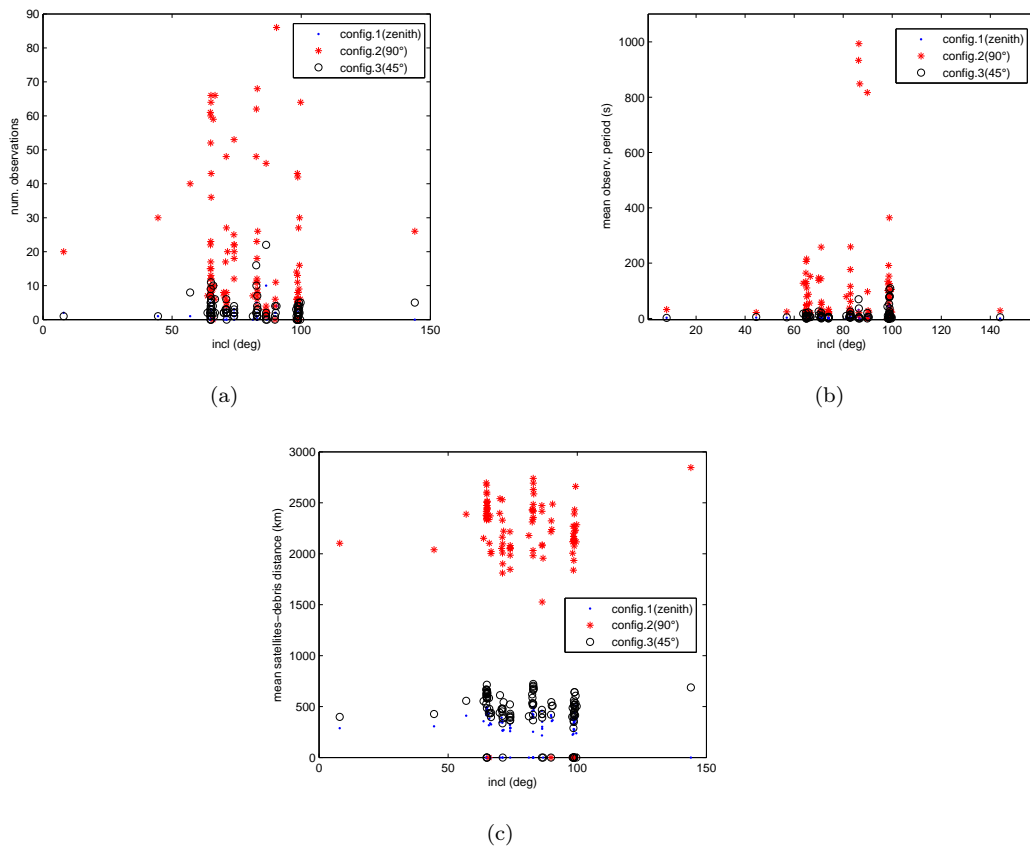
(a)

(b)

(c)

Figure 5.12: Simulation results as function of orbit inclination

Chapter 6

Conclusion

In this thesis the space debris problem has been discussed in order to understand the debris environment, the risk for operative satellites and surveillance systems. Debris in LEO region has been considered because they cover an important and populated region for space activities and because they are easily observed in this region. LEO region has been usually analysed with radar stations, but an innovative surveillance system based only on optical debris observations has been discussed in this thesis.

In this study simulated debris observations are created for analyses with assumptions decided by the *Carlo Gavazzi Space* in the ESA SSA feasibility study. The debris simulated observations software interface between STK and Matlab tools and the debris detection analysis program have been developed in this thesis with these assumptions. It has been also analysed an interface information of data structure to exchange data between different softwares, very useful when different actors and softwares must exchange data and results.

From simulated debris observations achieved with ad-hoc STK-Matlab Software Interface, it is possible to conclude that debris with a 5 cm diameter are often detected from a ground station network (7 optical stations around the world) in some observation weeks. This result is similar to real observations of the most powerful telescopes in the world for LEO debris observations and they are not very different from actual ESA radars performances. In this thesis a lot of conservative assumptions for debris observations have been hypothesized, so results here showed should be better: it's possible to detect 2-3 cm size debris. Simulations from 3 cm size objects are required to understand the real potentiality of simulated observations and to compare these results with actual and in progress telescopes and radars in the world. It is important to remind that these results consider the debris detection and not the debris orbit determination.

It is possible to consider different debris optical observation assumptions and for this purpose it's fundamental to have a more realistic debris albedo model and a debris magnitude model to be used alternatively to the model for the asteroid field in order to have more realistic debris observations, even so this thesis wants to show that asteroid magnitude model is a good approximation for debris magnitude model. The study of optical debris characteristics (e.g. albedo) is very important for future optical debris observations analyses. The telescope can also operate in different modes (survey or tasking mode). It is possible to use a different S/N model for debris

detection and in particular simulations in a tasking mode for LEO resident objects are required, considering a S/N model for a fixed debris.

In the LEO debris population is possible to distinguish resident LEO debris and transient LEO (TLEO) debris because simulated observations show two very different behaviours: it is difficult to observe TLEO debris, in particular HEO debris with an high eccentricity orbit, in the 2 months simulated period. HEO debris include GTO debris, very important to prevent collisions with the most important launchers in the world. A simulation over 6 months is required in order to better understand HEO debris detectability over a long observation period.

Debris here analysed are usually unknown objects from the ESA population file, considering also operative satellites; so it is possible to detect very small debris, but also large objects like unknown operative satellites.

Simulated observations in this thesis refer to debris in LEO region, but the system and the software interface is adaptable to other regions around Earth. In fact during twilight hours telescope can observe LEO debris, while in the middle of the night it can perform a conventional GEO or GTO debris search. It is possible to change some observation parameters (e.g. the observation exposure time) and the detection model (S/N equations) in order to obtain simulated debris observations in GEO or MEO regions and also to observe NEO; the software interface and the system structure are the same for LEO debris developed in this thesis. It is important to have a telescope co-located with radar installations that enable simultaneous radar and optical observations for a better debris detection.

Bibliography

[1] J. Africano, P. Kervin. *Understanding photometric phase angle corrections*, NASA document, 2005.

[2] V. Agapov, T. Schildknecht et al. *Results of GEO space debris studies in 2004-2005*, IAC-06-B6.1.12, 2006.

[3] D. K. Barton, D. Brillinger, A. H. El-Shaarawi, P. McDaniel, K. H. Pollock, M. T. Tuley. *Final Report of the Haystack Orbital Debris Data Review Panel*, NASA, Technical Memorandum 4809, 1998.

[4] E. Bowell et al. *Application of photometric models to asteroids*, 1989.

[5] D. Bruton. *Conversion of Absolute Magnitude to Diameter for Minor Planets*. Department of Physics and Astronomy (Stephen F. Austin State University), 2008.

[6] Carlo Gavazzi Space. *TELAD: Co-V Telescopes Analysis and Design*, Final Report to ESA study 6261/09/D/CS, January 2010.

[7] Carlo Gavazzi Space. *System support for SSA requirements analysis: SARA ('Feasibility study of an innovative system for debris surveillance based on the combination of UHF radar and optical telescopes for the SSA program'), 'LEO optical camera'*, Final Report to ESA study 5953/09/D/HK, July 2009.

[8] T. Donath, T. Schildknecht, P. Brousse et al. *Proposal for a European Space Surveillance System*, ESA document, 2005.

[9] ESA Director General's Office. *Space Debris Mitigation for Agency Projects*, 2008.

[10] ESA-ESOC. *System support for SSA requirements analysis. Part I-Feasibility study of an innovative system for debris surveillance in LEO regime*, statement of work, May 2009.

[11] ESA-ESOC. *Co-V Telescopes Analysis and Design*, statement of work, November 2009.

[12] D. Farnocchia, G. Tommei, A. Milani, A. Rossi. *Innovative methods of correlation and orbit determination for space debris*, 2009.

[13] T. Flohrer, J. Peltonen, A. Kramer, T. Eronen et al. *Space-based optical observations of space debris*, ESA document, 2005.

[14] T. Flohrer, T. Schildknecht, R. Musci. *Proposed strategies for optical observations in a future European Space Surveillance network*, Advances in Space Research, Cospar 41, pp. 1010-1021, 2008.

[15] Flury, Massart, Schildknecht, Hugentobler, Kuusela, and Sodnik. *Searching for Small Debris in Geostationary Ring. Discoveries with the Zeiss 1-metre Telescope*, ESA Bulletin 104, pp. 92-100, 2000.

[16] S. Fukushige et al. *Comparison of Debris Environment Models: ORDEM2000, MASTER2001 and MASTER2005*, Engineering Review, Vol. 40, N. 1, February 2007.

[17] M. A. Garcia Matatoros, D. Kuijper, P. L. Righetti. *NAPEOS: ESOC Navigation Package for Earth Observation Satellites*, ESA document.

[18] G.F. Gronchi, L. Dimare, A. Milani. *Orbit Determination with the two-body Integrals*, 2009.

[19] D. J. Kessler and K. S. Jarvis. *Obtaining the properly weighted average albedo of orbital debris from optical and radar data*, COSPAR, Houston, TX October, 2002.

[20] H. Klinkrad, F. Alby, D. Alwes, C. Portelli. *Space debris activities in Europa*, ESA document, 2005.

[21] H. Klinkrad, R. Tremayne-Smith, F. Alby, D. Alwes. *The proposal for a European Space Surveillance System*, ESA Bulletin 133, pp. 42-48, February 2008.

[22] H. Krag, P. Beltrami-Karlezi, J. Bendisch, H. Klinkrad et al. *PROOF: The Extension of ESA's MASTER Model to Predict Debris Detections*, Acta Astmnautica Vol. 47, Nos. 2-9. pp. 687-697, 2000.

[23] K. S. Jarvis, G. Stansbery. *Working Toward an Albedo Distribution Model: SiBAM- Size-Based Albedo Model*, The orbital debris Quarterly News, Vol.8, Issue 2, April 2004.

[24] R. Jehn. *Debris Detection and Observation Systems*, International Interdisciplinary Congress on Space Debris, McGill University, Montreal, May 2009.

[25] K. Jorgensen J. Africano, K. Hamada, E. Stansbery, P. Sydney, P. Kervin. *Physical properties of orbital debris from spectroscopic observations*, Advances in Space Research 34, pp. 1021-1025, 2004.

[26] *IADC Space Debris Mitigation Guidelines*, October 2002.

[27] R. Jehn. *Debris Detection and Observation Systems*, International Interdisciplinary Congress on Space Debris, McGill University, Montreal, 7-9 May 2009.

[28] Jer-Chyi Liou, M.J. Matney, P. D. Anz-Meador, D. J. Kessler. *The New NASA Orbital Debris Engineering Model ORDEM2000*, NASA/TP-2002-210780, May 2002.

[29] P. Maskell, L. Oram. *Sapphire: Canada's Answer to Space-Based Surveillance of Orbital Objects*

[30] D. Mehrholz, L. Leushacke, W. Flury, R. Jehn, H. Klinkrad, M. Landgraf. *Detecting, Tracking and Imaging Space Debris*, ESA Bulletin 109, February 2002.

[31] A. Milani, G.F. Gronchi, D. Farnocchia, G. Tommei, L. Dimare. *Optimization of space surveillance resources by innovative preliminary orbit methods*, Proc. of the Fifth European Conference on Space Debris, April 2009.

[32] A. Milani, G.F. Gronchi, Z. Knezevic, M. Vitturi.*Orbit Determination with Very Short Arcs. I Admissible Regions*, Celestial Mechanics and Dynamical Astronomy 90, pp. 59-87 2004.

[33] A. Milani, G.F. Gronchi, Z. Knezevic, M.E. Sansaturio, O. Arratia. *Orbit Determination with Very Short Arcs. II Identifications*, Icarus. 79, pp. 350-374 2005.

[34] A. Milani, G.F. Gronchi.*The theory of orbit determination*, Cam- bridge University Press, 2009.

[35] A. Milani, L. Denneau, F. Pierfederici, R. Jedicke. *Data Exchange Standard (2.02) for solar system object detections and orbits. A tool for Input/Output definition and control*, University of Hawaii, Institute for Astronomy, Pan-STARRS Project, 2007.

[36] A. Milani, A. Villani and M. Stiavelli. *Discovery of very small asteroids by automated trail detection*, Earth, Moon, and Planets, Volume 71, Number 3, pp. 257-262, 1995.

[37] A. Morbidelli, R. Jedicke, W.F. Bottke, P. Michel, E.F. Tedesco. *From magnitudes to diameters: the albedo distribution of Near Earth Objects and the Earth collision hazard*, Icarus 158, pp. 329-342, 2002.

[38] K. Muinonen, E. Bowell, K. Lumme. *Interrelating asteroid size, albedo, and magnitude distribution*, Astronomy and Astrophysics 293, pp. 948-952, 1995.

[39] M. K. Mulrooney, M. J. Matney. *Derivation and Application of a Global Albedo Yielding an Optical Brightness to Physical Size Transformation Free of Systematic Errors*, NASA document, 2007.

[40] R. Musci, T. Schildknecht, T. Flohrer, G. Beutler. *Concept for a catalogue of space debris in GEO*, ESA document, 2005.

[41] NASA. *Handbook for limiting orbital debris*, NASA-HANDBOOK 8719.14, 2008.

[42] NASA. The orbital debris Quarterly News, Vol.12, Issue 1, January 2008.

[43] F. Paolillo, F. Guarducci, C. Cappelletti, L. Ridolfi, L. Murrali. *Microsatellites formation flying for optical space debris in-orbit observation*, IAC-08 E2.3.3.

[44] C. Pardini and L. Anselmo. *Long-Term Evolution of Geosynchronous Orbital Debris with High Area-to-Mass Ratios*, Trans. Japan Soc. Aero. Space Sci. Vol. 51, No. 171, pp. 22-27, 2008.

[45] A. Rossi. *The Earth orbiting space debris*, Serb. Astron. J. 170, 2005.

[46] G. Ruiz, L. Leushacke, R. Jehn, R. Keller. *Improved FGAN/MPIFR Bi-static debris observation campaign: experiment outline, analysis algorithms and first results*, IAC-06-B6.1.07, 2006.

[47] T. Schildknecht, R. Musci, T. Flohrer. *Properties of the high area-to-mass ratio space debris population at high altitudes*, Advances in Space Research 41, pp. 1039-1045, 2008.

[48] T. Schildknecht, R. Musci, M. Ploner, G. Beutler, W. Flury, J. Kuusela, J. de Leon Cruz, L. de Fatima Dominguez Palmero. *Optical observations of space debris in GEO and in highly-eccentric orbits*, Advances in Space Research 34, pp. 901-911, 2004.

[49] T. Schildknecht, U. Hugentobler, and M. Ploner. *Optical Surveys of space debris in GEO*. Advances in Space Research 23, pp. 45-54, 1999.

[50] T. Schildknecht, R. Musci, M. Serra Ricart, J. de León Cruz, L. Domínguez Palmero, P. Beltrami, K.D. Bunte. *Geostationary Transfer Orbit Survey*, Final Report to ESA study 12568/97/D/IM , December 2006.

[51] T. Schildknecht, R. Musci, M. Ploner et al. *Geostationary orbit objects survey*, Final Report to ESA study 11914/96/D/IM, 2004.

[52] D. B. Spencer, K. Kim Luu et al. *Orbital Debris Hazard Assessment Methodologies for Satellite Constellations*, Journal of Spacecraft and rockets Vol. 38, No. 1, January-February 2001.

[53] S. Stabroth, M. Oswald, C. Wiedemann, P. Vörsmann. *Historical evolution of the small particle debris environment*, IAC-06-B6.2.4, 2006.

[54] G. Stansbery, J.L. Foster, Jr. *Completeness of measurements of the orbital debris environment*, NASA document, 2005.

[55] E. Stoveken, T. Schildknecht. *Algorithms for the optical detection of space debris objects*, ESA document, 2005.

[56] L. G. Taff, D. L. Hall. *The use of angles and angular rates. Initial orbit determination*, Celestial Mechanics and Dynamical Astronomy. 16, pp. 481-488, 1977.

[57] G. Tommei, A. Milani, D. Farnocchia, A. Rossi. *Correlation of space debris observations by the virtual debris algorithm*, Proc. of the Fifth European Conference on Space Debris, April 2009.

[58] G. Tommei, A. Milani, A. Rossi. *Orbit Determination of Space Debris: Admissible Regions*, Celestial Mechanics and Dynamical Astronomy, 97, pp. 289-304 (2007).

[59] United Nations Commitee on the peaceful uses of outer space. *Technical Report on Space Debris*, 1999.

[60] G.B. Valsecchi, A. Milani, A. Rossi, and G. Tommei. *The SRT, Near-Earth objects, and space debris*, Mem. S.A.It. Suppl. Vol. 10, 186, 2006.

[61] F. Vilas, F. Anz-Meador, D. Talent. *Observations of the orbital debris complex by the Midcourse Space Experiment (MSX) satellite*, 1997.

[62] C. Wiedemann, M. Oswald, S. Stabroth and P. Vörsmann.*Cost of Space Debris Impacts on a LEO Satellite*, AIAA 2004-5922.

[63] C. Wiedemann, M. Oswald, S. Stabroth, P. Vörsmann, H. Klinkrad. *Prediction of the Space Debris Particle Flux on Satellite Surfaces using MASTER 2005*, AIAA 2006-7222.

[64] D. Wright. *Colliding Satellites: Consequences and Implications*, February 2009.

[65] http://www.esa.int/SPECIALS/ESOC/SEMN2VM5NDF-mg-24-s-b.html (April-June 2010)

[66] http://www.physics.sfasu.edu/astro/asteroids/sizemagnitude.html (April-June 2010)

[67] http://celestrak.com/events/collision.asp (April-June 2010)

[68] http://www.esa.int/SPECIALS/Space-Debris/index.html (April-June 2010)

[69] http://www.esa.int/SPECIALS/SSA/index.html (April-June 2010)

[70] http://orbitaldebris.jsc.nasa.gov/photogallery/photogallery.html (April-June 2010)

[71] http://orbitaldebris.jsc.nasa.gov/measure/optical.html (April-June 2010)

[72] http://orbitaldebris.jsc.nasa.gov/measure/radar.html (April-June 2010)

[73] http://orbitaldebris.jsc.nasa.gov/measure/surfaceexam.html (April-June 2010)

[74] http://www.golombek.com/TLE-format.html (April-June 2010)

[75] http://celestrak.com/columns/v04n03/ (April-June 2010)

[76] http://www.fas.org/spp/guide/russia/facility/plesetsk.htm (April-June 2010)